The Implications of Fibulin-5 on Elastin Assembly and its Role in the Elastic Fiber

Florence Joelle Ferron

Department of Anatomy and Cell Biology
McGill University, Montreal
June 2007

A thesis submitted to McGill University in partial fulfillment
of the requirements of the degree of Master of Science

Your file Votre référence
ISBN: 978-0-494-38397-1
Our file Notre référence
ISBN: 978-0-494-38397-1

ABSTRACT

The extracellular matrix (ECM) is the material found surrounding the cells in a tissue. One component of the ECM is the elastic fiber, which confers the property of elasticity to its environment. Organs such as the lung, skin and major blood vessels have an abundance of elastic fibers so that they are able to expand and recoil. Elastic fibers are composed of two main components; elastin and microfibrils. Microfibrils are composed primarily of fibrillin-1 and provide a scaffold unto which tropoelastin monomers assemble. Elastic fibers interact with many other proteins in the ECM, one of which is fibulin-5. Based on the severe elastic fiber defects observed in the fibulin-5 null mouse, it was established that fibulin-5 plays an essential role in elastic fiber development. This role may be in the deposition of tropoelastin onto microfibrils and/or in stabilizing the elastic fibers in the extracellular matrix. In the present study, the relationship between fibulin-5 and the elastic fiber was investigated through a number of *in vivo* and *in vitro* experiments. To test the hypothesis that fibulin-5 requires the presence of elastin to assemble in the ECM, full-length recombinant fibulin-5 (rF5) was purified from transfected cells and used to make a fibulin-5 antibody. Solid-phase binding assays using rF5 showed that fibulin-5 binds tropoelastin at two sites; the initial portion of the C-terminus and the first calcium-binding epidermal growth factor-like domain at the N-terminus. Immunofluorescence staining of elastin null mouse embryonic fibroblast cultures revealed that fibulin-5 does not require elastin to be present in the ECM in order to assemble. Subsequently, solid-phase binding assays showed that fibulin-5 can bind to the N-terminus of

fibrillin-1. To determine if fibulin-5 could exist independent of elastin and/or fibrillin-1 *in vivo*, an immunohistochemical analysis was conducted on heart, liver, lung, colon, spleen, testis and kidney. All three proteins were co-localized in all organs except in the kidney, where fibrillin-1 was found to independently stain the capillary tufts of the renal corpuscles and renal tubules. Thus, fibulin-5 may be co-regulated with elastin and is not present on elastin-independent microfibrils. Additionally, novel locations of elastic fibers were uncovered in the heart, liver, colon, spleen and testis. Overall, this study provides important insights as to the role of fibulin-5 in elastic fiber structure and assembly and also reveals the complexity in understanding the pathogenesis of diseases involving elastic fiber proteins.

RÉSUMÉ

La matrice extracellulaire (MEC) est la matière qui entoure les cellules dans un tissu. Une des composantes de la MEC est la fibre élastique, qui confère l'élasticité à son environnement. Des organes comme le poumon, la peau et les prinicipaux vaisseaux sanguins contiennent des fibres élastiques en abondance pour leur permettre de se dilater et se rétracter. Les fibres élastiques sont composées de deux constituants principaux: l'élastine et les microfibriles. Les microfibriles sont composés principalement de fibrilline-1 et fournissent l'échafaudage sur lequel la tropoélastine s'assemble. Les fibres élastiques peuvent interagir avec d'autres protéines dans la MEC, en particulier la fibuline-5. Sur base des défauts sévères observés dans les fibres élastiques de la souris sans fibuline-5, il a été établi que la fibuline-5 jouait un rôle essentiel dans le développement de la fibre élastique. De plus, ce rôle peut être dans le dépôt de la tropoélastine sur les microfibriles ainsi que dans la stabilisation des fibres élastiques dans la MEC. Au cours de cette étude, la relation entre la fibuline-5 et la fibre élastique a été poursuivie à travers une série d'expériences *in vivo* et *in vitro*. L'hypothèse a été avancée que la fibuline-5 nécessitait la présence d'élastine pour s'assembler dans la MEC. Une protéine recombinante de longueur complète de fibuline-5 (rF5) a été purifiée de cellules transfectées et a servit à créer un anti-corps fibuline-5. En utilisant rF5, les essais de fixation en phase solide ont montré que la fibuline-5 se fixe à la tropoélastine en deux sites; la portion initiale au terminus-C, et le premier facteur de croissance épidermal qui fixe le calcium au terminus-N de la protéine. L'immunofluorescence d'une culture de cellules sans élastine provenant de

fibroblastes d'embryon de souris, a révélé que la fibuline-5 ne necessite pas l'élastine pour s'assembler dans la MEC. Ultérieurement, il a été trouvé par essais de fixation en phase solide que la fibuline-5 se fixait au terminus-N de la fibrilline-1. Pour determiner si la fibuline-5 peut exister sans l'élastine et/ou la fibrilline-1 *in vivo*, une analyse immunohistochimique du coeur, foie, poumon, colon, rate, testicule et rein a été entreprise. Les trois protéines étaient localisées ensemble dans tous les organes à l'exception du rein où seule la fibrilline-1 a été trouvée marquant les touffes capillaires du corpuscule rénal et les canaux rénaux. En conséquence, il a été conclu que la fibuline-5 peut être co-réguleé avec l'élastine, et qu'elle ne pourrait pas être présente sur les microfibrilles sans l'élastine. De plus, de nouveaux emplacements de fibres élastiques ont été découverts dans le coeur, le foie, le côlon, la rate et le testicule. Cette étude apporte des enseignements importants sur le rôle de la fibuline-5 dans la structure et l'assemblage des fibres élastiques et révèle aussi la complexité de la compréhension de la pathogènese des maladies relatives aux protéines des fibres élastiques.

To
Mom and Dad
et
Nonna

ACKNOWLEDGEMENTS

I would like to thank Dr. Elaine Davis, for giving me the chance to be part of her lab. For opening the door for me and for all the experience, guidance, and support she provided me over the course of my master's. I must thank Dr. Kerstin Tiedemann, who took me under her wing with patience and kindness, and taught me the secrets of proteins, Westerns blots, and cells. I would also like to express my gratitude to Dr. Dieter Reinhardt who provided me with valuable knowledge, fibrillin-1 protein and antibodies as well as the use of his Äkta purifier. I would also like to thank Dr. Hiromi Yanagisawa for providing us with fibulin-5 null mice and fibulin-5 antibody and constructs, Dr. Dean Li for providing the lab with elastin null mice and Dr. Robert Mecham for providing the lab with tropoelastin protein and antibody. Thanks go to my advisory committee members: Dr. Dieter Reinhardt, Dr. Louis Hermo and Dr. Janet Henderson for the feedback and advice they gave me over the course of my project. Special thanks goes to Ailian Li from Dr. Henderson's lab and Rujuan Huo and Shaozhen Fang from the Bone Center for embedding and cutting all those sections and doing an amazing job. To the past and present members of the Davis Lab: Andreas, Brendan, Faisal, Jiwon, Katie, Kaitlyn, Kerstin, Mansa, Nikolaus, Rachel, Sharon and Tania as well as the members of the Reinhardt Lab: Dr. Dirk Hubmacher and Christine Fagotto – thank you all for your help, friendship, for keeping me sane and making the lab a great place to work. I would like to further express my gratitude and appreciation to Dr. Dirk Hubmacher for giving me precious fibulin-2 protein from his personal secret stash. To Jiwon Choi, who patiently taught me all the staining

techniques, and then patiently taught me all the shortcuts to the staining techniques. To Katie Leonard for all her toils and troubles with mice and genotyping, and for her awesome shaving skills, of which I doubt I shall see such caliber again. To Roger, for his habit of suddenly appearing and making us laugh, and to all my friends who belonged outside of the extracellular matrix bubble, for their friendly patient smiles whenever I ranted or raved about extracellular matrix.

Last but not least, I would like to thank and honour my family for their constant love and support during the "highs" and the "lows". To my brothers Mathieu and Etienne for tethering me down and keeping me rooted to where I come from. To my parents who had to suffer through all my "lows" but who always picked me up and straightened me out, brushed me off and pushed me through the door – gently.

TABLE OF CONTENTS

REVIEW OF THE LITERATURE

Extracellular Matrix

In simple terms, extracellular matrix is the material found surrounding the cells. Composed of a complex interacting system of fibers, ground substance and tissue fluid [1], the extracellular matrix imparts structural integrity and function to tissues and organs of an organism. The composition of the extracellular matrix will vary and change depending on the location and function of the tissue; conferring special properties to the tissue and thus the organ. The most obvious function of extracellular matrix is structural, supporting organs and cells. It also has an immunological role by providing a physical barrier to the dispersion of microorganisms and a nutritional role by serving as a medium through which nutrients and metabolic wastes can be exchanged between cells and blood vessels [1]. The prominent role played by the extracellular matrix is underlined in the gravity of diseases caused by mutations, defects or disruptions in extracellular matrix proteins, which lead to illnesses such as Cutis laxa and Marfan syndrome [2, 3]. These diseases demonstrate the necessity of a "healthy" extracellular matrix and the important role it plays in the normal function of organs and tissues, right down to the basic unit - the cell. The relationship between cells and extracellular matrix is vast and complex but essential to maintain. The exact functions and roles of many of the extracellular matrix proteins, however, have yet to be completely defined but nonetheless, the importance of the matrix has been clearly established.

Elastic Fibers

An important component of the extracellular matrix is the elastic fiber. Elastic fibers are found in almost every organ and tissue in the body. Elastic fibers confer the property of stretch and resilience to tissues, such as blood vessels, lung and skin. Elastic fibers are composed of two integral proteins, elastin and microfibrils. Elastin makes up 90% of the elastic fiber and forms the internal core, which is surrounded by a lattice of microfibrils [4]. The structure of elastic matrices differs among tissues, thereby providing the different tissues with specialized functional properties. The tissue–specific architectures are determined by the organization of the microfibril template, the orientation of the cells that deposit them and the forces acting on the tissue [5, 6]. For example, in the aorta and elastic arteries, the elastic fibers are organized into concentric fenestrated lamellar layers within the media that interact with the vascular smooth muscle cells. The internal and external elastic laminae are thick concentric elastic fiber layers that separate the intima from the media and the media from the adventitia, respectively. Elastic fibers can also be found in the media of the smallest arteries. In the developing aorta, subendothelial microfibril bundles are oriented parallel with the direction of blood flow and provide elastic anchorage for the endothelial cells [7, 8]. This organization gives the arterial blood vessel the ability to accommodate blood pressure and stress. In lungs, the elastic fibers form a delicate, highly branched network that is present throughout the respiratory tree. The fibers are concentrated in areas of stress such as the openings of alveoli and alveolar junctions. This provides an architectural foundation but, most importantly, it allows for the stretch and recoil necessary for the alveoli to accommodate the intake of air [9]. In

skin, elasticity is imparted by an abundant elastic fiber network that extends from the dermal-epidermal junction as a series of microfibril bundles known as oxytalan fibers, into perpendicular elaunin fibers in the papillary dermis (these fibers contain small amounts of elastin), and finally to the thick horizontally aligned elastic fibers in the reticular dermis [10].

Elastin

Elastin makes up approximately 90% of the elastic fiber and it is the physical properties of elastin that are considered to be responsible for the function of elastic tissues [4, 11]. Elastin constitutes 30-57% of the aorta, 50% of elastic ligaments, 28-32% of major vascular vessels, 3-7% of lung, 4% of tendons and 2-5% of the dry weight of skin [12]. Elastin, which forms the internal core of the elastic fiber, is an insoluble and robust protein. It is estimated to have a half-life of 70 years and with a very low turnover rate in healthy tissues [13]. Elastin is secreted as a soluble monomer called tropoelastin, which has a size range from 62 to 75 kDa due to alternative splicing [6, 14-16]. Degradation of elastin is especially slow due to the extensive crosslinking of tropoelastin within the elastic fiber [6, 14, 16, 17]. Due to this characteristic, once elastic fibers are damaged, they are very poorly repaired or are lost altogether.

Elastin Gene and Structure

Human tropoelastin is encoded by a single-copy gene on chromosome 7 [6, 14-16]. The human tropoelastin gene contains 34 exons and differs from bovine, porcine, feline, canine and mouse genomes in that it has 2 less exons, which have been lost through primate evolution [18]. The tropoelastin gene is distinguished by a periodicity

of exons where distinct hydrophobic and crosslinking domains are encoded by separate alternating exons. The tropoelastin protein thus has a multidomain structure (Figure 1), with repeating hydrophobic and lysine-rich crosslinking domains, each encoded by a separate exon [19, 20]. The C-terminal exon of tropoelastin contains the only two cysteine residues found in tropoelastin. These form an intramolecular disulfide bond creating a hairpin loop and a positively charged pocket which is thought to be important for elastic fiber assembly [12, 19]. The N-terminal region is another region of interest because it contains a fibrillin-1 binding site [12, 20], although the identity of the specific exon responsible for the interaction is unknown. Similarly, fibulin-5 binds tropoelastin but the binding site has not been identified. The primary tropoelastin transcript undergoes widespread alternative splicing. This leads to the translation of various tropoelastin isoforms [21]. At least seven human isoforms have been discovered due to alternatively spliced exons [22, 23]. The most frequently observed human tropoelastin isoform lacks exon 26A and is reported to be only expressed in certain diseased states [24]. Due to alternative splicing the elastin protein, ranges from 62 to 75 kDa [6, 14-16]. The various splicings of the exons may be used to customize the structural function of the protein in different tissues [25].

Regulation of Tropoelastin Expression

The production of elastin is a tightly regulated process, this process is called elastogenesis. Elastogenesis occurs primarily during late fetal and early neonatal periods in several types of cells including smooth muscle cells, fibroblasts, endothelial cells, chondroblasts and mesothelial cells [26]. Once elastin synthesis ceases there is very little turnover of elastin during adult life, unless the elastic fibers are injured which induces neosynthesis of elastin [27]. Both pre- and posttranscriptional control

mechanisms have been identified for tropoelastin expression. The 5′ end of the elastin gene contains typical housekeeping elements that serve as potential sites for transcription–regulatory factors [26]. Exogenous factors that alter elastin transcription include nuclear factor-1 family members [28], insulin-like growth factor-1 [29, 30], basic fibroblast growth factor [31, 32], tumor necrosis factor-α [33], interleukin-1-β [34] and interleukin 10 [35]. Expression is also extensively controlled at the posttranscriptional level, where the messenger RNA (mRNA) decay is likely the principal regulatory mechanism [36]. Transforming growth factor (TGF β1) is known to be a strong stimulator of elastin expression and is believed to affect elastin mRNA stability [37].

Tropoelastin Secretion

Once tropoelastin mRNA is ready to be transported from the nucleus to the rough endoplasmic reticulum (rER), translation of tropoelastin will be able to start on the surface of the rER. The tropoelastin formed is a 70 kDa polypeptide with an N-terminal signal sequence, which is cleaved once the protein enters the rER [38]. To prevent any unwanted intracellular self-aggregation and premature degradation while traveling through the rER, tropoelastin associates with elastin-binding protein (EBP) [39]. This 67 kDa protein, binds predominantly to the hydrophobic domains on tropoelastin and chaperones tropoelastin intracellularly [39]. Tropoelastin also associates with FKBP65, a 65 kDa peptidyl-prolyl *cis/trans* isomerase [40], in the rER and together with EBP, move through the rER and Golgi apparatus and are secreted to the cell surface. Once outside the cell, tropoelastin can exist as a monomer in solution in two forms; an open globular molecule and a distended polypeptide [6, 14-16]. Two

major processes required for the incorporation of tropoelastin into a growing elastic fiber are coacervation and crosslinking. Crosslinking is essential for the structural integrity and function of elastin. Two types of crosslinking domains exist in tropoelastin; domains rich in alanine and domains rich in proline. Within the alanine-rich domains, lysine groups are usually found in clusters of two or three amino acids, separated by two or three alanine groups [41]. Within the proline-rich domains, lysine pairs are separated by one or more proline groups and are flanked by prolines and bulky hydrophobic amino acids [41]. Individual monomers of tropoelastin form an insoluble elastin polymer through lysine mediated crosslinks [15]. Crosslinking of tropoelastin is initiated through the action of the copper-dependent amine oxidase enzyme, lysyl oxidase (LOX) [42], or other family members such as the LOX-like proteins 1 through 4 [19]. Lysyl oxidase catalyses the oxidative deamination of lysine groups [42] within tropoelastin to form allysine [43]. Allysine are the precursors to a variety of inter- and intramolecular crosslinks found in elastin, particularly the crosslink desmosine [44]. Desmosine crosslinks are unique to elastin and are formed by the condensation of two allysine groups on one tropoelastin molecule and one allysine group and one lysine group on another tropoelastin molecule [41]. Desmosines have not been found associated with proline-rich domains [41]. The oxidation of lysine groups by lysyl oxidase is the only known posttranslational modification of tropoelastin. In order for tropoelastin molecules to be crosslinked, they must first associate and align with each other so as to facilitate the generation of crosslinks between neighbouring lysines. Coacervation is the proposed molecular means by which this occurs [45]. Coacervation refers to "an inverse temperature transition whereby tropoelastin molecules aggregate with increasing temperature" [12].

This means that at low temperatures, tropoelastin is soluble in solution but with increasing temperature, the solution becomes opaque as the tropoelastin molecules associate and become ordered by interactions between the hydrophobic domains of tropoelastin [12]. Evidently, the arrangement of sequences in tropoelastin is very important to the process of coacervation and it is no surprise that the process of coacervation is precisely adjusted to the physiological conditions of the extracellular matrix. Optimal coacervation of human tropoelastin occurs at 37°C, 150 mM NaCl and at a pH of 7 to 8 [46].

Microfibrils

In developing elastic tissues, microfibrils are the first components of the elastic fiber to appear in the extracellular matrix. They are thought to act as a scaffold for the deposition, orientation and assembly of tropoelastin monomers. They are 10 nm in diameter and lie parallel to the long axis of the developing elastin fiber [47]. Microfibrils are comprised of several macromolecules. The main integral component of the microfibril is fibrillin-1 [48], and to a lesser extent fibrillin-2, [49] and MAGP-1 [50], a microfibril-associated glycoprotein. The fibrillins are large, 350 kDa, acidic, cysteine-rich glycoproteins that appear as extended, flexible molecules when viewed by electron microscopy. Their primary structure is dominated by calcium-binding epidermal growth factor-like repeats [5]. MAGP-1 is an acidic, 31 kDa glycoprotein that is covalently linked to the microfibrils [50]. It colocalizes widely with microfibrils and was detected in purified microfibril preparations by mass spectrometry [51]. Other proteins that are found to be associated with the microfibrils

include latent transforming growth factor β-binding proteins (LTBPs) [5], microfibrillar associated proteins (MFAP) and members of the fibulin family [52-55] (Figure 2). It also has been shown that proteoglycans such as biglycan and decorin [56] interact with microfibrils and help confer specific properties to the surrounding extracellular matrix including hydration, impact absorption, molecular filtering, regulation of cellular activities, mediation of growth factor association and release and transport within the extracellular matrix [57].

Expression of Fibrillins

There are three members of the fibrillin protein family. Fibrillin-1 and fibrillin-2 are encoded by genes on chromosomes 15 and 5, respectively, and have partially overlapping expression patterns [49, 58, 59]. Fibrillin-1 is the most prominent protein expressed among the three fibrillin proteins, whereas, fibrillin-2 is strongly expressed in developing tissues [49, 59]. Not much is known about fibrillin-3, except that it is expressed in humans and birds but not in rodents [60]. Purified microfibrils from three different adult tissues have been analyzed by mass spectrometry and have identified abundant fibrillin-1, but fibrillin-2 was not present [51]. Immunofluorescence and immunochemical studies using antibodies specific for either fibrillin-1 or fibrillin-2 have shown that both fibrillins colocalize in some microfibrils [59]. A recent study by Carta *et al.*, 2006 [61], on the contribution of fibrillin-1 and fibrillin-2 to vasculogenesis using double knockout mice, indicated that both fibrillins perform partially overlapping functions during aortic development [61]. In this study, the fibrillin-1 null mice died perinatally from ruptured aortic aneurysms. In contrast, the fibrillin-2 null mice had normal aortic development. Double null mice

died *in utero* and had a much more severe vascular phenotype than the fibrillin-1 null mice alone.

Fibrillin-1 Structure

The human fibrillin-1 gene (*FBN1*) consists of 65 exons that extend over 200 kb and encodes a protein of approximately 350 kDa. The protein is composed of multiple domains (Figure 1) with the most abundant being tandem repeats of calcium-binding epidermal growth factor (cbEGF)-like domains. There are 47 epidermal growth factor (EGF)-like domains of which 43 are calcium binding. In the presence of calcium these domains adopt a linear conformation [49, 58, 60]. The cbEGF-like domains are interspersed by eight cysteine containing TGF-β binding domains [49, 58, 60]. Within each cbEGF-like domain, six cysteine residues form three intradomain disulfide bonds making the protein a rigid, rod-shaped molecule [62]. Fibrillin-1 has 14 *N*-glycosylation sites and an integrin-binding arginine-glycine-aspartate (RGD) motif in the center of the molecule. The N-terminus of fibrillin-1 has a unique cysteine containing motif as well as a potentially flexible proline-rich region, perhaps making it able to interact with a high number of extracellular matrix molecules, including MAGP-1, fibulin-5 and other fibrillin-1 monomers [63]. Once at the surface of the cell, the newly secreted fibrillin-1 monomers appear as thread-like filaments composed of beaded strings. The beaded strings subsequently assemble together with other components into thread-like filaments, which in turn give rise to macroaggregates with or without elastin [64].

Microfibril Assembly

Microfibril assembly is a multistep process. As fibrillin-1 monomers are secreted from the cell, they undergo N-terminal and C-terminal processing by enzymes

of the furin/PACE family [63, 65, 66]. This step serves as a precursor for lateral interactions and molecular additions in a linear fashion. Fibrillin-1 molecules associate laterally and linearly, through specific N-terminal and C-terminal interactions [63, 65, 66] and the newly assembled microfibrils are then stabilized by transglutaminase crosslinks [67]. The molecular interactions involved in microfibril assembly have been elucidated using recombinant fibrillin-1 fragments and *in vitro* binding assays [66, 68, 69]. From these studies, high-affinity binding was seen between N-terminal fragments, between furin-processed C-terminal fragments and between N-terminal and C-terminal fragments [66]. These interactions most likely drive the linear and lateral assembly of the microfibrils. Other proteins that are suspected to play an important role in microfibril assembly through interactions with fibrillin-1 are MAGP-1 and heparin. MAGP-1 strongly binds an N-terminal sequence in a calcium dependent manner [70, 71]. This interaction inhibits N-terminal and C-terminal interactions but not the homotypic N-terminal interactions [66]. Heparin was shown not to inhibit fibrillin-1 N-terminal and C-terminal interactions but heparin competes both with MAGP-1 to bind the fibrillin-1 N-terminus and with tropoelastin to bind a central fibrillin-1 sequence [72].

Elastic-Fiber Interface Molecule: Fibulin-5

Fibulin-5, also known as EVEC/DANCE, is an extracellular matrix protein that binds elastin and is essential for elastic fiber development [55]. It is not an integral structural component of the elastic fiber but rather an elastin-microfibril interface located molecule. Fibulin-5 is an integrin-binding [54] and calcium dependent elastin-binding protein that potentially functions as a scaffold protein to link cells to the

elastic fibers [55]. Since the molecules and mechanisms involved in elastogenesis are still unclear, knowledge about the seemingly "small players" in this process is as important as the knowledge acquired about the "big players" in elastic fibers.

The Fibulin Family

Fibulin-5 is one of five fibulin family members, which are all secreted extracellular matrix glycoproteins [73]. The name "fibulin" comes from the Latin word, *fibula*, meaning clasp or buckle [73]. The fibulins are highly conserved and exhibit a 90% homology between the mouse and human gene sequences [73]. The fibulins are part of a larger extracellular matrix family because of their capability to bind integrins and structures of the extracellular matrix and thus provide stability and organization to extracellular matrix structures such as the elastic fibers and basement membranes [74]. The fibulins are important in development and expression is largely decreased in adulthood; however, the fibulins can be upregulated in injury and their expression modified in disease states [74]. The involvement of the fibulins in functions such as cell morphology, adhesion, growth and motility remains unclear as well as their implicated role in regulating organogenesis, vasculogenesis, fibrogenesis and tumourigenesis [73-75].

Fibulin Family Genes and Structures

The fibulin gene family comprises five distinct genes that encode more than eight protein products due to alternative splicing [76, 77]. The fibulin proteins have three structural domains; I, II and III (Figure 3). Domain I is found at the amino terminus of the protein and is unique for each of the five fibulin members. Both fibulin-1 and fibulin-2 contain three anaphylatoxin-like (AT) modules in their domain I, whereas fibulin-3, fibulin-4 and fibulin-5 contain modified cbEGF-like modules

[73]. Fibulin-2 also contains cysteine-rich and cysteine-free subdomains, making it the largest member of the fibulin family [73, 76]. Domain II is composed of a series of cbEGF-like modules essential for the structural integrity of the protein. These modules assist in protein-to-protein interactions as a result of their tertiary structure and may play a crucial role in the interactions between fibulins and other proteins [78]. Finally, domain III is common to all members of the fibulin family and is known as the fibulin-type carboxyl terminus (FC) module [73, 79]. Fibulin-1 differs from the other fibulin members because it has four splice variants, fibulin-1A, 1B, 1C and 1D, each differing at the FC module and serving distinctive functions [76, 77].

Fibulin-5 Protein

Fibulin-5 is a secreted 448 amino acid glycoprotein and has a molecular weight of 55 kDa [80]. Fibulin-5 is highly expressed in the developing stages of the vascular system [80]. Synthesis significantly decreases in adult tissue although it can be restimulated in response to vascular injury [81]. Northern blot analysis of fibulin-5 shows that it is expressed in most tissues except in brain, liver, thymus, prostate and peripheral blood leukocytes [80, 82]. Fibulin-5 has six cbEGF-like domains. Five of these have six cysteine residues that form typical intramolecular disulfide bonds [80]. The most amino terminal cbEGF-like domain, however, contains a proline and tyrosine-rich insert, two additional cysteine residues and an integrin binding arginine-glycine-aspartate (RGD) motif [80, 81]. Cell surface integrins bind this RGD motif and initiate a cascade of signaling events inside the cell [83]. *In vitro*, fibulin-5 binds $\alpha_v\beta_3$, $\alpha_v\beta_5$ and $\alpha_9\beta_1$ integrins and endothelial cell adhesion to fibulin-5 has been shown to be mediated by the RGD motif [54, 81]. *In vivo*, fibulin-5 has been shown to localize to the surface of elastic fibers [55]. The induction of tropoelastin expression is

followed by the expression of fibulin-5 suggesting that fibulin-5 expression could be directly or indirectly mediated by tropoelastin [84]. Solid-phase binding assays have shown that fibulin-5 strongly binds tropoelastin and suggest that the cbEGF-like motifs of fibulin-5 are responsible for the interaction between the two proteins [55]. Using solid-phase binding assays, it was also shown that fibulin-5 interacts with the N-terminus of fibrillin-1, thus fibulin-5 interacts with microfibrils [85]. There was earlier evidence of an interaction occurring between fibulin-5 and fibrillin-1 with the tight skin (*Tsk*) mouse, where a mutation in fibrillin-1 affected its association with fibulin-5 [86]. In the skin of this mouse, fibulin-5 fibers normally found at the connective tissue/muscle interface were absent [86]. The decrease in fibrillin-1 also led to an overall decrease in fibulin-5 in the extracellular matrix of the *Tsk* mice and the appearance of irregular elastic fibers in the hypodermis [87]. Overall, fibulin-5 may be playing a role in the deposition of tropoelastin onto microfibrils by bridging elastin to microfibrils as well as having a role in stabilizing the elastic fibers in the extracellular matrix by linking them to the surrounding cells.

Elastic Fiber Assembly

The accepted theory of elastic fiber assembly starts with the deposition of soluble, newly secreted tropoelastin molecules onto assembled microfibrils. This is then followed by the accumulation of additional tropoelastin monomers that become covalently cross-linked by one or more members of the LOX enzyme family to form the insoluble elastin core of the elastic fiber. There are many interactions occurring during this process that are necessary in order to have a functioning elastic fiber. The following is a summary of some of the necessary interactions between the proteins of

interest. The N-terminus of tropoelastin will interact with two high affinity binding sites located near the center of the fibrillin-1 protein on the N-terminal side. Tropoelastin can become transglutaminase crosslinked to a specific fibrillin-1 sequence in one of these sites [71]. The surrounding cells can interact with elastin through EBP, which binds the tropoelastin hexapeptide VGVAPG [88-90]. The C-terminus of elastin also interacts with integrin $\alpha v\beta 3$ but not in an RGD mediated manner since elastin lacks this motif [91]. In addition to this, a cell interaction site exists within the last 17 C-terminal residues of tropoelastin, which mediates cell adhesion through cell surface proteoglycans containing heparan sulphate and/or chondroitin sulphate [92]. As mentioned previously, the N-terminus of fibrillin-1 with its cysteine containing motif and its proline-rich region is able to interact with a large number of extracellular matrix molecules, including fibulin-5. Although it was known that the N-terminus of fibrillin-1 and fibulin-5 interact [85], the exact binding site between these two proteins has only recently been determined to be on the first hybrid domain of fibrillin-1 [93]. Fibulin-5 and fibrillin-1 both contain single RGD motifs. Fibrillin-1 mediates cell adhesion mainly through its RGD motif located in the center of the protein [94] It was shown that fibrillin-1 interacts with human smooth muscle cells through the $\alpha v\beta 3$ integrin [94-96]. It also has been demonstrated that fibulin-5 interacts directly with vascular cells through its RGD motif, a function that may contribute in elastic fiber deposition [54, 55, 76]. Finally, solid-phase binding assays have shown that fibulin-5 strongly binds tropoelastin and suggest that both an N-terminal cbEGF-like domain and a C-terminal region (a.a. 342 - 399) are involved [55, 97]. The exact binding site has not yet been determined. From these studies, it is

evident that elastic fiber assembly must involve a complex network of interactions. All three proteins, elastin, fibrillin-1 and fibulin-5, can bind cells, either through an RGD mediated or non-RGD mediated mechanism and all three can bind each other. The absence or dysfunction of any one of these proteins can therefore have disastrous effects on the structure, stability and function of the elastic fiber.

Mouse Models

Mouse models have proven to be very valuable tools for *in vivo* studies of diseases linked to mutations in genes. These mice have been designed to harbour targeted mutations in genes of interest and very often provide the first animal models for human diseases. The mouse models allow for a better understanding and insight of these diseases as well as new discoveries. Over the years, many mouse models have been engineered to reflect connective tissue diseases found in humans, including mouse models that have been designed to have mutations in the genes for fibrillin-1 (*fbn1*), fibulin-5 (*fbln5*) and elastin (*eln*) genes.

Fibrillin-1 Mouse Models

The mgΔ Fibrillin-1 Mouse Model

In 1997, Dr. L. Pereira generated a mouse that had an allele (mgΔ = marfan gene deleted) that produced a truncated fibrillin-1 monomer that was only expressed at 5 to 10% of normal levels [98]. This study was important because it showed that a mouse with a targeted mutation in the fibrillin-1 gene recapitulated the vascular aspects of Marfan syndrome. Heterozygous mgΔ/+ mice were born normally and

showed only occasional and subtle skeletal abnormalities late in life [98]. There were no vascular changes seen and life expectancy was normal. Homozygous mgΔ/ mgΔ mice were also born at the expected frequency and appeared normal but died prior to weaning. Autopsies revealed aortic dilatation and dissection leading to hemopericardium and hemothorax in all the homozygous mutant mice that died [98]. Upon closer inspection, the aortic media showed disruption of elastic laminae and loss of elastin content with the accumulation of amorphous matrix elements as seen in mature human lesions [98]. Surprisingly, these lesions were very localized, with the bulk of the aorta showing linear, uninterrupted and parallel elastic fibers. The mgΔ mouse model provided evidence that very little and malfunctioning microfibrils were adequate to support the deposition of elastin to form elastic fibers but that fibrillin-1 plays a very prominent role in elastic fiber homeostasis [98].

The mgR Fibrillin-1 Mouse Model

The early death of the homozygous mgΔ/ mgΔ mice made the analysis of the pathological changes leading to the formation of an aneurysm difficult. A second mutant mouse line resulting from an aberrant targeting event was therefore developed by Dr. Pereira in 1999 [99]. This mouse model differed from the mgΔ model because it allowed for the study of the progression of an aneurysm. This mutation caused the allele (mgR = marfan gene reduced) to express structurally normal fibrillin-1 but only at 15% of normal levels. Heterozygous mgR/+ mice had no abnormalities throughout life [99]. The homozygous mgR/mgR showed normal prenatal and perinatal development but died between the ages of three and four months. Upon investigation of the aorta (and other arteries), focal calcifications of intact elastic laminae were

observed as early as six weeks of age. The calcified segments became more numerous and merged with each other over time [99]. It was also observed that intimal hyperplasia with excessive and disorganized deposition of matrix components occurred at approximately nine weeks of age. The infiltration of mixed inflammatory cells into the media layer was associated with the expression of matrix metalloproteinases, intense elastolysis and the eventual structural collapse of the vessel wall [99]. The longer life span of the mice allowed the observation of bone overgrowth, a telltale sign of Marfan syndrome [99]. Ultrastructural analysis of aorta from mgR/ mgR mice revealed the initial events of the destructive changes in the media layer. Elastic laminae link neighbouring endothelial and smooth muscle cells through an intermediate structure composed of microfibrils [7, 8]. These connections are thought to contribute to the structural integrity of the vessel wall through cell anchorage and to coordinate contractile and elastic tensions [8]. Homozygous mgR/ mgR mice showed a loss of these connections prior to elastolysis, a breach that would eventually allow infiltration of inflammatory cells into the media and structural collapse of the vessel wall [100]. This mouse model allowed for the establishment of a pathogenetic model of Marfan syndrome.

Fibulin-5 Mouse Model

In 2002, Dr. H. Yanagisawa and Dr. T. Nakamura, simultaneously generated mice deficient in fibulin-5 [54, 55]. Their separate studies both determined that fibulin-5 is essential for elastic fiber formation *in vivo*. Fibulin-5 null mice survive to adulthood with a relatively mild phenotype. The most affected tissues were the elastin-rich organs such as the skin, lung and aorta, which all showed severely

disrupted and disorganized elastic fibers. One of the most apparent phenotypes observed in fibulin-5 null mice is severely loose and sagging skin. The skin of the fibulin-5 null mouse showed a sparse and fragmented elastic fiber network that manifested in a loss of elastic recoil causing the skin to hang in folds. The knockout mice also had enlarged airspaces and distended alveoli in the lung. The pulmonary elastic fibers were short and fragmented and ultimately resulted in emphysema and pulmonary hypertension leading to enlargement and hypertrophy of the right ventricle [54]. The most concerning phenotype was a tortuous and elongated aorta and aortic branches which exhibited a loss of compliance. In these vessels, the medial elastic laminae were severely disrupted and disorganized, with the exception of the most internal laminae found near the intimal layer of the vessel [54, 55]. Systolic blood pressure was increased as a result of the loss of elasticity in the wall of the aorta, while the mean and diastolic blood pressures remained normal [55]. The loose skin seen in fibulin-5 null mice due to the lack of fibulin-5 suggested that mutations in the fibulin-5 gene (*fbln5*) might cause cutis laxa in humans. This led to the discovery of a homozygous mutation, S227P, in a large consanguineous family with an autosomal recessive form of cutis laxa [2]. In addition to this homozygous mutation, a dominant negative effect of a 22kb tandem gene duplication in *fbln5* was also found in patients with cutis laxa [101]. In the majority of cutis laxa patients, however, cutis laxa does not result from a mutation in *fbln5* but involves other extracellular matrix proteins, the main one being elastin. Since the elastinopathy in fibulin-5 null mice is neither caused by elastolytic activity nor by inflammation mediators, it is clear that fibulin-5 itself must play a key role in elastic fiber development. As the mice age, the phenotypes worsened but the lifespan of the mice was unaffected [54, 55]. The fibulin-5 null

mouse is thus a valuable tool to elucidate the role of fibulin-5 in elastic fiber assembly and vascular development *in vivo*.

Elastin Mouse Model

The Elastin Null Mouse Model

In 1998, Dr. D.Y. Li generated mice deficient in elastin by deleting exon 1 and 4 kb of the elastin promoter, resulting in a null mutation [102]. The elastin null mice survived birth but died within three days from a subendothelial accumulation of proliferating smooth muscle cells that eventually occluded the vascular lumen. These lesions were also found in systemic and pulmonary arteries of all sizes. It is unknown through which mechanism elastin is able to exert its effects on the smooth muscle cells but it is interesting to note that disruption of elastin may participate in the obstructive arterial pathology by altering the proliferation rate of vascular cells at the site of injury [102].

The Elastin Heterozygous Mouse Model

The elastin heterozygous (*eln*+/-) mouse proved to be a useful model since the phenotype reproduced loss of function mutations linked to supravalvular aortic stenosis (SVAS) [103] (see below). The *eln*+/- mice are the same as the wildtype in gross appearance, behaviour and life expectancy [104]. Northern blot analysis showed that *eln*+/- vessels had approximately a 50% decrease in elastin mRNA when compared to wildtype mice at birth [104]. Histological examination of arterial structure demonstrated an increased number of lamellar units in both the ascending and descending aorta from *eln*+/- mice but with the lamellae being about 50% thinner then in the wildtype mice [104]. The changes are apparent at birth which suggested that the

alterations in the vessel wall were occurring early in development. The *eln*+/- mouse did not exhibit all of the phenotypes of human SVAS, such as the development of stenotic lesions, but has revealed some traits of the human disease that were until then, unknown.

Clinical Significance

As very often happens, when "something" is missing, not functioning or diseased, we realize too late how important and vital that "something" is. This is often seen with genetic disorders, but we must learn from these genetic errors and acquire the knowledge necessary to eventually undo or compensate for the genetic mistakes. Such is the case with genetic disorders that affect elastic fibers, which are often life threatening. The clinical studies of patients with altered elastic fiber structure and function stress the importance of elastic fibers in all elastic connective tissues, but in particular, the cardiovasculature system.

Marfan Syndrome

Marfan syndrome is a relatively common autosomal dominant hereditary disorder of connective tissue, with major cardiovascular, skeletal and ocular defects [105, 106]. It is caused by mutations in the gene for fibrillin-1 (*FBN1)* [107, 108]. Most families have unique mutations due to large heterogeneity among *FBN1* mutations [109, 110]. However, 25% of cases of Marfan syndrome result from sporadic parental germinal *de-novo* missense mutations in *FBN1* with no prior family history [107, 108]. Most mutations occur within the 47 tandemly repeated EGF-like

domains, many disrupting one of the six predictably spaced cysteine residues that interact via disulfide linkage to determine domain folding and calcium binding. Such disturbances can lead to enhanced cleavage and proteolytic degradation [111, 112]. Premature death is most often caused by aortic dissection following elastic fiber degeneration and progressive dilatation of the ascending aorta. Mutations in *FBN1* may cause Marfan syndrome as a direct consequence of an alteration or reduction in the secretion of mutant fibrillin-1 molecules or due to aberrant assembly of mutant fibrillin-1 molecules into microfibrils. Microfibrils that contain mutant fibrillin-1 molecules have an increased susceptibility to proteolytic damage [107]. Fibrillin-1 mutations have been identified in a range of overlapping Marfan syndrome-like conditions, or what has been collectively called, type-1 fibrillinopathies. These include Marfan syndrome, neonatal Marfan syndrome, atypically severe Marfan syndrome, ectopia lentis, kyphoscoliosis, familial arachnodactyly, familial ascending aortic aneurysms and dissections, MASS phenotype (mitral valve prolapse, aortic valve dilation without dissection, skeletal and skin abnormalities), Shprintzen-Goldberg syndrome, isolated skeletal features, 'new variant of Marfan syndrome' and Weill-Marchesani syndrome [113]. The Marfan syndrome pathology has recently been strongly associated with excess TGF-β signaling [114, 115]. The excess TGF-β signaling results in developmental defects, such as defective mitral valvulogenesis [115] and a widening of distal airspaces due to failure of alveolar septation [114], as well as TGF-β mediated increased cell proliferation and altered extracellular matrix deposition and turnover. In some cases, familial thoracic aortic aneurysms and dissections is not caused by mutations in *FBN1*, but rather the TGF-β receptor

(TGFBR) II gene [116, 117]. Loeys-Dietz aortic aneurysm syndrome is a disorder that phenotypically overlaps with Marfan syndrome with aggressive cardiovascular defects that is also caused by enhanced TGF-β signaling due to mutations in TGFBRI and II [118]. Very recently, it has been shown that an angiotensin II type 1 receptor blocker, Lorsartan, can prevent the increased TGF-β signaling associated with Marfan syndrome [119]. Lorsortan is currently in widespread clinical use for treatment of hypertension and prevention of strokes in adults and children. Given its exceptional tolerance profile in all age groups, clinical trials in patients with Marfan syndrome are underway [119].

Supravalvular Aortic Stenosis

Supravalvular aortic stenosis (SVAS) is caused by mutations in the elastin gene (*ELN)*, including deletions and point mutations in the 5′ and middle region of the gene, many of which lead to premature termination codons and unstable mRNA [103]. SVAS is inherited in an autosomal dominant manner. The symptoms of SVAS involve a decreased deposition of elastin associated with increased vascular cell proliferation that leads to an obstructive vascular disease [102, 104, 120, 121]. Haploinsufficiency of elastin underscores the pathology of SVAS, but correlations between gene dosage to physical manifestation have proven difficult. Patients with severe SVAS may present with angina and dyspnea, systolic murmur and left ventricular hypertrophy leading to congestive heart failure. Some SVAS patients demonstrate a diffuse narrowing of the ascending aorta, with disorganized elastic fiber lamellae and smooth muscle cell hypertrophy in the medial layer. Others develop a

localized fibrous ring above the aortic valves or, more commonly, demonstrate an increased medial thickness with fibrous thickening. The pulmonary, coronary, carotid and renal arteries have also been identified to have developed stenosis and a thickening of the vessel wall [103].

Cutis Laxa

Cutis laxa (CL) is a heterogeneous group of disorders characterized by excess, sagging and inelastic skin [2, 101, 113, 122, 123]. There are at least three recessive heritable forms of cutis laxa: CL type I, CL type II and De Barsy syndrome, as well as an X-linked form and an autosomal dominant form. Mutations in the elastin gene mostly occurring in the 3′end have been shown to cause the autosomal dominant form of cutis laxa [23, 122, 124-126]. In at least one case, the mutant protein was secreted and interfered with deposition of normal elastin in a dominant negative manner [123]. The autosomal recessive form of cutis laxa can also be caused by mutations in the gene encoding fibulin-5 [2]. There has even been a recently described recessive cutis laxa syndrome shown to be caused by a mutation in the gene for fibulin-4 gene; a gene that has also been associated with vascular tortuosity and bone fragility [127]. There is yet another form of cutis laxa termed acquired cutis laxa. Although this cutis laxa is caused by dermal inflammation and associated elastic fiber degeneration, its pathogenesis involves an underlying genetic susceptibility in which the interaction of specific elastin and fibulin-5 gene alleles render the elastic fibers predisposed to inflammatory destruction [128]. The apparent disease links between the affected proteins underline the important relationship that exists between elastin and fibulins in the elastic fiber system.

Age-Related Macular Degeneration

Age-related macular degeneration (AMD) has been shown to be caused, in a small percentage of cases, by selected missense mutations in *fbln5* which result in defects in the elastic fibers of Bruch's membrane of the eye [129]. These mutant fibulin-5 molecules may not be effectively secreted and thus the reduced content of fibulin-5 may be a factor in this pathology [130]. The vision loss in AMD patients is due to choroidal neovascularization, which develops as choroidal blood vessels penetrate Bruch's membrane, leading to the accumulation of blood below the retinal pigment epithelium which adversely affects the retina [131, 132]. Fibulin-5 may not be a major factor in AMD but genetic mutations in the *fbln5* predisposes patients to the development of the disease [130].

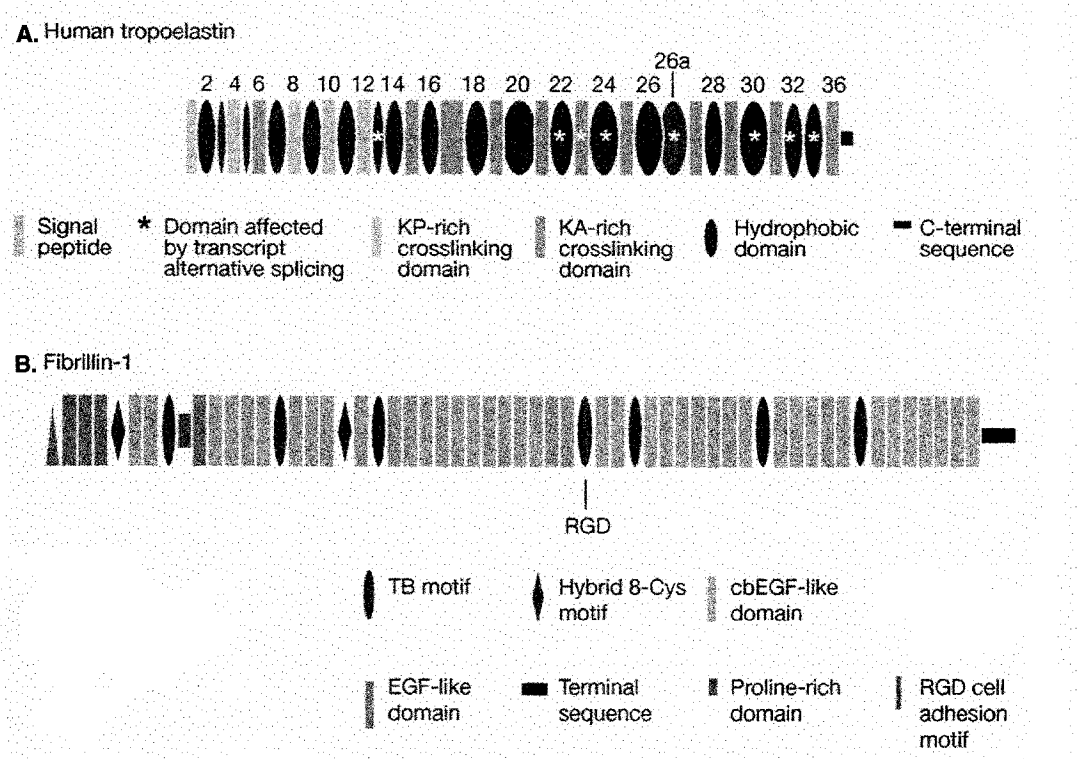

Figure 1: Domain Structure of Elastin and Fibrillin-1. A. Tropoelastin comprises alternating hydrophobic and crosslinking (KP- or KA-rich) domains. It undergoes complex alernative splicing in different elastic tissues. The unique C-terminal domain contains the only 2 cysteine residues. **B.** Fibrillin-1 is a large multidomain glycoprotein comprising 47 epidermal growth factor (EGF)-like domains, 43 of which are calcium binding (cbEGF-like domains). These domains are interspersed with seven TB (8-cysteine) motifs and two "hybrid" domains that have similarities to both EGF-like domains and TB motifs. There are 14 N-glycosylation sites, and a potentially flexible proline-rich region is present towards the N-terminus. At the N-terminus, there is a unique cysteine-containing motif (shown as a triangle). Adapted from Keilty, C. *Expert Reviews in Molecular Medicine.* **8**, 19 (2006).

Molecule	Elastic-fibre location
Fibrillin-1	Microfibrils
Fibrillin-2	Microfibrils
Fibrillin-3	Unknown – likely in microfibrils
MAGP-1	Microfibrils
MAGP-2	Some microfibrils
LTBP-1	Some microfibrils; also fibronectin
LTBP-2	Microfibrils, elastic fibres
LTBP-3	Fibrillar structures
LTBP-4	Fibrillar structures, fibrillin
Decorin	Microfibrils, microfibril–elastic-fibre interface
Biglycan	Elastic-fibre core
Versican	Some microfibrils
Heparan sulphate	Microfibrils, elastic-fibre core
Perlecan	Microfibrils
MFAP-1	Some microfibrils
MFAP-3	Some microfibrils
MFAP-4 (MAGP-36)	Some microfibrils
βIgH3	Elastic-fibre–collagen interface
Tropoelastin	Elastic-fibre core
LOX	Newly secreted tropoelastin, microfibril–elastin interface
LOXL	Microfibril–fibulin-5–elastin interface
Fibulin-1	Elastic-fibre core
Fibulin-2	Elastin–microfibril interface
Fibulin-4	Unknown – likely in elastic-fibre core
Fibulin-5	Elastic-fibre–cell interface
Emilin-1	Elastin–microfibril interface
Emilin-2	Elastin–microfibril interface
Elastin-binding protein	Newly secreted tropoelastin
Vitronectin	Some microfibrils in dermal tissues
Amyloid	Some microfibrils in dermal tissues
Collagen VIII	Vascular elastic fibres
Collagen XVI	Dermal microfibrils
Endostatin (C-terminus of collagen XVIII)	Vascular elastic fibres
Collagen VI	Some microfibrils

Abbreviations: βIGH3, also known as transforming growth factor-β-inducible gene-H3 and as keratoepithelin, on chromosome 5q31; LOX, lysyl oxidase; LOXL, lysyl oxidase-like; ITBP, latent-transforming-growth-factor-β-binding protein; MAGP, microfibril-associated glycoprotein; MFAP-1, microfibril-associated protein-1.

Figure 2: Structural and Associated Molecules of Microfibrils and Elastic Fibers. Many proteins have been identified to compose or interact with elastic fibers. They are either found in the elastic fiber core, with the microfibrils or at the elastin-microfibril interface. Since publication of this list, fibulin-5 has also been found to be located at the elastin-microfibril interface. This list is to demonstrate the rich and complex environment of the elastic fiber. Adapted from Kielty, C. *Expert Reviews in Molecular Medicine.* **8,** 19 (2006).

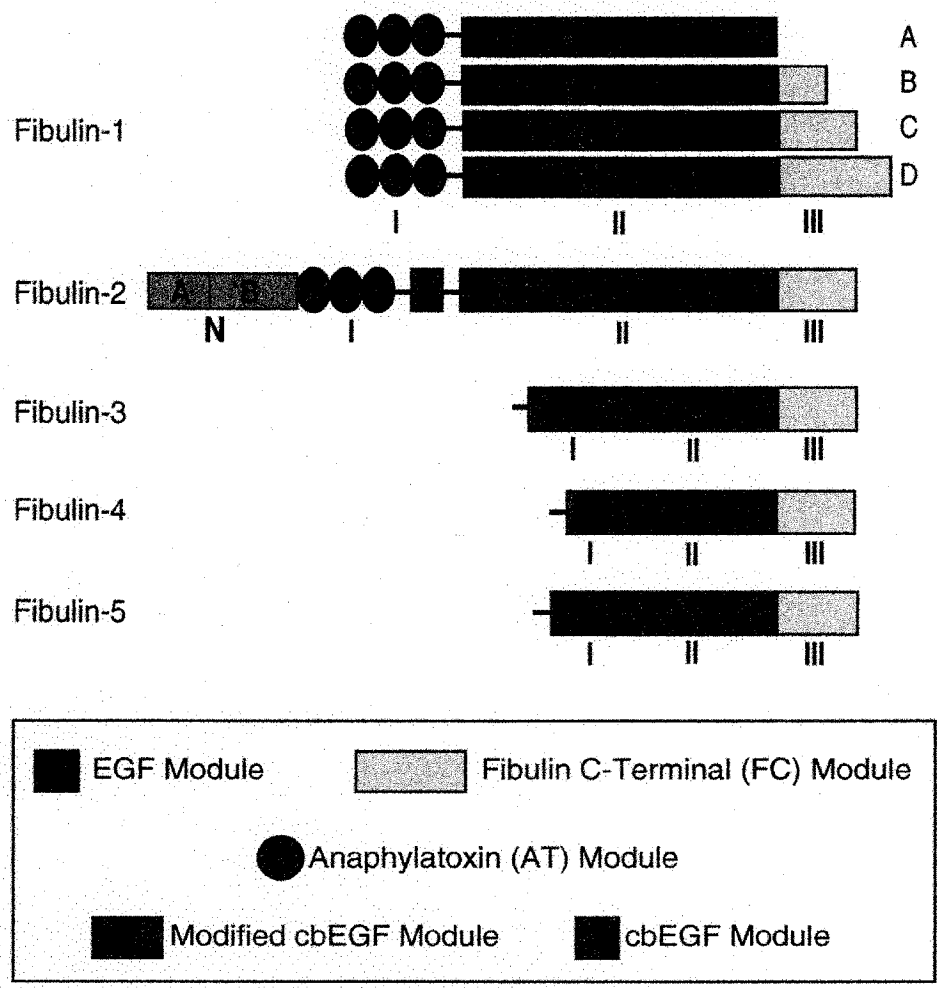

Figure 3: The Modular Domain Structure of Fibulins. The fibulin family members have 3 characteristic modules; domains I, II and III. Fibulin-1 has four splice variants (A-D) which differ at the C-terminal. Domain N, which is unique to fibulin-2, has a cysteine rich region (A) and a cysteine free region (B). Fibulins 3, 4 and 5 are very similar, all with an N-terminus modified cbEGF module, followed by 5 typical cbEGF modules and a C-terminal FC-module. Adapted from Timpl, R. *et al. Nat. Rev. Mol. Cell Biol.* **4,** 480 (2003).

INTRODUCTION

The extracellular matrix has proven to be a very important and complex part of the everyday functionings of an organism. Indeed, it provides structure and support, as well as protection, signal transduction and the ability to monitor, change and control the local environment. This study focuses on a specific and special component of the extracellular matrix: the elastic fiber. Elastic fibers in the extracellular matrix give the extracellular matrix the property of stretch and recoil and thus they are found predominantly in tissues and organs that require this ability to function such as the aorta, lung and skin.

The elastic fiber is composed mainly of elastin and microfibrils and other molecules called associated or interface proteins such as fibulin-5. This study has centered on these three players of the elastic fiber. Elastin is the insoluble core of the elastic fiber and is made up of cross-linked monomers of tropoelastin. Through a multistep process, tropoelastin is deposited on a scaffold of microfibrils made primarily of fibrillin-1. Fibulin-5 is able to bind both elastin and fibrillin-1 [54, 55, 85] and its role most likely involves orienting and helping in the assembly of the elastic fiber [133, 134]. Based on the fibulin-5 knockout mouse and its elastic fiber defects [54, 55] as well as findings from our own lab that show EM localization of fibulin-5 to the elastin-microfibril interface [135], this role has begun to be elucidated. Thus, it is clear that there is a functional relationship between elastin and fibulin-5.

The objective of the present study was to further investigate fibulin-5 and its relationship to elastin and elastic fibers. It is hypothesized that fibulin-5 requires elastin

to assemble in the matrix. To carry out this work, the appropriate reagents needed to be made and tested. This included a purified recombinant full-length fibulin-5 protein as well as a fibulin-5 antibody. With these reagents and well established models, it was then possible to evaluate the hypothesis with solid-phase binding assays, immunoprecipitation, cell culture and a tissue survey using of immunohistochemical analysis.

MATERIALS AND METHODS

Animals

Transgenic mice lacking the elastin gene (*eln*) were generated as previously described [102] and were generously provided for this study by Dr. Dean Li (Department of Oncological Sciences, University of Utah, Salt Lake City). For the experiments using *eln* mice, mouse embryonic fibroblasts (MEF) cells were harvested (see below) from *eln* +/+ and -/- littermates at the embryonic age of 12.5 days (E12.5).

Transgenic mice lacking the fibulin-5 gene (*fbln5*) were generated as previously described [55] and were kindly provided for this study by Dr. Hiromi Yanagisawa (University of Texas Southwestern Medical Center, Dallas). For the experiments using these mice, MEF cells were harvested from littermates at E12.5 (see below). For the remaining experiments, mice aged 2-3 months were used.

All mice were on a C57/BL6 background and were kept under pathogen-free conditions. All the studies using mice were carried out in accordance with McGill Animal Care Committee regulations and protocols.

Antibodies

For detection of fibulin-5 on Western blots, solid-phase binding assays and cell culture, and for staining of fibulin-5 on frozen tissue sections, an affinity-purified rabbit polyclonal anti-fibulin-5 antibody raised against full-length recombinant rat

fibulin-5 protein was used (see below). This antibody was specifically generated for this study.

For detection of fibrillin-1 on Western blots and solid-phase binding assays, and for fibrillin-1 staining on frozen tissue sections, an affinity-purified rabbit polyclonal anti-fibrillin-1 antibody, raised against a C-terminal fibrillin-1 construct known as rF6H, was used. For solid-phase binding assays, an affinity-purified rabbit polyclonal anti-fibrillin-1 antibody, raised against an N-terminal fibrillin-1 construct known as rF16, was also used. The fibrillin-1 antibodies were generously provided by Dr. Dieter Reinhardt (McGill University, Montreal).

For staining of elastin on frozen tissue sections and cell culture, a histidine-tagged bovine tropoelastin construct (exons 2-36) in pQE30 was expressed in M15 bacteria strain. The expressed protein was purified using Ni^{2+} affinity column (Probond, Invitrogen, Carlsbad CA) and used to produce a polyclonal antibody. This anti-tropoelastin (anti-TE) was generously provided by Dr. Robert Mecham (Washington University School of Medicine, St. Louis).

Protein Purification of Recombinant Fibulin-5

A vector containing a construct of full-length rat fibulin-5 cDNA was stably transfected into 293 cells (the construct was generously provided by Dr. Hiromi Yanagisawa). The cells were plated in 8 triple-layered flasks and the transfected cells were selected with 100 μg/ml Neomycin G418 (Invitrogen, Montreal, QC). Once the cells reached confluency, the cells were incubated in serum-free Dulbecco's Modification Eagle's Medium (SF-DMEM or SFM) (Wisent Inc, Saint-Jean-Baptiste

de Rouville, QC). A total of 4 L of SFM was collected every second day for 3 weeks and kept frozen. Verification of the expression and secretion of the recombinant full-length fibulin-5 protein in the SFM was done by Western blot analysis (see below). For protein purification, the SFM was thawed and treated with 0.1 M PMSF to prevent protein degradation. The SFM was filtered using a 5 μm membrane (Millipore, Bedford, MA) under vacuum and concentrated by ultrafiltration (10,000 MWCO) (Millipore) to ~ 50 ml using Amicon stirred ultrafiltration cells (series 8000 system, Millipore) at 4°C. The concentrate was centrifuged at 11,000 *g* and the supernatant was dialyzed using a Spectra/Por membrane (MWCO 12-14,000) (Spectrum, Rancho Dominguez, CA) against filtered 500 mM NaCl in 20 mM Hepes buffer [pH 7.2], twice overnight at 4°C. The dialyzed concentrate was passed through a 1 ml chelating HisTrap affinity column (Amersham Biosciences, Baie d'Urfé, QC) using an Äkta purification system (Amersham Biosciences). The bound protein was eluted with a linear gradient of 1 M imidazole, 500 mM NaCl, in 20 mM Hepes buffer [pH 7.2]. Samples of 30 μl from every third fraction were separated by sodium dodecyl sulfate-polyacrylamide gel electrophoresis (SDS-PAGE) followed by Coomassie Blue staining to determine the presence of recombinant full-length fibulin-5 protein. The fractions containing the recombinant protein were then pooled and dialyzed using a Spectro/Por membrane (MWCO 12-14,000) against 0.1 mM EDTA in Tris-Buffered Saline (TBS) [pH 7.4], twice overnight at 4°C. The dialyzed, pooled fractions were verified by SDS-PAGE, followed by Coomassie Blue staining. The protein concentration was determined by using a BCA assay kit (Pierce, Rockford, IL) and an

Ultrospec 2100 pro UV/visible spectrophotometer (Fisher, Mississaga, ON). Pooled fractions were aliquoted and stored in -80°C.

Western Blotting to Verify Protein Production

To verify that the protein present in the fractions was the purified recombinant protein, the following Western blot was performed. A 1 ml sample of the SFM, taken from the media collected every two days from confluent 293 cells stably transfected with full-length recombinant fibulin-5 cDNA, was analyzed for protein content. The sample was TCA precipitated (see below) and the pellet dissolved in 30 µl of 1 x sample buffer containing 0.3 µl of 1 M dithiothreitol (DTT). To increase the pH of the samples, 1 µl of 2 M Tris-HCL [pH 7.5] was added. Samples were then heated at 95°C for 3 min and the entire sample was loaded and separated by SDS-PAGE. After transfer to nitrocellulose using a 10 mM Borax buffer, non-specific binding sites were blocked with 5% dry milk in TBS for 1 hr at room temperature (RT). The membrane was then incubated with an anti-His (C-Term) monoclonal antibody (Invitrogen) diluted 1:250 in 5% dry milk in TBS, overnight at 4°C. The following day, the membrane was washed 3 x 5 min with 0.05% Tween-20 in TBS and incubated with a monoclonal HRP-conjugated secondary antibody (Invitrogen) diluted 1:3000 in TBS with 5% dry milk for 1 hr at RT. The membrane was washed 3 x 5 min with 0.05% Tween-20 in TBS and incubated with a chemiluminescent substrate (Pierce) for 5 min before exposure to film. This procedure was repeated with a previous fibulin-5 antibody (made by Dr. Yanagisawa) to confirm the identity of the protein in the fractions (data not shown). A Western blot was also performed to verify the

specificity of the new fibulin-5 antibody made in the lab, except pure and impure fractions from the original purification of fibulin-5, as well as protein derived from whole lung tissue, were used as a substrate.

Fibulin-5 Antibody Production

Purified full-length recombinant fibulin-5 protein was used as an antigen to produce a fibulin-5 antibody in two rabbits. The injections, bleeds and final exsanguinations of each rabbit was carried out by staff at McGill Animal Resources Center (ARC). Included in the bleeds was a pre-bleed consisting of 10 ml of blood taken from each rabbit prior to antigen injection. For the first injection, 250 μg of antigen was mixed with Freund's Complete Adjuvant provided by the ARC. The first bleed (10 ml from each rabbit) was collected after a three-week interval and frozen at -80°C. The remaining three injections were mixed with Freund's Incomplete Adjuvant and administered at three-week intervals. For the second, third and fourth injections, 100 μg of antigen was injected. At each three-week time interval, 10 ml of blood was collected and frozen. Three weeks following the fourth injection, exsanguination was carried out and approximately 100 ml of blood was collected and frozen from each rabbit. After collecting all of the bleeds, testing and characterizing of the antibody was conducted to verify and ascertain its function and quality.

Rapid IgG Purification of Antibody

Seventy-five μl of Protein A Sepharose 4B (Zymed, San Francisco, CA) was resuspended in 500 μl of Phosphate Buffered Saline (PBS), followed by centrifugation

at 2000 *g* for 5 min. The supernatant was discarded and the pellet was resuspended in 500 µl of PBS and centrifuged at 2000 *g*, two more times. The clean Protein A Sepharose pellet was then resuspended in 250 µl of anti-sera and rotated overnight at 4°C. The following day, the sepharose beads were washed 3 x with 500 µl of cold PBS and centrifuged at 2000 *g* for 5 min in between each wash. The supernatant was discarded and 75 µl of 0.1 M glycine [pH 3.0] was added. The supernatant was then rotated for 20 min at 4°C, followed by centrifugation at 2000 *g* for 5 min. Finally, the supernatant was transferred to a fresh eppendorf tube and 7.5 µl of 1 M Tris [pH 7.4] was added.

ELISA

Full-length recombinant fibulin-5 protein was plated, in duplicate, on a 96-well plate (Nalge Nunc International, Rochester, NY) at a concentration of 5 µg/ml in 50 µl TBS and left overnight at 4°C. The next day, the plate was washed 3 x with washing buffer (20 mM Tris-HCl [pH 7.4], 150 mM NaCl, 2 mM $CaCl_2$ and 0.05% Tween-20) and blocked for 1 hr with 75 µl of blocking buffer (20 mM Tris-HCl [pH 7.4], 150 mM NaCl, 2 mM $CaCl_2$ and 5% non-fat milk powder) at RT on a shaker. The anti-fibulin-5 antibody was serially diluted in a 1:3 ratio with binding buffer (20 mM Tris-HCl [pH 7.4], 150 mM NaCl, 2 mM $CaCl_2$ and 2% non-fat milk powder) starting at a concentration of 150 µg/ml (initial dilution was 1:50). The plate was incubated with 50 µl of antibody, following the dilution scheme, for 1.5 hr at RT with gentle shaking. After washing 3 x with washing buffer, the plate was then incubated with anti-rF16 or anti-rF6H antibodies for 1 hr at RT with gentle shaking. The plate was washed 3 x

with washing buffer before detecting the primary antibody with a rabbit polyclonal HRP-conjugated secondary antibody (Invitrogen). Finally, the plate was washed 4 x with washing buffer before detection. Colour development was performed with 1 mg/ml 5-aminosalicylic acid in 20 mM phosphate buffer [pH 6.8], including 0.045% (v/v) H_2O_2 (100 µl/well) for 3-5 min and stopped by adding 100 µl of 2 M NaOH to each well. In one case, fibulin-2 protein extracts and full-length recombinant fibulin-5 protein were plated at the same concentration (5 µg/ml in 50 µl TBS) in order to test for cross-reactivity. The fibulin-2 protein was provided by Dr. Dirk Hubmacher (McGill University, Montreal QC) and was extracted as described in Sasaki *et al.*, 1996 [136]. Colour yields were determined at 490 nm using a Microplate EL310 autoreader (Bio-Tek Instruments, Winooski, VT). All assays were repeated 3 to 5 times, resulting in similar binding profiles each time. Nonspecific binding of the antibody to either the blocking reagents or the plastic surface was subtracted from the binding profiles.

Cell Culture

All cultured cells were kept in a sterile environment and handled with sterilized solutions and equipment. Cells were grown at 37°C in 5% carbon dioxide in DMEM and 10% Fetal Bovine Serum (FBS) (Wisent).

The rat pulmonary artery smooth muscle cells (PAC-1) were grown to confluency and then incubated with SFM for 24 hr before collection. The SFM was collected, then centrifuged at 10,000 *g* for 10 min at 4°C to remove cell debris. Cell lysates were collected by washing the dish 3 x with PBS and incubating the cells with

1 ml of lysis buffer (25 mM Tris-HCL [pH 7.4], 5 mM ethylenediamine-tetraacetic acid (EDTA), 250 mM NaCl and 1% Triton X-100) containing protease inhibitors (Complete Protease Inhibitor Cocktail, Roche, Laval, QC) for 30 min. The cell lysates were centrifuged at 10,000 *g* for 10 min at 4°C to remove insoluble material.

To obtain MEF cells, embryos were surgically removed from the uterus at E12.5. The embryos were separated from the placenta and the heads removed and kept for genotyping. The livers were then removed from each torso and the torsos passed individually through 18 gauge needles. Cell homogenates from each torso were plated in separate wells of a 6-well plate in 10% FBS in DMEM. The media was changed the following day and any unattached tissue was carefully removed until the cell population became confluent and was ready to be trypsinized. Cell cultures were kept separate until genotyping.

Sample Preparation for Western Blot

i/ TCA Precipitation

To 1 ml SFM, that was collected from confluent PAC-1 or 293 cells, 390 µl of a solution containing 1% triton X-100 and 55% TCA was added and shaken. The samples were left on ice for 10 min, followed by centrifugation at 8000 *g* for 5 min at RT. The supernatant was discarded and the pellet was washed with 500 µl of ice-cold acetone and vortexed. After the sample was centrifuged at 8000 *g* for 5 min at RT, the supernatant was discarded and the pellet was left to air-dry for 1 hr. The pellet was then dissolved in sample buffer before being separated by SDS-PAGE.

ii/ Protein Isolation from Whole Organs

Lungs were dissected from of *fbln* +/+, *fbln* +/- and *fbln* -/- mice and frozen in liquid nitrogen. The organs were then ground under liquid nitrogen using a mortar and pestle. The nitrogen liquid served to keep the organ in a frozen, powder form once ground up. The powder was transferred to pre-weighed tubes and stored at -80°C. Lysis buffer containing protease inhibitors (Roche) was added at a 1:100, powder (mg) to lysis buffer (µl). The samples were further dissolved by sonification (Branson, Danbury, CT), and then centrifuged at 16,000 *g* for 10 min until the supernatant was clear. The supernatant was transferred to a fresh eppendorf tube and stored at -20°C and the pellet was discarded.

Solid-Phase Binding Assay

Full-length recombinant fibulin-5 protein (rF5) was plated, in duplicate, on a 96-well plate (Nalge Nunc International) at a concentration of 5 µg/ml in 50 µl TBS overnight at 4°C. The next day, the plate was washed 3 x with washing buffer (20 mM Tris-HCl [pH 7.4], 150 mM NaCl, 2 mM $CaCl_2$ and 0.05% Tween-20) and blocked for 1 hr with 75 µl of blocking buffer (20 mM Tris-HCl [pH 7.4], 150 mM NaCl, 2 mM $CaCl_2$ and 5% non-fat milk powder) at RT on a shaker. Two constructs of fibrillin-1, N-terminal (rF16) and C-terminal (rF6H), were used as soluble ligands (the constructs were generously provided by Dr. Dieter Reinhardt). Each ligand, starting at a concentration of 150 µg/ml, was serially diluted in a 1:3 ratio with binding buffer (20 mM Tris-HCl [pH 7.4], 150 mM NaCl, 2 mM $CaCl_2$ and 2% non-fat milk powder). The plate was incubated with 50 µl of ligand, following the dilution scheme, for 1.5 hr

at RT with gentle shaking. After washing 3 x with washing buffer, the plate was incubated with 100 µl of anti-rF16 or anti-rF6H antibodies (1:500 diluted in binding buffer), for 1 hr at RT with gentle shaking. The plate was washed 3 x with washing buffer before detecting the primary antibody with 100 µl of rabbit polyclonal HRP-conjugated secondary antibody (1:800 diluted in binding buffer) (Invitrogen) for 1.5 hr. Finally, the plate was washed 4 x with washing buffer before detection. Colour development was performed with 1 mg/ml 5-aminosalicylic acid in 20 mM phosphate buffer [pH 6.8], containing 0.045% (v/v) H_2O_2 (100 µl/well) for 3-5 min and stopped by adding 100 µl of 2 M NaOH to each well. For the assays involving tropoelastin protein, plates were coated with tropoelastin at a concentration of 5 µg/ml in 50 µl TBS, rF5 and the other recombinant fibulin-5 domain mutants were used as soluble ligands (starting concentration of 150 µg/ml). These assays were carried out as described above. The tropoelastin protein was provided by Dr. Robert Mecham (Washington University School of Medicine, St. Louis, MO) and generated as previously described [92]. Colour yields were determined at 490 nm using a Microplate EL310 autoreader (Bio-Tek Instruments). All solid-phase binding assays were repeated 3 to 5 times, resulting in similar binding profiles each time. Nonspecific binding of the soluble ligands to either the blocking reagents or the plastic surface was subtracted from the binding profiles.

Immunoprecipitation

PAC-1 cells were plated and grown until confluency, then incubated for 24 hr with SFM. The next day, the media and cell lysate were collected as described above.

i/ Media Samples

Media (500 µl) was pre-incubated with 40 µl of Sepharose A beads (Zymed) overnight at 4°C with gentle rotation. The next day, the sample was centrifuged at 2000 *g* for 2 min, after which the supernatant was collected and incubated with 10 µl of anti-fibulin-5 antibody. After 3 hr at RT, 40 µl of washed Sepharose A beads was added to the sample and incubated for 4 hr at 4°C with gentle rotation. After the incubation period, the supernatant was discarded and the beads were washed 3 x 5 min with 500 µl TBS and centrifuged at 2000 *g* between each wash. Once the final wash was completed and discarded, 65 µl of 1 x sample buffer containing 6.5 µl of 1 M DTT was added to the beads and heated at 95°C for 5 min. The same procedure was repeated with an additional 500 µl of media using10 µl of anti-TE antibody. A negative control consisted of replacement of the primary antibody with 2 µl normal rabbit serum (Invitrogen).

ii/ Cell Lysate Samples

Cell lysate (400 µl) was incubated with 10 µl of anti-fibulin-5 antibody overnight at 4°C. The next day, 40 µl of washed Pansorbin (Calbiochem, Mississaga, ON) was added to the sample and then incubated for 1 hr at 4°C with gentle rotation. After the incubation period, the supernatant was discarded and the Pansorbin was washed 2 x 5 min with 40 µl of lysis buffer and centrifuged at 2000 *g* between each wash. After a final wash with a non-detergent lysis buffer (lysis buffer without 1% TritonX-100), the Pansorbin was resuspended in 65 µl of 1 x sample buffer containing

6.5 µl of 1 M DTT and heated at 95°C for 5 min. This procedure was repeated with an additional 400 µl of cell lysate using 10 µl of anti-TE antibody. A negative control consisted of replacement of the primary antibody with 2 µl normal rabbit serum (Invitrogen).

iii/ Western Blot of Immunoprecipitated Protein

Immunoprecipitated media and cell lysate samples were separated by SDS-PAGE and transferred to nitrocellulose membrane. The membranes were then incubated with either anti-TE antibody at a 1:1000 dilution or anti-fibulin-5 antibody at a 1:1000 dilution. As a positive control for the blot incubated with anti-TE as primary antibody, 1 ml of SFM collected from the PAC-1 cells was TCA precipitated (as described above) and the resulting pellet was dissolved in 30 µl of 1 x sample buffer containing 0.3 µl of 1 M DTT. As a positive control for the blot incubated with anti-fibulin-5 as primary antibody, 10 µl from a fraction containing purified rF5 was added to 20 µl of 1 x sample buffer containing 0.3 µl of 1 M DTT. The positive controls were separated by SDS-PAGE along with the media and lysate samples on the appropriate gel.

Cell Culture Immunofluorescence

Wildtype and elastin null MEF cells were plated in a four-well chamber slide (Nalge Nunc International) at a concentration of 50,000 cells per 1 ml. After eight days, the media was removed and the cell layer was washed with PBS and fixed with a 70% MeOH /30% acetone solution for 5 min at RT. The cell layer was then washed

with PBS and blocked for 1 hr at RT with normal goat serum (Jackson Laboratories, West Grove, PA) diluted 1:20 in PBS. This was followed by 1 hr incubation at RT with primary antibody. The cell layer was washed 3 x 5 min with PBS and gentle shaking, before detecting the primary antibody with FITC-conjugated anti-rabbit IgG antibody (Cappel, Irvine, CA) for 1 hr at RT. Finally, the cell layer was washed 3 x 5 min with PBS and gentle shaking. Coverslips were mounted onto the slides with GelTol Aqueous Mounting Medium (Thermo, Pittsburgh, PA). Omission of primary antibody was used as a negative control. Images were taken with Zeiss AxioCam digital camera mounted on a Zeiss Axioskop fluorescence microscope (Carl Zeiss, North York, ON).

Histochemical Analysis – Paraffin Sections

To prepare tissue for paraffin embedding, organs were removed from wildtype mice and fixed overnight in 4% paraformaldehyde in PBS. The following day, the tissues were dehydrated in a graded series of ethanol solutions for 5 min each, starting with a 50% ethanol solution and finishing at 100% ethanol. The tissues were then infiltrated and embedded in paraffin wax. Sections (5μm) were cut, mounted on glass slides, de-paraffinized 3 x 5 min in CitriSolv (Fisher), and then washed in a 1:1 ratio of CitriSolv and ethanol for 5 min. The sections were then rehydrated in a series of graded ethanol solutions for 5 min each, starting with 100% ethanol and ending with 50% ethanol, and finally rinsed in tap water for 5 min. The sections were ready to be stained by one of the following methods.

i/ Hart's Staining

For elastic fiber staining, a modified Hart's stain was used [137]. After hydration, the sections were immersed in resorcin-fuchsin stock dissolved in 70% ethanol and HCl for at least 4 hr. The duration of time in the stain was dependent on the age of the solution; more time was required for newly made stain. Sections were then washed in distilled water for 10 min and counterstained with 0.2% metanil yellow for 2 min. Finally, the sections were rinsed in tap water for 1 min and dehydrated in 95% and 100% ethanol solutions for 1 min each. The dehydration process was continued further by immersing the slides in a 1:1 solution of CitriSolv (Fisher) and ethanol for 3 min and then in a solution of pure CitriSolv for 10 min. Coverslips were mounted over the sections with Permount (Fisher).

ii/ Hematoxylin and Eosin Staining

To stain for general morphology, hydrated sections were immersed in hematoxylin (Sigma, Oakville, ON) for 10 min. The sections were then washed in tap water for 5 min and differentiated by dipping in acid alcohol (1% HCl in 70% ethanol). The nuclei were made blue by dipping the sections in a water bath of 0.3% ammonia hydroxide. The sections were counterstained with eosin (Sigma) for 2 min, rinsed in tap water for 1 min and dehydrated in 95% and 100% ethanol solutions for 2 min each. The dehydration process was continued further by immersing the slides in a solution of CitriSolv (Fisher) for 5 min. Coverslips were mounted over the sections with Permount (Fisher).

Immunohistochemistry on Frozen Sections

Organs removed from wildtype mice were fixed overnight in 4% paraformaldehyde in PBS prior to being cyroprotected. To reduce freezing artifact, the tissues were infiltrated with 1:2, 1:1 and 2:1 ratios of 5% sucrose/PBS to 20% sucrose/PBS and then left in 20% sucrose/PBS overnight at 4°C with gentle rotation. The next day, the tissues were infiltrated in a mixture of two parts 20% sucrose/PBS to one part O.C.T. embedding medium (Canemco-Marivac, St. Laurent, QC) for 30 min at RT before freezing. The tissues were positioned in an embedding mold and frozen in fresh infiltration mixture consisting of 2:1 ratio of 20% sucrose/PBS:O.C.T. freezing medium. Following cutting, sections were washed in PBS and then fixed in 0.4% paraformaldehyde in PBS for 15 min at RT. Sections were then further fixed with cold acetone for 5 min, followed by another wash with PBS, and then blocked in 10% dry milk in PBS, overnight at 4°C. The next day, the sections were incubated with anti-fibulin-5 antibody for 1 hr at RT. The sections were washed 3 x 10 min with PBS and blocked with normal goat serum (Jackson Laboratories) diluted 1:20 in PBS for 30 min at RT. The primary antibody was then detected with FITC-conjugated anti-rabbit IgG antibody (Cappel) for 1 hr at RT. The sections were washed 3 x 10 min with PBS and mounted with GelTol Aqueous Mounting Medium (Thermo). For fibrillin-1 staining, slides were incubated with anti-rF6H. For elastin staining, slides were incubated with an affinity-purified rabbit polyclonal anti-TE antibody. Omission of primary antibody was used as a negative control. Images were taken with Zeiss AxioCam digital camera mounted on a Zeiss microscope (Carl Zeiss).

RESULTS

Recombinant Fibulin-5 Protein Production

To investigate the effects and interactions of fibulin-5 in various experimental models, it was necessary to produce fibulin-5 protein. The production of full-length fibulin-5 recombinant protein (rF5) was the first step in this study so that an important anti-fibulin-5 antibody could be generated. Recombinant fibulin-5 protein was also necessary in order to carry out experiments involving narrowing down of interaction sites between fibulin-5 and other elastic fiber proteins.

As described previously in the methods and materials, secreted rF5 was purified from SFM collected from 293 cells. SFM containing the fibulin-5 protein was loaded onto a chelating HisTrap affinity column and eluted with 1 M imidazole (Figure 4A). The blue line on the chromatogram represents the absorbance of protein and the yellow line corresponds to the increasing imidazole gradient. The imidazole will compete with the proteins and fibulin-5 for the binding sites on the column. The numbered red line represents the points of absorbance at which fractions were collected. Starting from the left of the chromatogram, unbound and loosely bound protein were the first to come off the column. As the imidazole gradient increases, the more tightly bound proteins were eluted. The rF5 has a high affinity for the column due to its His-tag group, leaving it to be eluted further away from the unwanted protein, at around fraction 20 (the asterix on Figure 4A).

To verify in which fraction the rF5 was found, fractions including the original sample, flow-through and rinse were collected and separated by SDS-PAGE and

stained with Coomassie blue (Figure 4B). The rF5 was found in fractions 16 through 24 in a clean and pure state. The fractions were pooled according to their purity and verified by SDS-PAGE after staining with Coomassie blue (Figure 5A). Fractions 16 and 17 were pooled, fractions 18 to 21 were pooled and fractions 22 and 23 were pooled. Clearly, the pooled fractions 22 and 23 and fraction 24 were the cleanest fractions and therefore the purest. Fraction 24 was kept separate as not to dilute its purity. The rF5 in the pooled fractions was confirmed by Western blot analysis using an anti-His-Tag antibody against the His-tag group on the protein (Figure 5B). This procedure was repeated with fibulin-5 antibody provided by Dr. Yanagisawa to confirm the identity of the protein contained in the fractions (data not shown).

The number of purifications and the amount and concentration of rF5 produced is detailed in Table 1. There were five batches of fractions from five separate purification runs. The fractions were labeled ID1, ID2 *etc*, according to which purification the fractions came from.

Constructs

Using the preceding method, it was possible to purify other recombinant fibulin-5 proteins from cells stably transfected with a number of different fibulin-5 constructs (generously provided by Dr. Hiromi Yanagisawa). The recombinant proteins purified are shown in Figure 6. In addition to the rF5 protein, the constructs include: (a) del 1 - a fibulin-5 construct with the first cbEGF module (also known as the modified cbEGF module located in domain I) deleted, (b) del 6-C - a fibulin-5 construct with the sixth cbEGF module (also known as the fifth cbEGF module located

in domain II) and fibulin-module deleted, (c) RGE - a fibulin-5 construct where the aspartamic acid (D) of the RGD motif is replaced with glutamic acid (E), and (d) del EB - a fibulin-5 construct with amino acids 342 to 399, found at the beginning of the fibulin module and predicted to contain the elastin-binding domain [97], deleted. All constructs including rF5 were tagged with V5 and His to facilitate identification and purification. The rF5 and all the recombinant fibulin-5 domain mutants were generated and characterized as previously described in Zheng *et al.*, 2007 [97].

Production of Fibulin-5 Antibody

Production of a polyclonal anti-fibulin-5 antibody was described previously in the materials and methods. In order to use the antibody for experimentation, it was necessary to characterize the antibody to verify binding and specificity.

A. Characterization of Fibulin-5 Antibody – ELISA Assay

To detect binding and cross-reactivity between a protein and an antibody, an ELISA assay can be performed. An ELISA assay is a modification of a solid-phase binding assay. It omits the protein ligand step and goes straight to primary antibody that has been serially diluted. After receiving each bleed (including the pre-bleed) from rabbits 4075 and 4076, the antibody was tested for binding with rF5 and for cross-reactivity with fibulin-2 protein (detergent, EDTA and urea extracts).

i/ ELISA Assay of the 3rd and Terminal Bleeds

To test the binding of the antibodies produced in the 3rd and final bleeds, an ELISA assay was performed. Antibodies from rabbits 4075 and 4076 reacted strongly

with the immobilized rF5 but the 4075 antibody exhibited a stronger reaction (Figure 7). A similar pattern was also seen when the 1st and 2nd bleeds were tested (results not shown). As expected, the terminal bleed from both rabbits, when tested with an ELISA assay, also showed a similar pattern (Figure 8). Pre-bleeds from rabbit 4075 and 4076 verified that the results seen with the bleeds following injection of the antigen into the rabbits were indeed due to the antigen and not from pre-existing non-specific immunoreactivity (Figure 8).

ii/ ELISA Assay to Test Cross-reactivity of Antibody

Cross-reactivity of the antibodies from both rabbits was tested by ELISA using immobilized ligands from a different fibulin protein. Detergent, EDTA and urea extracts of fibulin-2 protein were used to see if the antibodies would bind to fibulin-2 and therefore show that the anti-fibulin-5 antibody may cross-react with other similar proteins. The choice of fibulin-2 protein as a potential target for the antibody was because it is a member of the fibulin family and therefore has a similar domain structure as fibulin-5. Consequently, it can be assumed that if the anti-fibulin-5 does not recognize and bind to one of its family members, than it is less likely that this antibody will bind to distant or unrelated proteins. Figure 9 shows that there is no binding between the anti-fibulin-5 antibody from rabbit 4075 (Figure 9A) or rabbit 4076 (Figure 9B) with any of the extracts of fibulin-2 protein.

B. Characterization of Fibulin-5 Antibody – Western Blot Analysis

To test the quality of the antibody and its ability to be used in various experiments and assays, the antibody was analyzed by Western blot. Fibulin-5 from two different sources was used for the Western blots. One source came from fractions

collected from the original purifications of rF5 and the other from a lung extract from *fbln5* +/+, *fbln5* +/- and *fbln5* -/- mice.

i/ Western Blot Analysis Using Pure and Impure Fractions

Pure (fraction 22, Figure 4B) and impure fractions (fraction 14, Figure 4B) were separated by SDS-PAGE, transferred to nitrocellulose and incubated with anti-fibulin-5 antibody (Figure 10). The pure fraction contained only rF5, whereas the impure fraction contained a mixture of other proteins as well as rF5. The results clearly show a clean and distinct band at approximately 55 kDa for both the pure and impure fractions. Cross-reactivity of the antibody with the other proteins in the impure fraction was not seen. This indicated that the anti-fibulin-5 antibody only interacted with fibulin-5.

ii/ Western Blot Analysis Using Tissue Derived Whole Protein

To further test the specificity of the rF5 antibody, the antibody was used in a Western blot analysis with protein extracted from lungs of wildtype, heterozygous and knockout fibulin-5 mice (Figure 11). The Western blot showed a single band at approximately 55 kDa for wildtype lung and a less intense band for the heterozygous lung. No band was seen for the knockout lung. Cross-reactivity of the antibody with other proteins in the lung extract was not seen indicating that the anti-fibulin-5 antibody only interacted with fibulin-5 protein.

Immunoprecipitation

To confirm that an interaction between tropoelastin (TE) and fibulin-5 exists, co-immunoprecipitations of TE and fibulin-5 were performed.

Immunoprecipitation of TE

SFM and cell lysate were collected from confluent PAC-1 cells and incubated with anti-TE antibody overnight. Immunoprecipitated proteins were separated by SDS-PAGE, transferred to a nitrocellulose membrane and the membrane blotted with an anti-fibulin-5 antibody. As seen in Figure 12A, double bands were seen in the SFM and cell lysate lanes around the 54 kDa mark. The negative control (indicated as "- Control") in Figure 12A, was rabbit serum (IgG) that served to indicate any background staining or cross-reactivity. Nothing was observed in this lane on the membrane. The positive control was done to show that the anti-fibulin-5 antibody only recognized fibulin-5. A sample containing purified rF5 (indicated as rF5 in Figure 12A), showed a band below the 99 kDa mark. The molecular weight of fibulin-5 protein is approximately 55 kDa. To conclude, fibulin-5 protein was successfully "pulled-down" with TE protein.

Immunoprecipitation of Fibulin-5

The reverse of the preceding experiment was done with samples incubated with anti-fibulin-5 overnight and the membrane blotted with an anti-TE antibody. As seen in Figure 12B, intense bands appear in the SFM and cell lysate lanes above the 54 kDa mark. The negative control (indicated as "- Control") in Figure 12B, again served to indicate any background staining or cross-reactivity. Nothing was observed in this lane on the membrane. A sample of SFM collected from PAC-1 cells served as a positive control (indicated as "+ control" in Figure 12B) to show that the anti-TE antibody recognized tropoelastin. This showed a band at approximately the same molecular weight as the bands from the SFM and cell lysate samples, plus a higher

molecular weight band. The molecular weight of TE protein is approximately 70 kDa. To conclude, TE protein was successfully "pulled-down" with fibulin-5 protein.

Fibulin-5 Binding to Tropoelastin Protein

To further investigate the nature of the interaction between fibulin-5 and TE, a solid-phase binding assay was carried out. As seen in Figure 13, a strong binding affinity between TE and rF5 protein was seen. No binding was seen with the TBS blank control where no TE was present. This result confirmed that fibulin-5 has a strong binding affinity with TE.

TE interactions were also tested with different fibulin-5 constructs to narrow down the region of fibulin-5 that binds to TE (Figure 14). The strongest binding was seen between TE and rF5 (shown in light blue). To a lesser degree, binding was also seen with del 1 (red) and RGE (dark blue), with RGE having a slightly lower affinity than del 1. No binding was seen with del 6-C (yellow) or del EB (green). These results indicate that binding sites for TE on fibulin-5 are found in the regions deleted in the del 6-C and del EB constructs and that reduced binding is seen with the del 1 and RGE constructs.

MEF Cell Immunofluorescence

In the previous experiments, it was shown that fibulin-5 binds to and interacts with tropoelastin. Thus, to determine if the formation of a fibulin-5 matrix requires the deposition of elastin into the matrix, immunofluorescence was performed on *eln* knockout and wildtype MEF cells. A comparison between the *eln* knockout and

wildtype MEF cells at four days showed only a small amount of fibrillin-1 staining in both cultures and no elastin or fibulin-5 staining (data not shown). By eight days (Figure 15), an elastin matrix was clearly seen in wildtype MEF cultures and, as expected, no matrix staining was seen in the knockout MEF cultures. A similar degree of fibulin-5 and fibrillin-1 staining was seen in both wildtype and *eln* knockout MEF cultures. Fibrillin-1 staining verified the establishment of a microfibril network in both wildtype and knockout cell cultures. From these results, it was determined that the establishment of a fibulin-5 matrix does not require an elastin matrix to be formed.

Fibrillin-1 Binding to Fibulin-5 Protein

It was shown that fibulin-5 has a high binding affinity for TE but that fibulin-5 does not require the presence of elastin *in vitro* to form a matrix. Therefore, to test if fibulin-5 was binding to another elastic fiber protein, a solid-phase binding assay between fibulin-5 and fibrillin-1 was carried out. Two fibrillin-1 constructs were used: (a) rF6H - the C-terminal half of fibrillin-1, and (b) rF16 - the N-terminal half of fibrillin-1 (Figure 16). From Figure 17, the results showed there was a strong binding affinity between rF16 and rF5 but no interaction between rF6H and rF5. This indicated that the binding site for fibulin-5 on fibrillin-1 is located in the N-terminal half of fibrillin-1. This assay provides evidence that fibulin-5 can interact with another protein besides tropoelastin.

Organ Survey Using Immunofluorescence for Elastin, Fibulin-5 and Fibrillin-1

A survey of adult wildtype mouse tissues was done to determine the presence and location of fibulin-5 with respect to elastin and fibrillin-1. Hematoxylin and Eosin and Hart's staining were done on paraffin sections for each organ to show the general morphology and location of elastic fibers, respectively. Immunofluorescence localization of elastin, fibulin-5 and fibrillin-1 was done on frozen sections for each organ. The omission of primary antibody on one section for each organ served as a negative control.

Heart

Hematoxylin and Eosin staining of the heart showed an abundance of muscle tissue in the atrium (Figure 18A) and ventricle (Figure 18B). Hart's staining showed elastic fibers lining the interior wall of the atrium (Figure 18C) as well as in the coronary arteries (blood vessels that supply the cardiac muscle) found in the ventricle (Figure 18D). Immunolocalization confirmed the Hart's stain showing elastin in the intimal and adventitial layers of the coronary arteries as well as lining the interior of the atrium wall. A similar pattern of staining was also seen for fibulin-5 but the staining was much weaker when compared to the elastin staining. The staining seen for fibrillin-1 was the weakest staining. Fibrillin-1 only very faintly stained the intimal and adventitial layers of the coronary arteries and very faint staining could be seen at the apex of some of the trabeculae of the atrium wall. Figure 18E is the negative control.

Liver

Hematoxylin and Eosin staining of the liver showed liver lobules of hepatocytes aligned around a central vein. There were also hepatic portal triads in the corners of the lobules and larger blood vessels could be seen scattered across the organ (Figure 19A). Hart's staining showed that elastic fibers were present in the large blood vessels, including the blood vessels in the portal triads, as well as the central vein. Fibers could also be seen faintly under the capsule (Figure 19B). Immunostaining confirmed the Harts' staining. Elastin was present in all the blood vessels as distinct strands running parallel to the lumen. Elastin had a very strong localization under the capsule where the individual strands of elastin could clearly be seen in a meshwork lattice. There was also staining seen for fibulin-5 and fibrillin-1 in these regions but to a lesser degree when compared to the elastin staining. The orientation of the fibers in the central veins for both fibulin-5 and fibrillin-1 was not as clear as for elastin but they both seemed to be oriented parallel to the lumen of the vein. Fibulin-5 staining in the capsule, like the elastin staining, showed a meshwork but less intense. Fibrillin-1 in the capsule was weaker than fibulin-5 and showed single parallel strands following the outside of the liver. Figure 19C is the negative control.

Lung

Hematoxylin and Eosin staining of the lung showed large air spaces with many alveoli mixed with blood vessels and respiratory airway tracts (Figure 20A). Hart's staining showed that elastic fibers were present in the blood vessels and larger bronchioles, as expected. The fibers were barely noticeable under the pleura but were clearly present in the walls of the alveoli as single elastic fibers and also seen within

the alveolar tips (Figure 20B). By immunofluorescence, elastin was present around the lumen of the blood vessels, respiratory airway tracts and under the pleura. Fine strands of elastin staining were seen in the walls of the alveoli and alveolar tips. There was also strong staining seen for fibulin-5 with identical distribution. The staining seen for fibrillin-1 was the same as elastin and fibulin-5, in the blood vessels and airway tracts, but staining for fibrillin-1 in the alveoli and alveolar tips was sparser and weaker. Figure 20C is the negative control.

Colon

Hematoxylin and Eosin staining of the colon showed the mucosa lining the lumen of the colon followed by the layer of connective tissue of the submucosa, the layers of smooth muscle of the tunica muscularis and the serosa (Figure 21A). The mucosa is composed of an epithelium and supporting connective tissue, called lamina propria, which also contains the crypts of Leiberkühn. Hart's staining (Figure 21B) showed very little elastic fibers present, except in the wall of blood vessels, as well as a few random fibers in the connective tissue and epithelium (blue arrows). Surprisingly, there was very strong staining seen with all three antibodies. A "tree-shaped" pattern was observed in the connective tissue portion of the colon with the "trunk" starting in the submucosa and rising up to join the connective tissue in the lamina propria of the mucosa, forming the "branches". The "branches" in the lamina propria seemed to follow the supporting connective tissue found between the crypts of Leiberkühn. Figure 21C is the negative control.

Testis

Hematoxylin and Eosin staining of the testis showed the seminiferous tubules surrounded by a thick connective tissue capsule called the tunica albuginia. Each seminiferous tubule is supported by connective tissue called the tunica propria (also known as the limiting membrane) and the seminiferous tubules are separated by interstitial tissue which contains nerves and blood vessels (Figure 22A). Hart's staining showed very little elastic fibers present except for in the wall of blood vessels as well as a faint presence in the capsule (Figure 22B). Unexpectedly, there was very strong staining seen with all three antibodies, with elastin having the strongest signal. Elastin, fibulin-5 and fibrillin-1 were all present in the capsule and the tunica propria that surrounded the seminiferous tubules. There was also staining seen in small blood vessels found in the interstitial tissue between the seminiferous tubules (not shown for all three antibodies). Individual strands of elastin and fibulin-5 staining could be seen in the tunica propria of the seminiferous tubule in a meshwork lattice. It was also evident that there were more elastin and fibulin-5 fibers present in the capsule and tunica propria than there were fibrillin-1. The fibrillin-1 staining in the tunica propria was less distinct and the positive fibers were fewer in number and also seemed to be aligned parallel to the seminiferous tubules, the opposite of elastin and fibulin-5. Figure 22C is the negative control.

Spleen

Hematoxylin and Eosin staining of the spleen showed the demarcation between the red pulp (the red staining sections), which is rich in blood and the white pulp (the roundish bluish staining lobules), which are lymphoid nodules (Figure 23A). Hart's

staining showed that elastic fibers were strongly present in the capsule and in the trabeculae, which are extensions of the capsule into the parenchyma scattered across the organ. There was also elastic fibers present in the walls of the blood vessels of the spleen but they stained lighter than the elastic fibers of the capsule and the trabeculae (Figure 23B). By immunofluorescence, elastin stained strongly in the capsule and the trabeculae. There was also staining of short scattered fibers that seemed to be limited to the white pulp and that followed the circular pattern around the central arteriole of the white pulp. This same pattern was seen for fibulin-5 and fibrillin-1 although staining of the capsule and trabeculae were weaker when compared to the elastin staining. The fibrillin-1 fibers found in the white pulp around the central arteriole were shorter than the fibers stained with elastin but were similarly arranged. The fibulin-5 stained fibers found in the white pulp around the central arteriole were also shorter than the fibers stained for elastin and appeared more disorganized. Figure 23C is the negative control.

Kidney

Hematoxylin and Eosin staining of the kidney showed the outer cortex of the kidney staining a darker pink, whereas the medulla and renal sinus stained lighter. Renal corpuscles are found in the cortex, thick descending and ascending limbs of the loop of Henle are in the upper portion of the medulla, and thin limbs of the loop of Henle and collecting ducts are in the lower portion of the medulla. The ducts empty into the renal calyces that exits from the interior of the kidney (Figure 24A). Hart's staining only identified elastic fibers present in the blood vessels (Figure 24B). Using immunolabeling, strong staining could be seen in all of the layers of the blood vessels

for elastin and fibulin-5. There was much less staining seen with fibrillin-1 in blood vessels but staining of fibrillin-1 was clearly seen among the tubules in both the cortex (not shown) and medulla. Most interestingly was distinct staining in the interior of the renal corpuscle, around the capillary tufts, as well as staining of the outside of the renal corpuscle. This was not seen for either elastin or fibulin-5, with elastin and fibulin-5 staining only seen at the perimeter of the renal corpuscle. Figure 24C is the negative control.

Summary - Table 2

All blood vessels found in the seven organs had elastin, fibulin-5 and fibrillin-1 present in the intimal, adventitial and sometimes medial layers (depending on vessel size). The inner lining of the heart atrium demonstrated that there was elastin and fibulin-5 present but the presence of fibrillin-1 was questionable. All three proteins were present in the respiratory airways, including the alveolar tips and in the alveolar walls. Remarkably, the liver capsule had a considerable amount of elastin, fibulin-5 and fibrillin-1 present. The colon had a strong and interesting "tree" pattern in the lamina propria of the mucosa for elastin, fibulin-5 and fibrillin-1. All three proteins were strongly expressed in the tunica albuginea and tunica propria of the testis as well as the capsule and trabeculae of the spleen, in addition to short delicate strands seen in the white pulp. The kidney differed from the rest of the organs in that it was the only organ that showed one antibody staining in a location where the other antibodies did not. Fibrillin-1 was found to stain the perimeter and interior of the renal corpuscle and around tubules, whereas elastin and fibulin-5 were only found to be present around the

outside of the renal corpuscle, most likely associated with the afferent and efferent arterioles.

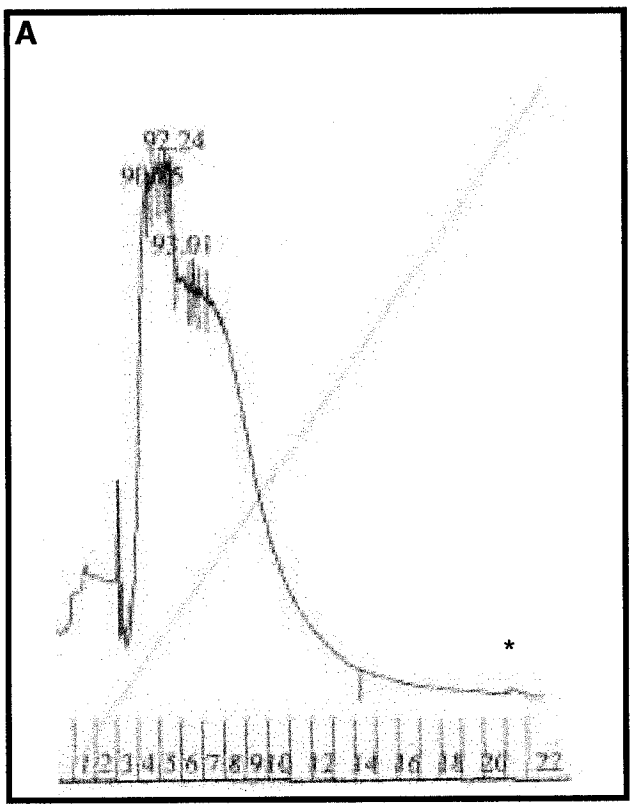

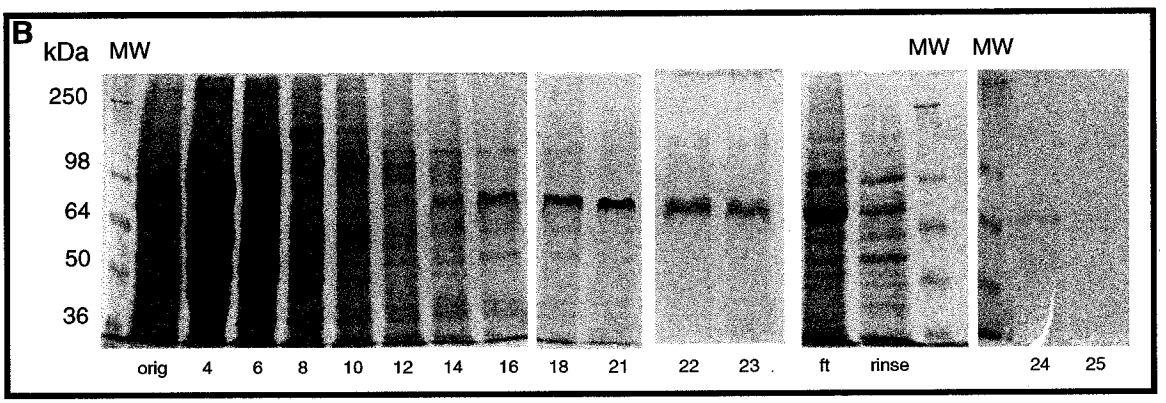

Figure 4: Purification of Full-length Recombinant Fibulin-5 Protein. **A.** Chromatogram of the purification of full-length recombinant fibulin-5 protein. The asterix indicates the absorbance peak corresponding to the full-length recombinant fibulin-5 protein. The yellow line corresponds to imidazole concentration gradient. **B.** To verify the purity of sample, SDS-PAGE of the fractions followed by Coomassie stain was done. The original sample (orig), the flow-through (ft) and the rinse were also tested.

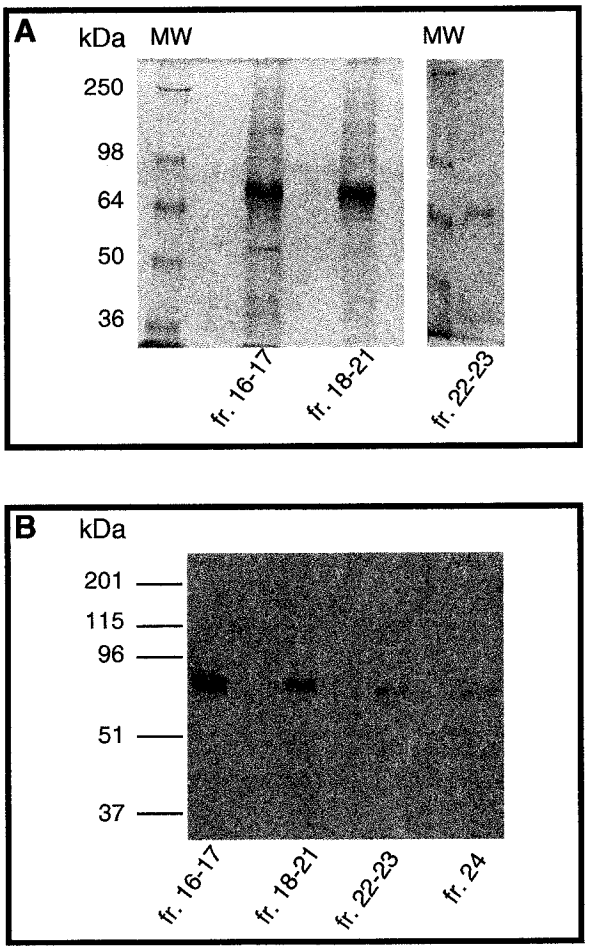

Figure 5: Purification of Full-length Fibulin-5 Recombinant Protein.
A. After dialyzation of the pooled fractions containing the full-length fibulin-5 recombinant protein, SDS-PAGE was done, followed by Coomassie staining to further verify purity of fractions. **B.** Western blot of the pooled fractions using an anti-His Tag antibody.

ID	mg/ml	Date	Volume (ml)	# of Vials	Fibulin-5 Construct	Comment
1	0.134	5/5/05	~8	4	Full-length (FL)	Used for Ab
1	0.7	5/5/05		1	FL	
2	0.153	5/5/05	0.5	1	FL	Used for Ab
3	0.408	4/7/05	0.5	1	FL	
3		11/7/05	0.5	1	FL	Frac. 17; very pure
4	0.5	13/7/05	~0.688	2	FL	
4	0.038	22/7/05	0.8	2	FL	frac.17
4	0.4	13/7/05	~1	2	FL	
5	0.262	10/10/05	~4	8	FL	frac. 18-21
5	0.273	10/10/05	~1.8	4	FL	frac. 16-17; semi-pure

Table 1: Full-length Fibulin-5 Recombinant Protein. Chart details the type of construct (full-length), the amount (ml) of protein, the concentration (mg/ml), the date the protein was frozen, which purification the protein comes from and the number of vials there is of the protein.

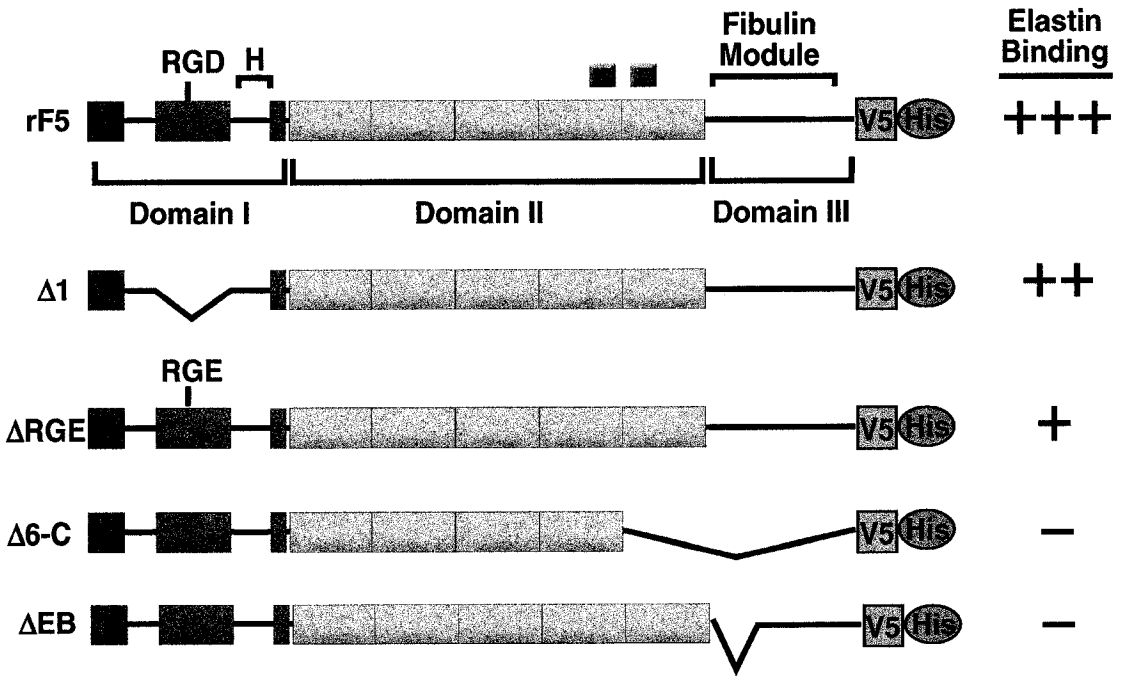

Figure 6: Recombinant Fibulin-5 Constructs. Schematic diagram of full-lenght recombinant fibulin-5 (rF5) and four other constructs used. Domain I contains the signal peptide (purple box), a modified cbEGF module which includes the RGD motif (blue boxes)and the specialized hinge (H) region. The light blue boxes in domain II are cbEGF modules and the red boxes represent glycosylation sites. Domain III is a conserved fibulin module. The Δ1 construct has the first modified cbEGF module deleted. The ΔRGE construct has the amino acid D changed to amino acid E. The Δ6-C construct has the fibulin module and the sixth cbEGF of domain II deleted. The ΔEB construct has deleted amino acids 342 to 399 from the fibulin module, deleted. All constructs were tagged with V5 and His to facilitate identification and purification. Adapted from Zheng, Q. *et al. Mol. Cell. Biol.* **3**, 27 (2007).

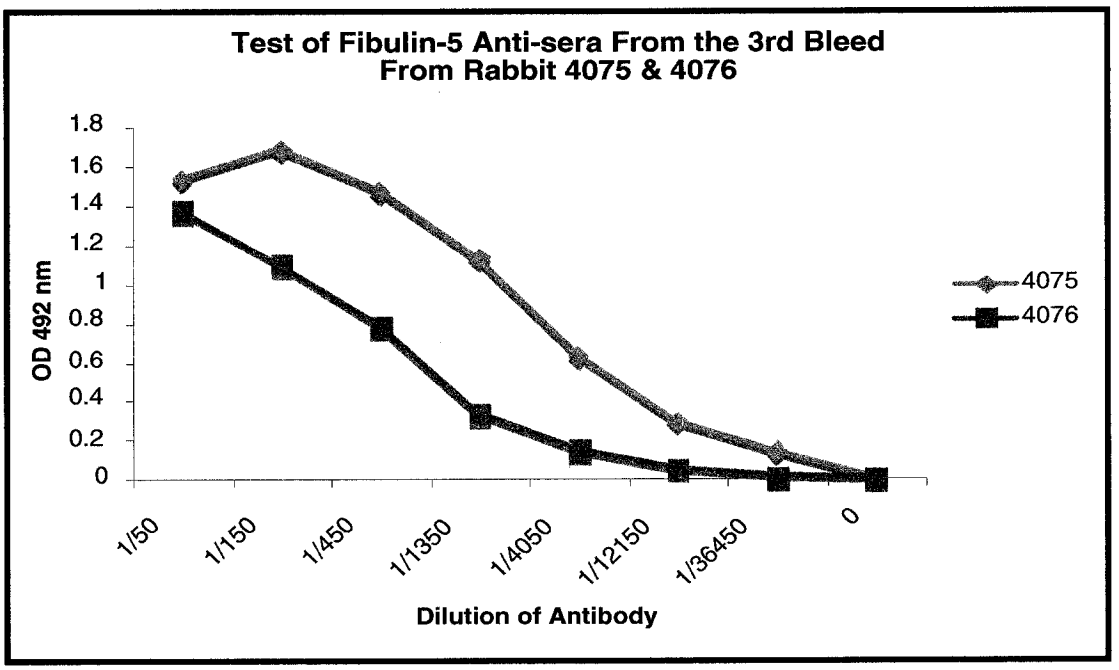

Figure 7: Test of Fibulin-5 Anti-sera From the 3rd Bleed From Rabbit 4075 & 4076. ELISA comparing the binding affinity of fibulin-5 anti-sera 4075 and 4076 to immobilized fibulin-5 protein.

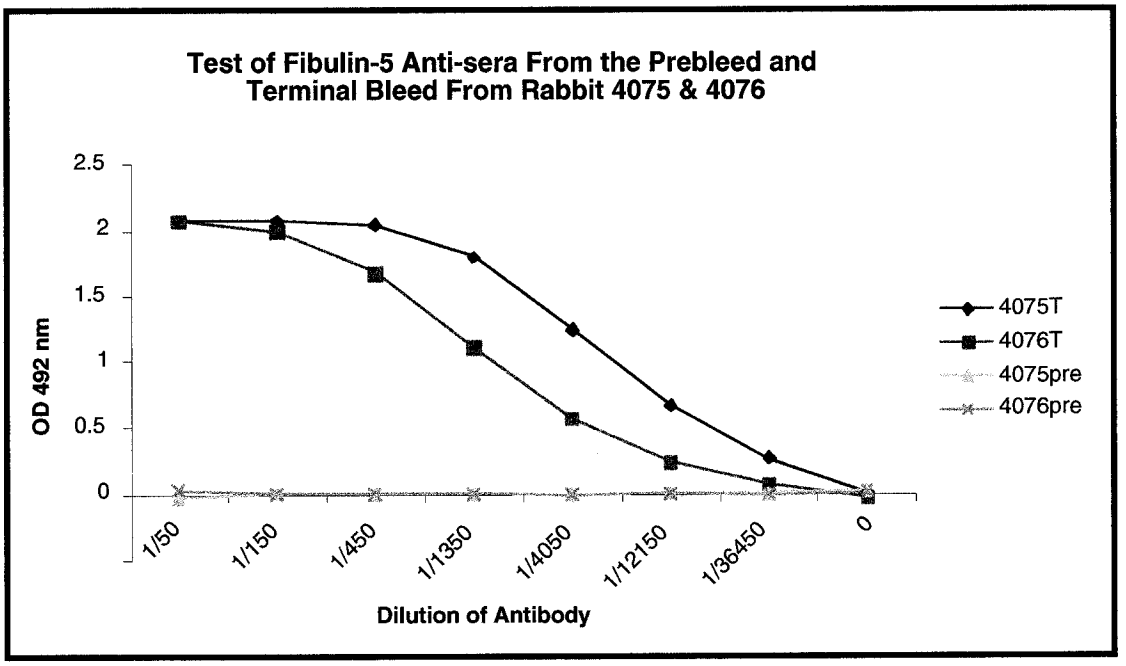

Figure 8: Test of Fibulin-5 Anti-sera From the Prebleed and Terminal Bleed From Rabbit 4075 & 4076. Elisa testing, comparing the binding affinity of fibulin-5 anti-sera from the terminal bleed (T) and prebleed (pre) from both 4075 and 4076.

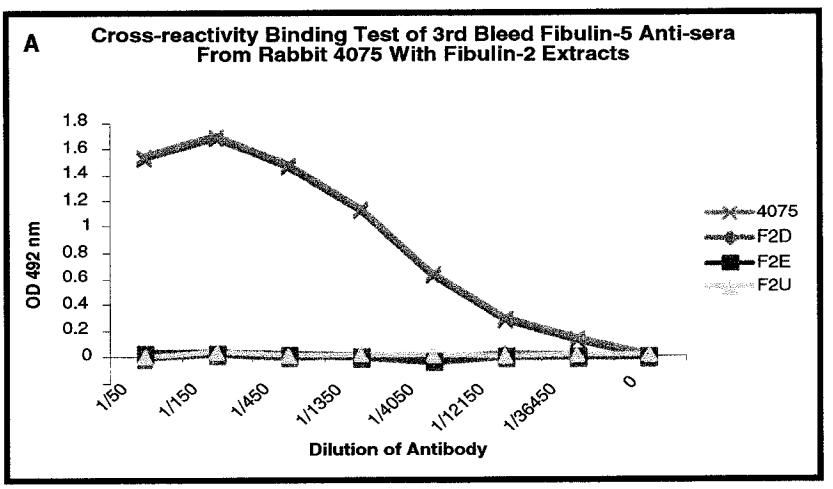

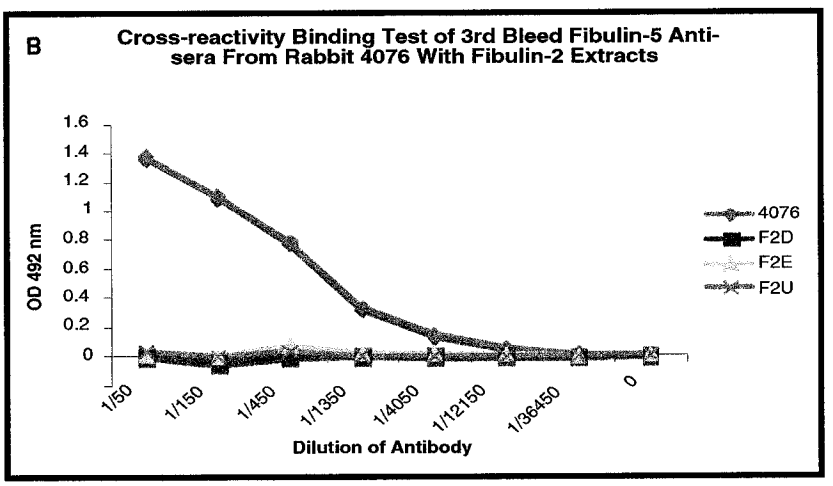

Figure 9: Cross-reactivity Binding Tests of 3rd Bleed Fibulin-5 Anti-sera From Rabbits 4075 & 4076 With Fibulin-2 Extracts.
A. Elisa testing for cross-reactive binding between immobilized fibulin-2 protein from a detergent extract (F2D), EDTA extract (F2E) and urea extract (F2U) with fibulin-5 anti-sera (4075). Graph also shows binding between immobilized fibulin-5 protein and fibulin-5 anti-sera (green-4075). **B.** Elisa testing for cross-reactive binding between immobilized fibulin-2 protein from a detergent extract (F2D), EDTA extract (F2E) and urea extract (F2U) with fibulin-5 anti-sera (4076). Graph also shows binding between immobilized fibulin-5 protein and fibulin-5 anti-sera (blue-4076).

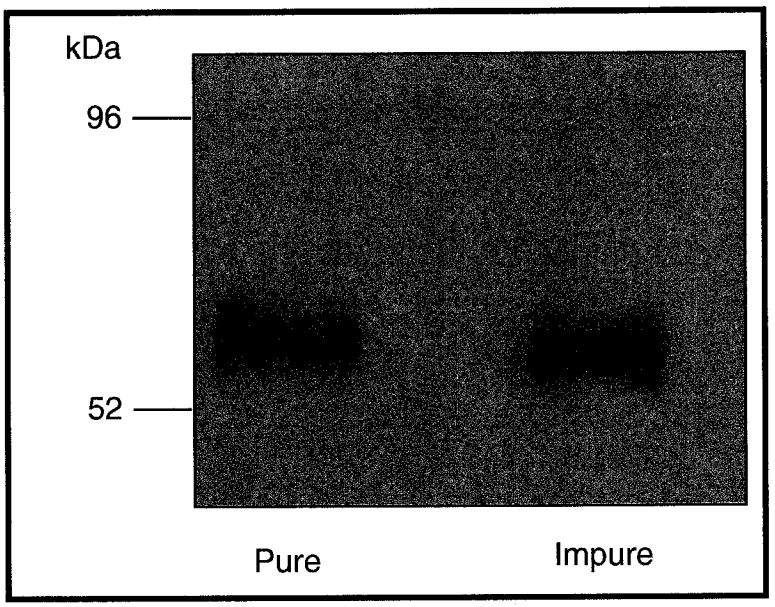

Figure 10: Western Blot Analysis to Test Anti-fibulin-5 Antibody Against a Pure and Impure Fibulin-5 Sample. Both pure and impure fractions from the original purification of fibulin-5, showed clear bands at approximately 55 kDa after incubation with the anti-fibulin-5 antibody.

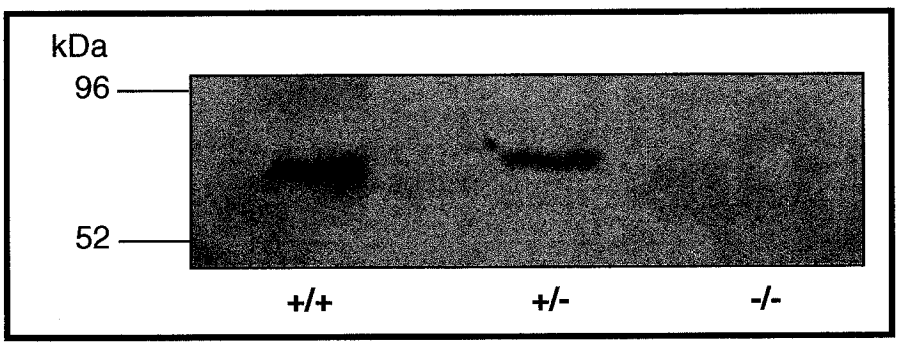

Figure 11: Western Blot Analysis of Anti-fibulin-5 Antibody on Lung Tissue From Fibulin-5 Wildtype (+/+), Heterozygous (+/-) and Knockout (-/-) mice. Antibody used was an IgG cut of anti-fibulin-5 from the 2nd bleed of rabbit 4075. The antibody clearly detected only fibulin-5 in +/+ lung tissue at approximately 55 kDa, with less reactivity in the +/- lung and no reactivity in the -/- lung.

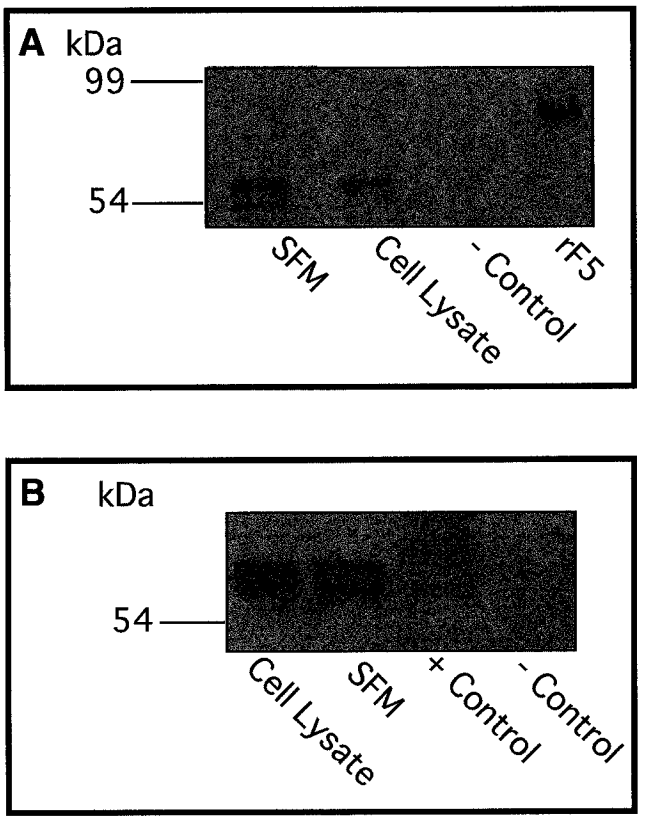

Figure 12: Immunoprecipitation of Fibulin-5 and Tropoelastin. A. Tropoelastin was immunoprecipitated from SFM and cell lysate collected from PAC-1 cells and then Western blotted for fibulin-5. The blot shows that fibulin-5 was "pulled-down" with tropoelastin due to an interaction. The appearance of double bands was consistent with repeats of this experiment. A positive control was done using purified full-length recombinant fibulin-5 (rF5) protein to verify the recognition of fibulin-5 by anti-fibulin-5 antibody. A negative control was done using rabbit serum (IgG), to verify no crossreactivity. **B.** Fibulin-5 was immunoprecipitated from SFM and cell lysate collected from PAC-1 cells and then Western blotted for tropoelastin. The blot shows that tropoelastin was "pulled-down" with fibulin-5 due to an interaction. A positive control was done using media (+ control) collected from PAC-1 cells to verify the recognition of tropoelastin by anti-tropoelastin antibody. A negative control was done using rabbit serum (IgG), to verify no crossreactivity. The molecular weight of fibulin-5 is 55 kDa and the molecular weight of tropoelastin is approximately 70 kDa.

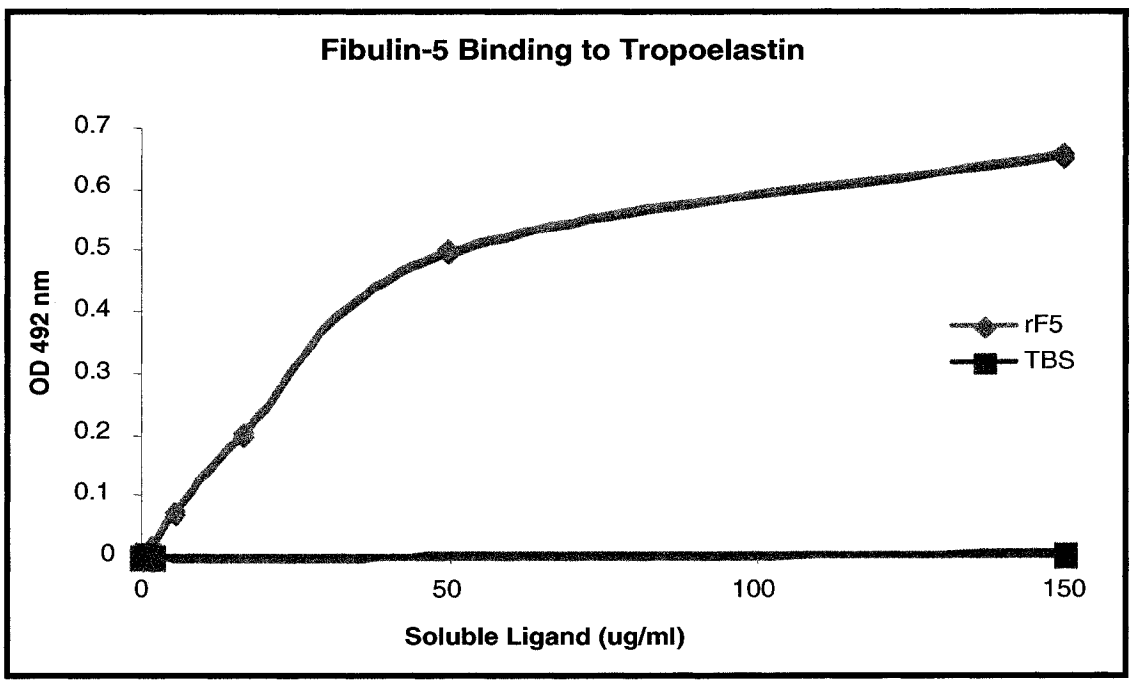

Figure 13: Solid-phase Binding Assay of Fibulin-5 With Tropoelastin. This graph shows the binding affinity between tropoelastin (TE) and full-length recombinant fibulin-5 (rF5). TE was used as the immobilised ligand and rF5 was the soluble ligand. Strong binding affinity between TE and rF5 was seen. There was no binding seen with the TBS blank control, which served to check for non-specific binding of rF5 to the plate.

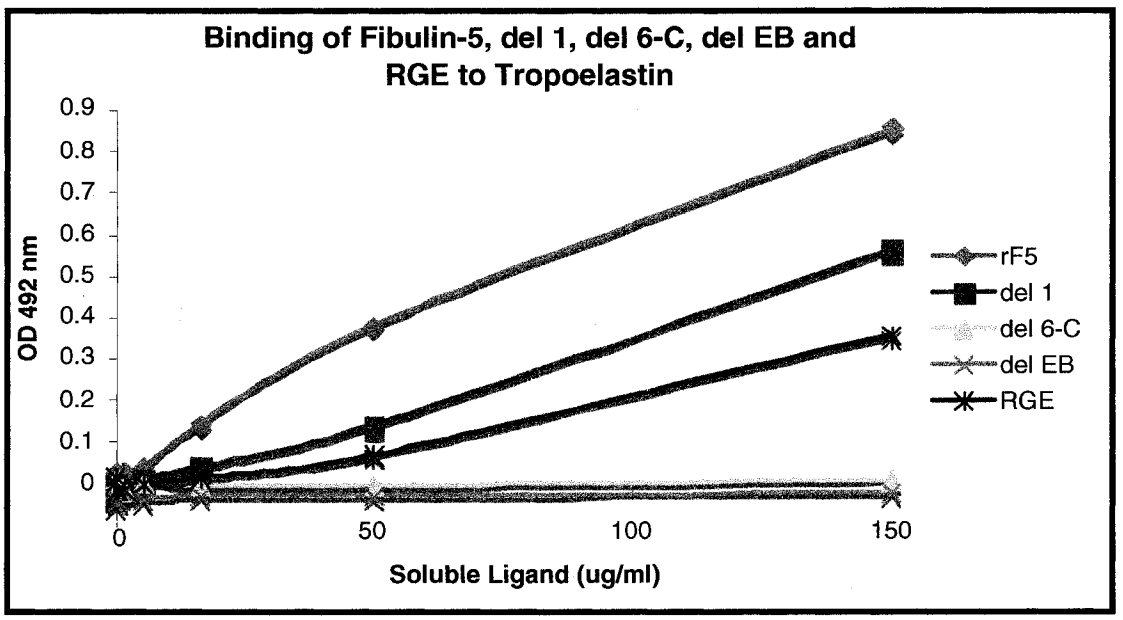

Figure 14: Solid-phase Binding Assay of Different Fibulin-5 Constructs With Tropoelastin. This graph shows the binding affinity between tropoelastin (TE) and different fibulin-5 constructs. TE was used as the immobilized ligand and full-length fibulin-5 recombinant (rF5) and the other constructs were used as soluble ligands. Strong binding affinity between TE and rF5 was seen. Weaker binding was seen between TE and the del 1 construct and between TE and the RGE construct. There was no binding seen between TE and the del EB or del 6-C constructs.

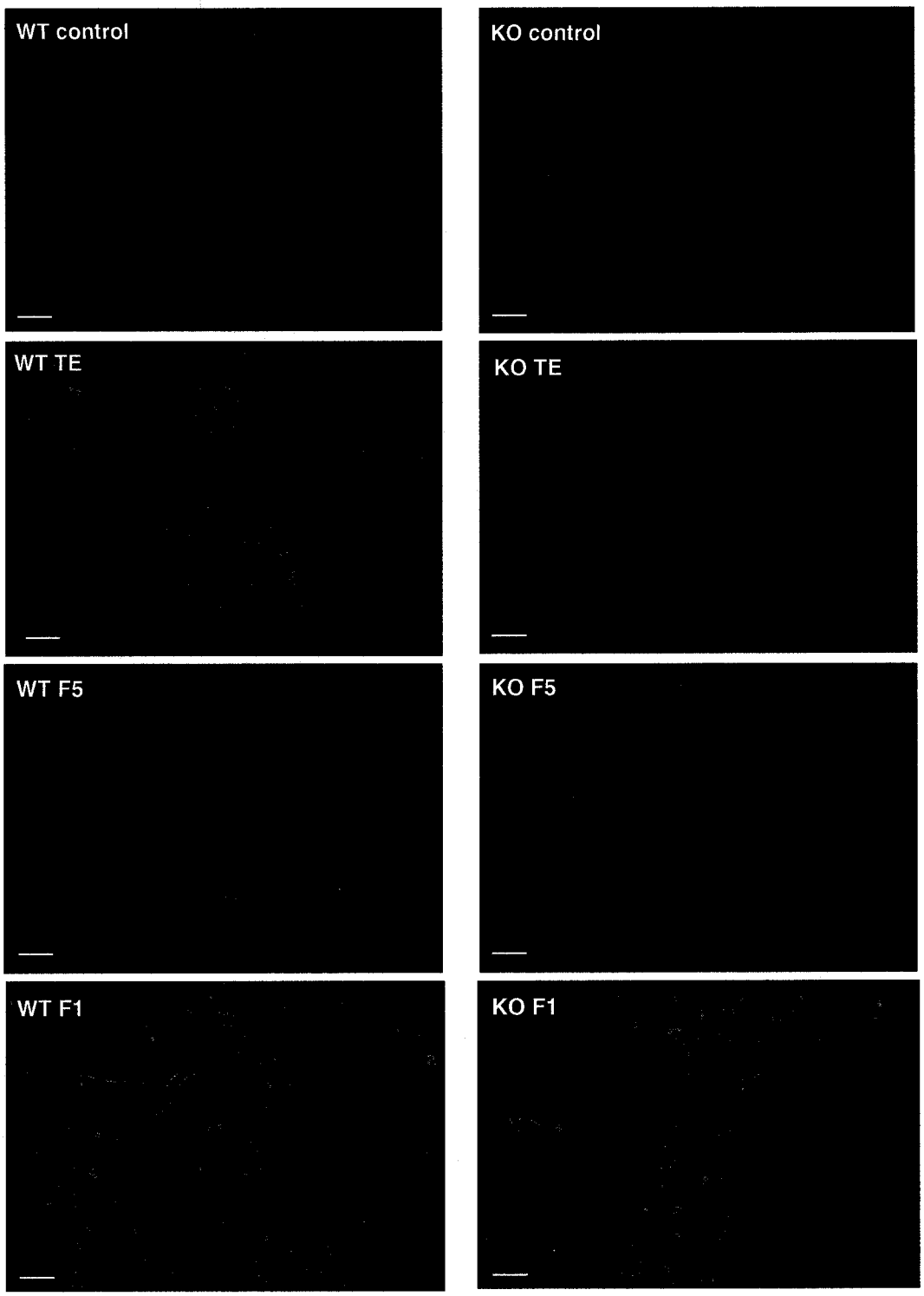

Figure 15: Immunofluorescence of Wildtype and Elastin-null MEF Cells After 8 Days in Culture. Wildtype (WT) and elastin-null (KO) MEF cells were stained for tropoelastin (TE), fibulin-5 (F5) and fibrillin-1(F1). Omission of primary antibody served as a negative control. Bar = 50 μm.

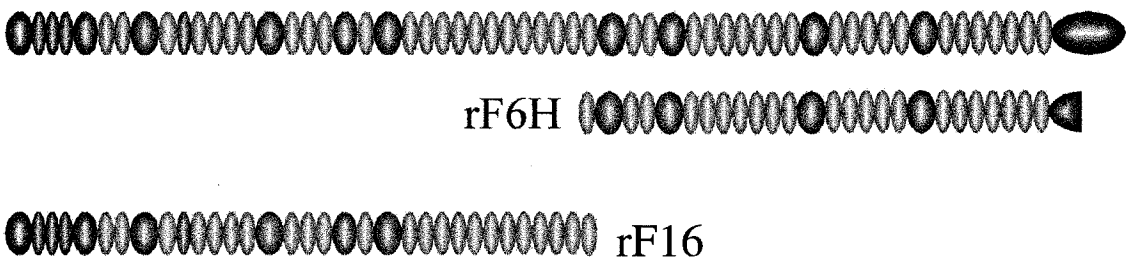

Figure 16: Recombinant Fibrillin-1 Constructs. The rF6H construct represents the C-terminal half of fibrillin-1 and rF16 construct is the N-terminal half. Full-length fibrillin-1 protein is shown for reference. Provided by and adapted from Dr. D. Reinhardt, McGill University, Montreal, QC.

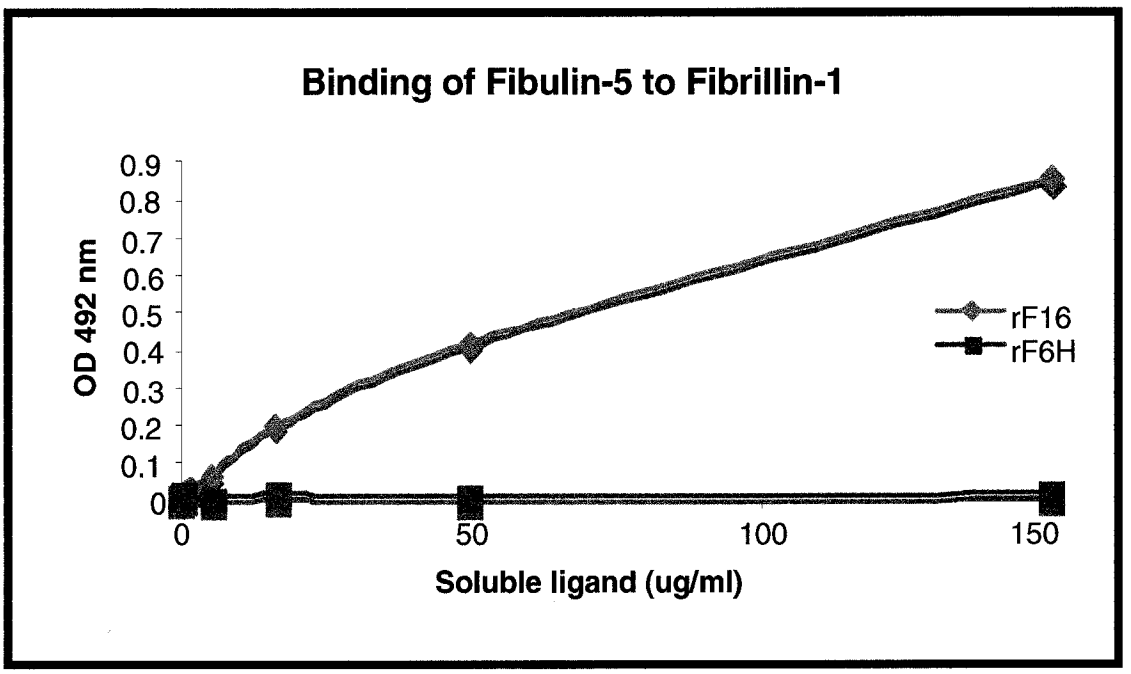

Figure 17: Binding of Fibulin-5 to Fibrillin-1. Solid-phase binding assay demonstrating the binding between full-length recombinant fibulin-5 (immobile ligand) and fibrillin-1 constructs (soluble ligands). Two constructs of fibrillin-1 (rF16 and rF6H) were used for this assay. Results show that fibulin-5 only binds the rF16 N-terminal construct.

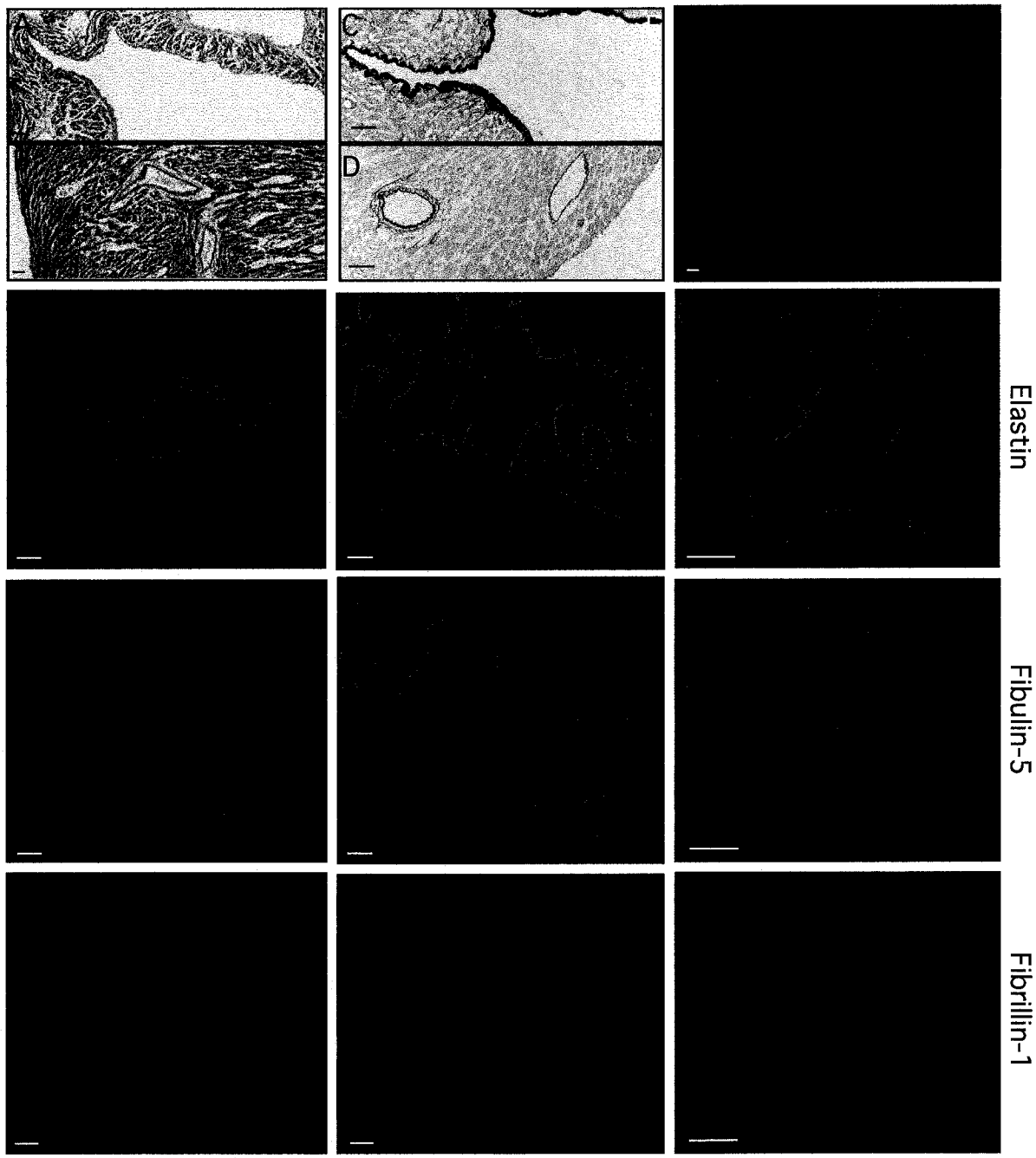

Figure 18: Immunohistochemical Analysis of Heart. Immunofluorescence microscope images of frozen sections of heart stained for tropoelastin, fibulin-5 and fibrillin-1. Omission of the primary antibodies serves as a negative control (**E**). Light microscope images of paraffin sections of heart were stained with Hematoxylin and Eosin for morphological purposes (**A**-atrium and **B**-ventricle) as well as a Hart's stain to show the presence of elastic fibers in the organ (**C**-atrium and **D**-ventricle). Bars = 50 μm.

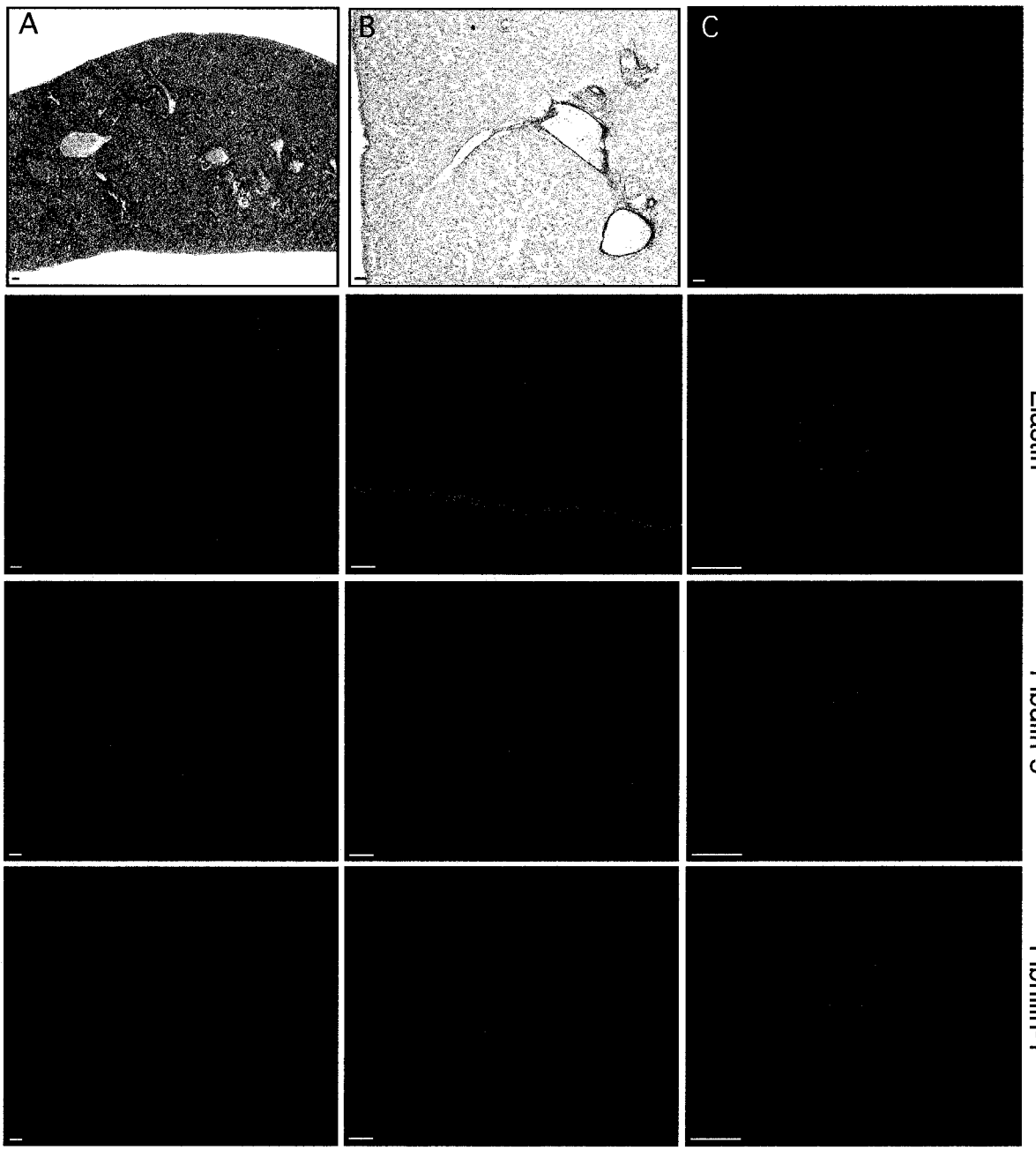

Figure 19: Immunohistochemical Analysis of Liver. Immunofluorescence microscope images of frozen sections of liver stained for tropoelastin, fibulin-5 and fibrillin-1. Omission of the primary antibodies serves as a negative control (**C**). Light microscope images of paraffin sections of liver were stained with Hematoxylin and Eosin for morphological purposes (**A**) as well as a Hart's stain to show the presence of elastic fibers in the organ (**B**). Bars = 50 μm.

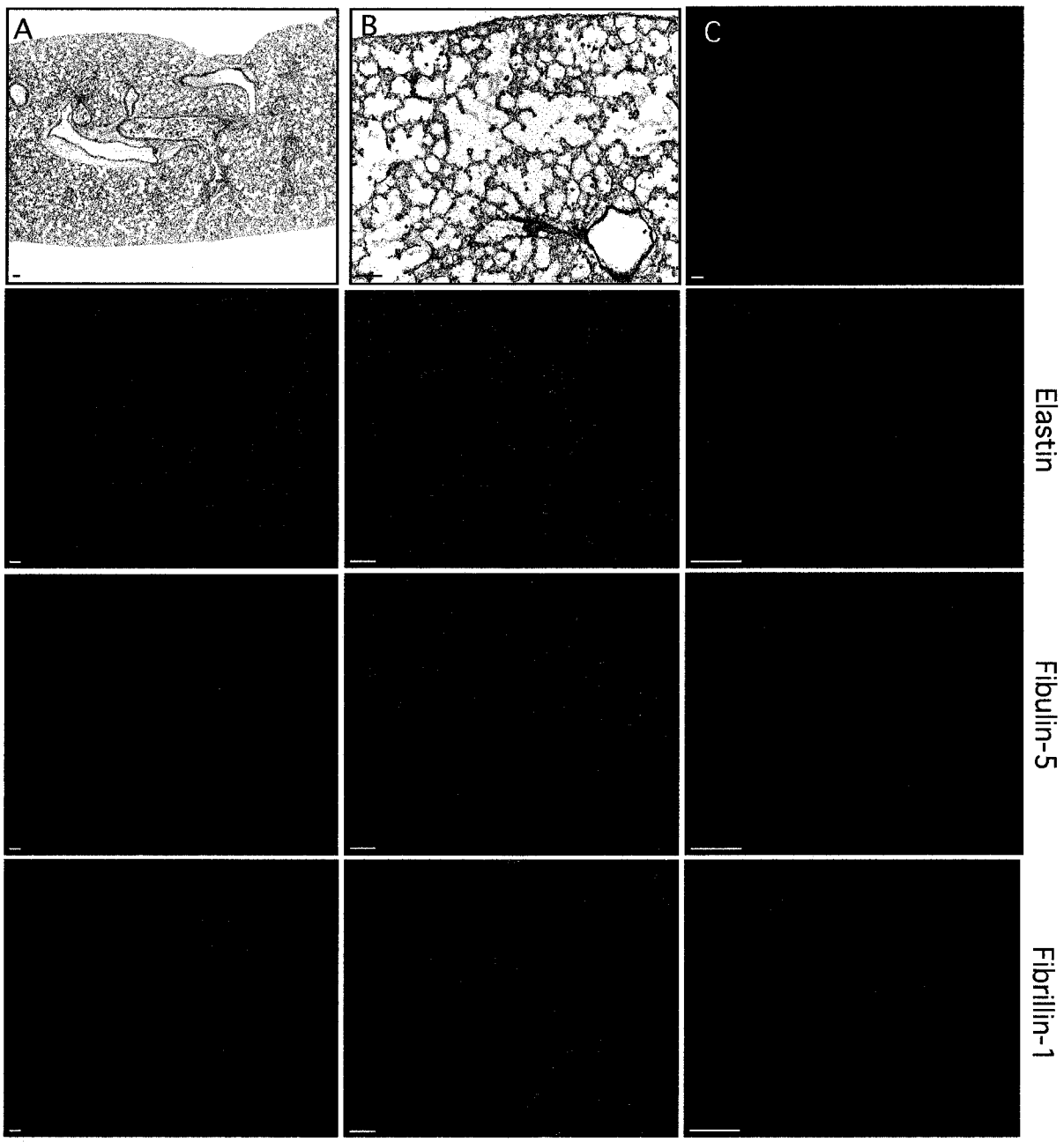

Figure 20: Immunohistochemical Analysis of Lung. Immunofluorescence microscope images of frozen sections of lung stained for tropoelastin, fibulin-5 and fibrillin-1. Omission of the primary antibodies serves as a negative control (**C**). Light microscope images of paraffin sections of lung were stained with Hematoxylin and Eosin for morphological purposes (**A**) as well as a Hart's stain to show the presence of elastic fibers in the organ (**B**). Bars = 50 μm.

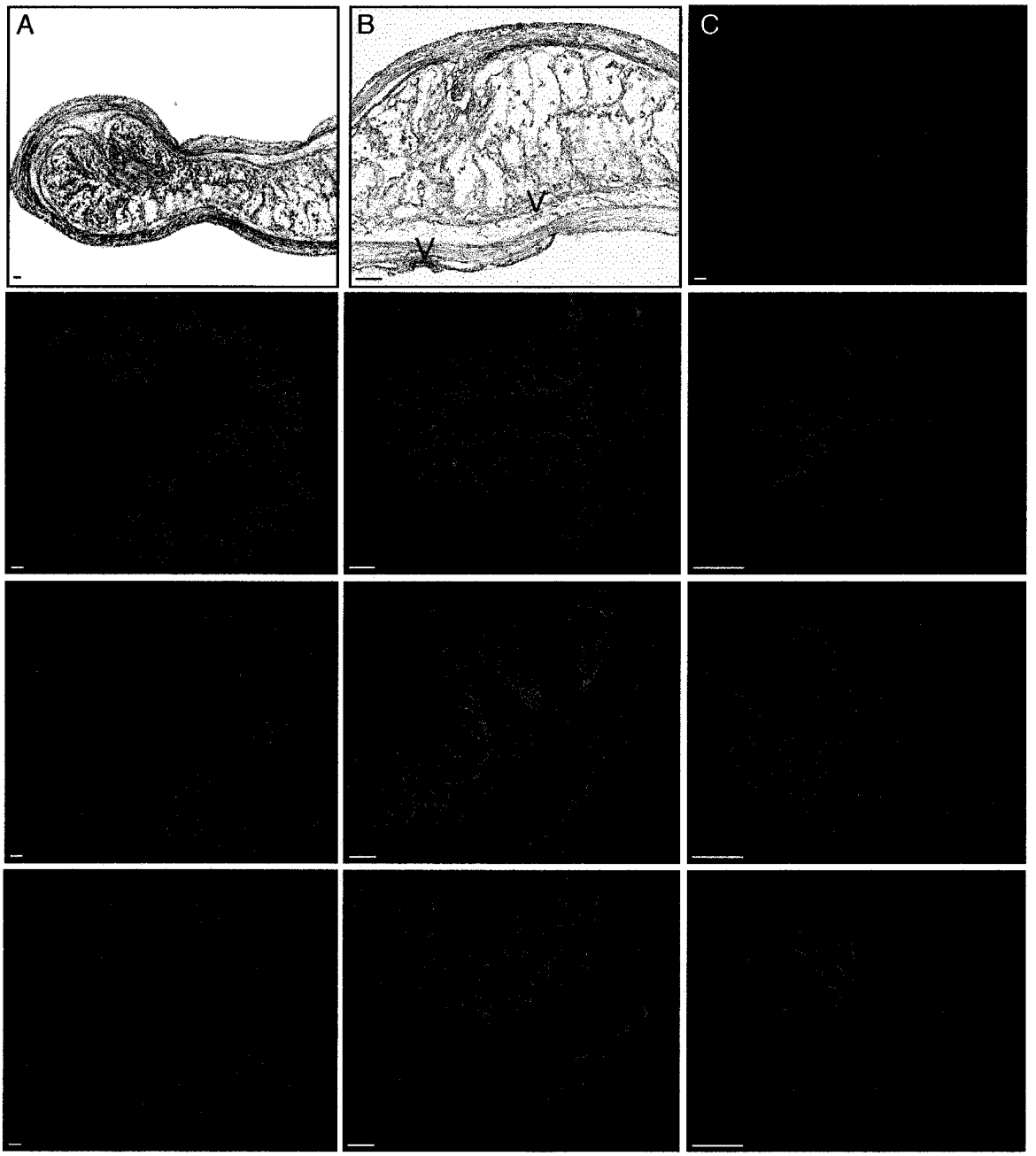

Figure 21: Immunohistochemical Analysis of Colon. Immunofluorescence microscope images of frozen sections of colon stained for tropoelastin, fibulin-5 and fibrillin-1. Omission of the primary antibodies serves as a negative control (**C**). Light microscope images of paraffin sections of colon were stained with Hematoxylin and Eosin for morphological purposes (**A**) as well as a Hart's stain to show the presence of the few elastic fibers (red arrows) in the organ (**B**). Bars = 50 μm.

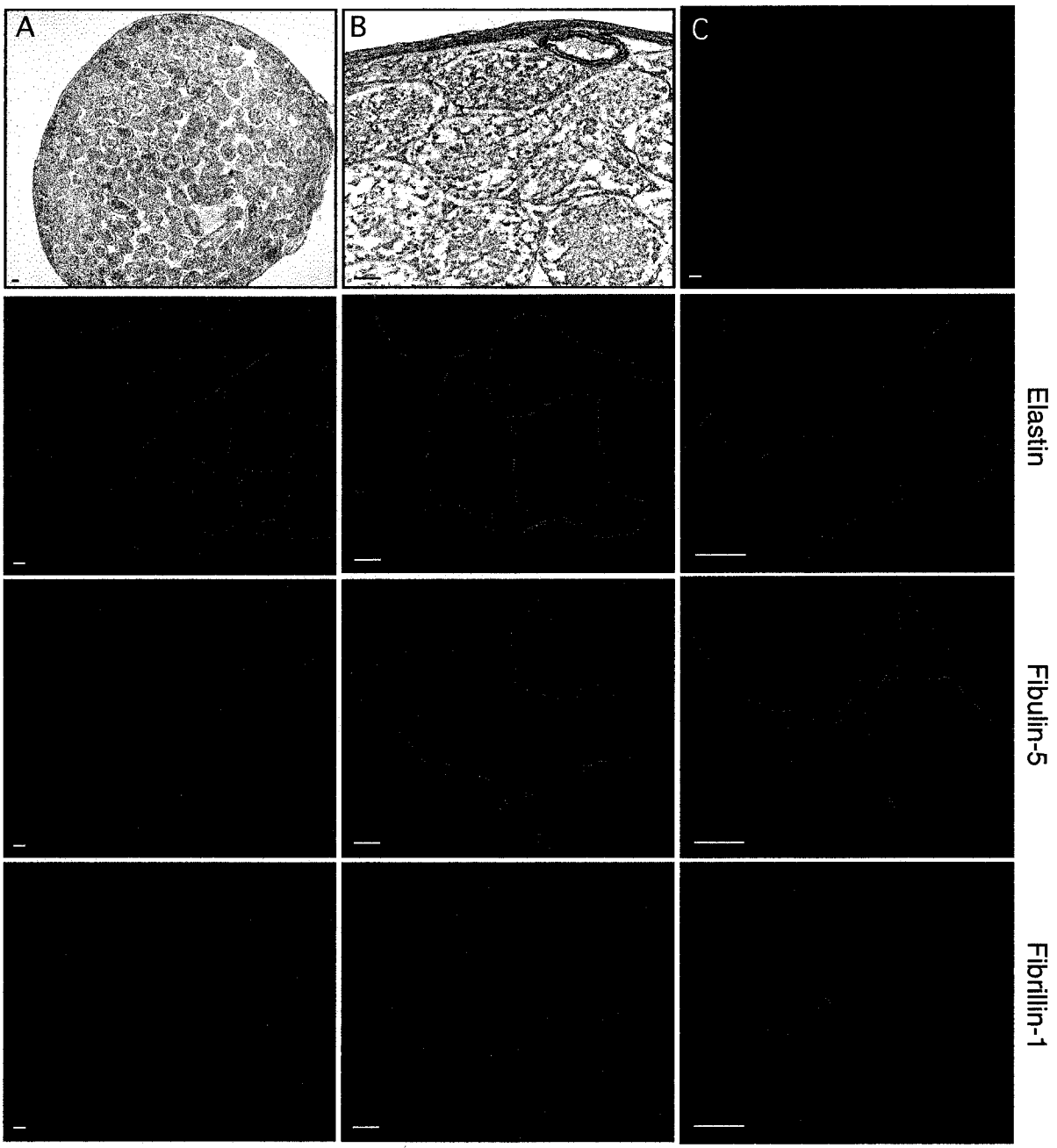

Figure 22: Immunohistochemical Analysis of Testis. Immunofluorescence microscope images of frozen sections of testis stained for tropoelastin, fibulin-5 and fibrillin-1. Omission of the primary antibodies serves as a negative control (**C**). Light microscope images of paraffin sections of testis were stained with Hematoxylin and Eosin for morphological purposes (**A**) as well as a Hart's stain to show the presence of elastic fibers in the organ (**B**). Bars = 50 μm.

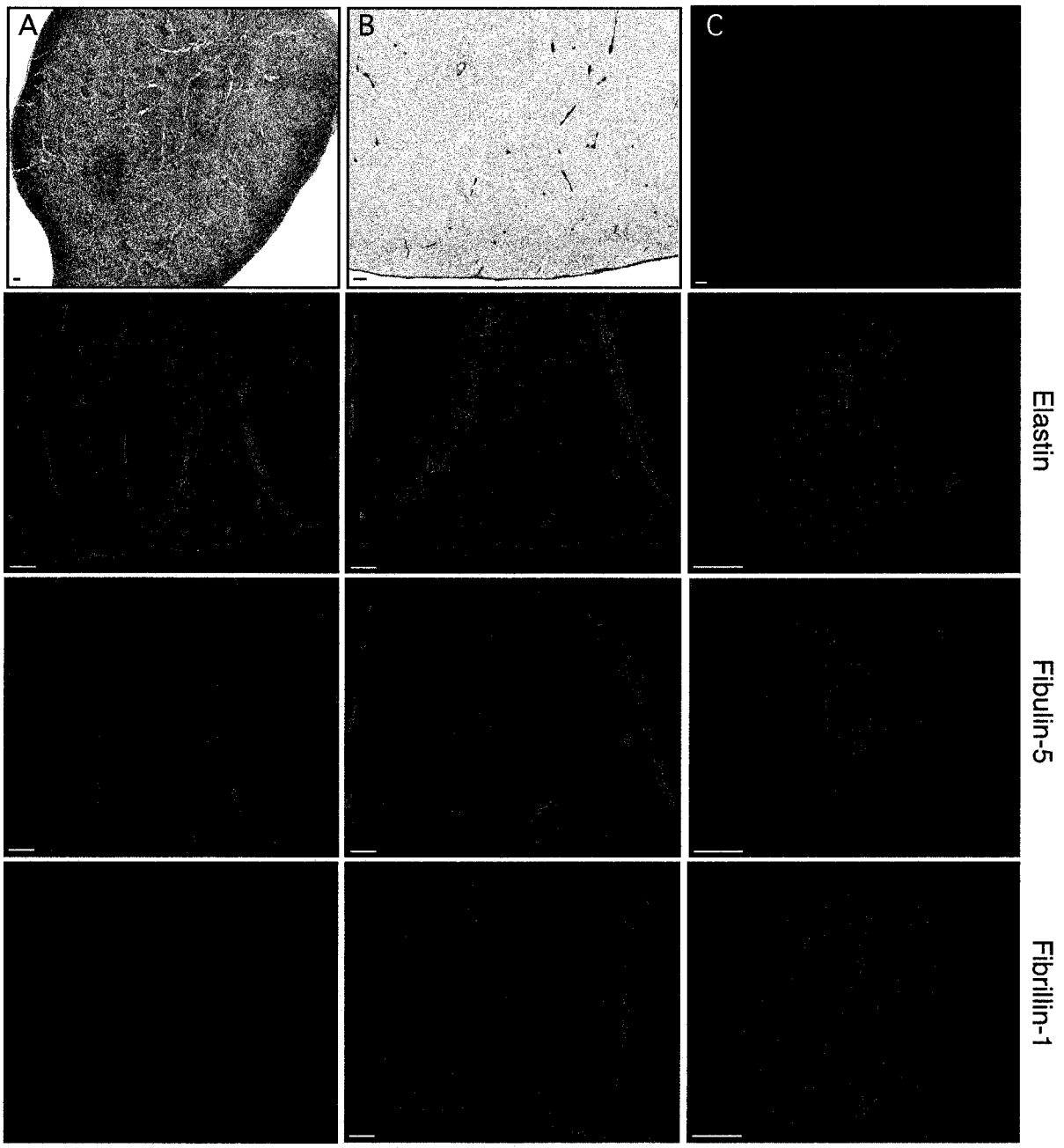

Figure 23: Immunohistochemical Analysis of Spleen. Immunofluorescence microscope images of frozen sections of spleen stained for tropoelastin, fibulin-5 and fibrillin-1. Omission of the primary antibodies serves as a negative control (**C**). Light microscope images of paraffin sections of spleen were stained with Hematoxylin and Eosin for morphological purposes (**A**) as well as a Hart's stain to show the presence of elastic fibers in the organ (**B**). Bars = 50 μm.

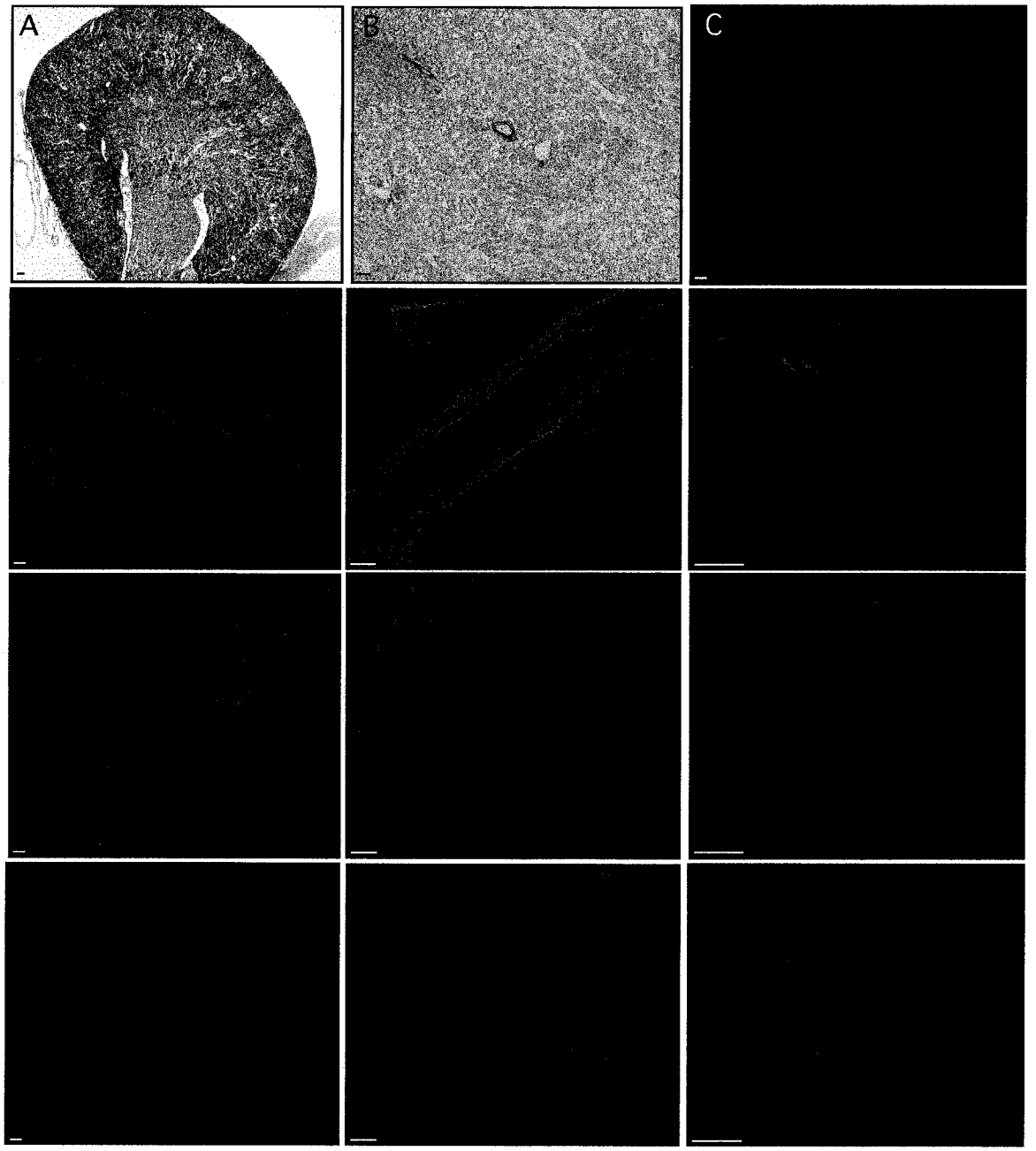

Figure 24: Immunohistochemical Analysis of Kidney. Immunofluorescence microscope images of frozen sections of kidney stained for tropoelastin, fibulin-5 and fibrillin-1. Omission of the primary antibodies serves as a negative control (**C**). Light microscope images of paraffin sections of kidney were stained with Hematoxylin and Eosin for morphological purposes (**A**) as well as a Hart's stain to show the presence of elastic fibers in the organ (**B**). Bars = 50 μm.

		Elastin	Fibulin-5	Fibrillin-1
Heart	Blood Vessels	✔	✔	✔
	Atrium	✔	✔	?
	Ventricle	✖	✖	✖
Liver	Blood Vessels	✔	✔	✔
	Capsule	✔	✔	✔
	Parenchyma	✖	✖	✖
Lung	Blood Vessels	✔	✔	✔
	Respiratory Airways	✔	✔	✔
	Alveolar Wall	✔	✔	✔
Colon	Blood Vessels	✔	✔	✔
	Lamina Propria	✔	✔	✔
Testis	Blood Vessels	✔	✔	✔
	Capsule	✔	✔	✔
	Tunica Propria	✔	✔	✔
Spleen	Blood Vessels	✔	✔	✔
	Capsule	✔	✔	✔
	Trabeculae	✔	✔	✔
	White Pulp	✔	✔	✔
Kidney	Blood Vessels	✔	✔	✔
	Interior Renal Corpuscle	✖	✖	✔
	Exterior Renal Corpuscle	✔	✔	✔
	Tubules	✖	✖	✔

Table 2: Summary of the Organ Survey. The seven organs are listed with their corresponding anatomy. They were stained with anti-tropoelastin (elastin), anti-fibullin-5 and anti-fibrillin-1 antibodies. The checkmarks indicate positive staining and the crosses indicate negative staining, the question mark indicates a result that was not clear. Note that the blood vessels in the liver include the central vein and the respiratory airways in the lung include the bronchioles,

DISCUSSION

The present study attempts to clarify the exact nature of the relationship between elastin, fibulin-5 and the fibrillin-containing microfibrils. Our data illustrate that not only does fibulin-5 interact with tropoelastin, but that it can bind tropoelastin at two different sites. Surprisingly, even though there is a strong interaction between elastin and fibulin-5, fibulin-5 does not require elastin to assemble into the matrix. This led to the hypothesis that fibulin-5 can interact with another protein of the elastic fiber, and indeed fibulin-5 was shown to bind to fibrillin-1. Furthermore, the tissue distribution of fibulin-5, elastin and fibrillin-1 was explored in several organs, in an attempt to elucidate the relationship of fibulin-5 with these two major elastic fiber proteins.

The necessary materials to attain the objectives and experiments set out in this study had to be initially made. The first half of this study was dedicated to producing a full-length recombinant fibulin-5 protein, which was used for solid-phase binding assays, and for the production of a polyclonal fibulin-5 antibody. The fibulin-5 antibody was essential in order to perform the ensuing experiments. With fibulin-5 protein and antibody, it was then possible to test the hypotheses and questions in the second half of this study.

The phenotype and severe elastic fiber defects seen in the fibulin-5 gene knockout (*fbln5-/-*) mouse demonstrated an essential role for fibulin-5 in the assembly of elastic fibers [54, 55]. The immunoprecipitation pull-down experiments for elastin and fibulin-5 showed the existence of an interaction between these two proteins *in*

vivo. It was not clear why there was a discrepancy between the molecular weight of fibulin-5 of the positive control and the other fibulin-5 bands, however, since the purified rF5, used as the positive control, had a His-tag added, this could have altered the molecular weight of the protein. The doublet bands seen for fibulin-5 around 55 kDa are likely due to processing of the protein while traveling through the Golgi, such as cleavage and/or glycosylation [81, 134] (Dr. Z. Urban - personal communication). For the elastin Western blot, alternate splice forms of elastin could explain the broad nature of the bands seen on the blot [6, 14-16].

Since it was not possible to determine if a direct or indirect interaction was occurring between elastin and fibulin-5 from whole cell lysate pull-downs, it was necessary to investigate the interaction of these two proteins with a solid-phase binding assay. Based on our results with this *in vitro* assay, strong binding between fibulin-5 and tropoelastin was shown, thereby demonstrating the existence of a direct interaction between these two proteins. These results are consistent with previous *in vivo* data showing that fibulin-5 localizes to elastic fibers using electron microscopic immunogold labeling of skin and aorta [55, 135], and by colocalisation immunostaining studies of cell culture matrices [54]. Furthermore, our results have recently been confirmed, using a similar solid-phase binding assay, in which fibulin-5 was shown to bind tropoelastin with high affinity [55]. Although, the interaction and binding of fibulin-5 to tropoelastin are not new data, it was important to test this interaction with our newly generated reagents. Once this interaction was established, an attempt to determine the specific binding site between fibulin-5 and tropoelastin was undertaken.

Using a number of deletion mutants, two binding sites for tropoelastin were identified on fibulin-5. One of the binding sites was found in the C-terminus based on the fact that the del 6-C construct of fibulin-5 did not bind tropoelastin. This site was further narrowed down by the observation that no binding was detected with the del EB construct. The results from this work identified the binding site for tropoelastin to be in the initial portion of the fibulin module (domain III). A second binding site for tropoelastin was also identified in the modified cbEGF module (domain I). The reduced binding seen with the N-terminal cbEGF module (domain I) deletion indicated that the presence of the C-terminal binding site alone, was not sufficient to mediate binding to tropoelastin. Rather, the C-terminal site required the N-terminal cbEGF domain to potentiate tropoelastin binding [97]. This result is consistent with the observation that tropoelastin binding of fibulin-5 can be inhibited by the absence of Ca^{2+} [55, 97], which is necessary to stabilize the cbEGF domains [73]. The rigidity of the cbEGF domains may thus impart a necessary structural stability to the elastin-binding region of the C-terminus to allow for binding [97]. Interestingly, modification of the RGD motif to RGE, a motif which is also found in the modified cbEGF module, showed a reduction in binding by one-half. The significance of this result remains unclear. This was collaborative work done with Dr. Hiromi Yanagisawa which has since been published [97]. In contrast to our study, however, that done by Dr. Yanagisawa and colleagues used whole media from protein-expressing cells [97]. Since whole media contains many other proteins besides the expressed fibulin-5, our results with purified proteins were important to validate this finding. Overall, these results indicate that the binding site in the C-terminus is essential for the ability of fibulin-5 to bind tropoelastin [97], but the nature of the functional association between

the elastin-binding region in the C-terminus and the first cbEGF domain at the N-terminus remains to be addressed.

This study also addressed the hypothesis that fibulin-5 requires the presence of elastin to properly assemble into the matrix. This hypothesis was based on several observations. First, our solid-phase binding assays have shown that fibulin-5 binds to tropoelastin. Second, immunogold labeling showed fibulin-5 localized to the surface of elastic fibers *in vivo* [55, 135] and immunostaining of cell culture matrices revealed that fibulin-5 colocalizes with elastin [54]. Third, it has been shown that fibulin-5 expression decreases upon RNA interference-mediated down-regulation of tropoelastin, suggesting co-regulation [84]. Finally, it has been reported that decreased fibulin-5 expression correlates with reduced elastin in thoracic aortic dissection [138]. Despite this supportive data, however, we determined that fibulin-5 can assemble into the matrix in the absence of elastin. This was a surprising result considering the strong data suggesting a physical and functional relationship between fibulin-5 and elastin. Since fibulin-5 appears to only form dimers and not a network on its own (Dr. Yanagisawa – personal communication), fibulin-5 must be binding to another protein present in the matrix.

To date, there have been many proteins identified to be part of, or associated with, elastic fibers (Figure 2). This led to the suggestion that one of these proteins must be helping fibulin-5 to assemble into the matrix. Due to the previously reported colocalization of fibulin-5 and elastic fibers seen in cell culture and the localization of fibulin-5 at the elastin-microfibril interface [55, 135], the most obvious candidate was fibrillin-1. From our solid-phase binding assay results, we showed that fibulin-5 binds to the N-terminal half of fibrillin-1. While working on this data, a paper was published

by Freeman *et al.,* 2005 [85] that showed similar results as ours. In this case they had more fibrillin-1 constructs to work with and narrowed down the binding site to a smaller region of the N-terminal. However, the solid-phase binding assays conducted by Freeman *et al.,* 2005 [85] were performed at the non-physiological temperature of 4°C. Thus, our results, obtained at room temperature, better reflect the normal environment in which these proteins exist. Recently, by using modified N-terminal fibrillin-1 constructs, it has been reported that fibrillin-1 interactions with fibulin-2, fibulin-4 and fibulin-5 depend on the first hybrid domain of fibrillin-1 [93]. Narrowing down the binding site is important because it allows for new insights into the molecular mechanism(s) by which fibulin-5 participates in the process of elastic fiber assembly. The fact that fibulin-5 can interact with fibrillin-1 is important because it suggests that fibulin-5 can be autonomous from elastin.

When first discovered, fibulin-5 was mainly emphasized as a protein associated with the vascular system since it was shown to be highly expressed in developing blood vessels as well as being upregulated after vascular injury [80]. Based on the *fbln-/-* mouse phenotype [54, 55], which showed loose skin and emphysematous lungs, fibulin-5 has been redefined as a critical regulator of elastic fiber formation in all tissues. Thus, to investigate the relationship between fibulin-5, fibrillin-1 and elastin *in vivo*, an organ survey was undertaken. Tissues examined were lung, liver, heart, colon, testis, spleen and kidney harvested from adult wildtype mice. The choice of these organs was based on previously published work on the expression of fibulin-5 by Northern blot analysis [81]. Based on this paper, all of the chosen organs except the liver showed high levels of fibulin-5 mRNA. Liver was therefore used in our study as a negative control.

As summarized in Table 2, elastin, fibrillin-1 and fibulin-5 were present in all blood vessels in all seven organs. As expected, there was a strong and similar staining pattern seen in the lung for all three proteins. Optimum antibody concentrations were determined with this organ because of its rich content of elastic fibers. Surprisingly, strong staining for all three proteins was also found in the liver capsule and the central venule of the liver lobules. This result was contrary to the published Northern blot data which showed no expression for fibulin-5 in liver [81]. However, this was most likely due to a dilution effect of mRNA by the large amount of liver cells not expressing the gene. Elastic fibers in the liver have been documented in the stroma of blood vessels found in the portal triad [139], but there has been no previous mention of elastic fibers in the liver capsule in the literature. Thus, it was very interesting to discover such a prominent elastic fiber network in the liver capsule. Elastic fiber staining in the heart was not a surprise since the left ventricle leads to the elastic fiber-rich aorta and the heart valves have been documented to contain elastic fibers [140, 141]. However, the extent of elastic fibers lining the interior of the atrial chamber is novel and suggests that a more detailed study of elastin and elastic fiber-related proteins in the heart is warranted. The very weak staining of fibrillin-1 in the atrium could indicate that there are fewer microfibrils present or perhaps there are more fibrillin-2 than fibrillin-1 molecules composing the microfibrils in the atrium since fibrillin-2 has been documented to have overlapping functions with fibrillin-1 but with distinct tissue localization [61].

The colon showed an interesting "tree" pattern for all three proteins that coincided with what has been described previously as a subepithelial elastic fiber system in the rat proximal colon [142]. Because of this elastic fiber system, the colon

is equipped to resist permanent distension or compression during digestion. The intense staining seen indicated an extensive and abundant elastic fiber presence in this tissue. The testis also stained very strongly for all three proteins in the tunica albuginea but mostly in the tunica propria (or limiting membrane). These results are consistent with early morphological studies on the testis which demonstrated the presence of elastic fibers in the tunica propria of human seminiferous tubules [143-145]. The intense staining seen in the colon and testis was surprising, however, because the Hart's staining did not indicate the presence of abundant elastic fibers. Perhaps, the elastic fibers in these tissues have a different organization whereby they are more diffuse than the normally thick strands of elastic fibers, and therefore possibly not detected by Hart's staining. Clearly, the only way to confirm this would be by electron microscopy of these tissues.

The spleen is usually associated with reticular fibers so it was relatively unexpected to observe such a strong presence of all three elastic fiber proteins in the capsule, trabeculae and white pulp. However, elastic fibers in the capsule, trabeculae and pulp have been identified by electron microscopy in rat spleen [146]. The rat study focused on the reticular fibers and did not mention the striking pattern of elastic fibers that we observed in the white pulp. Overall, it was suggested that a mixed meshwork of connective tissue fibers not only supports the organ as a whole but contributes to a contractile mechanism that regulates blood flow in concert with contractile elements in the capsule-trabecular system [146].

As mentioned earlier, the kidney was the only organ that differed from the rest with respect to the localization of the three proteins. It has already been shown that fibrillin-1 is located in the renal corpuscle mesangium as well as in the basement

membrane of the renal corpuscles and tubules, and around the renal blood vessels [147-149]. Our data is consistent with the published localization of fibrillin-1 in kidney but the function of fibrillin-1 in these locations, however, is not clear. What is especially noteworthy in the kidney is that fibulin-5 and elastin staining were not found inside the renal corpuscles or around the tubules, like fibrillin-1. Instead, elastin and fibulin-5 were only found to be associated with the major renal blood vessels, as well as with the afferent and efferent arterioles entering the renal corpuscle. Thus, it can be concluded that fibulin-5 is not a component of all microfibrils. From this data, one would anticipate that structures made exclusively of microfibrils, such as ciliary zonules of the eye [150-153], would not contain fibulin-5. This notion is supported by the fact that fibulin-2, which binds the same fibrillin-1 hybrid domain as fibulin-5 [93], was not found in the ciliary zonules [52]. Based on the fact that we have shown that fibulin-5 can assemble with fibrillin-1 in the absence of elastin *in vitro*, we reason that fibulin-5 must not be being expressed in those regions that contain "naked' microfibrils *in vivo*. This supports previously published data that suggests co-regulation of fibulin-5 and elastin expression [84].

Overall, the organ survey served two purposes. First, it demonstrated the tissue distribution of fibulin-5 in various organs and the prevalence of elastic fibers in organs where elastic fibers were not suspected to be present, such as in the atrium, liver capsule, colon and seminiferous tubules. Second, as summarized in Table 2, we discovered that fibulin-5 was never found without elastin and fibrillin-1, and that elastin was never found without fibulin-5 and fibrillin-1. However, fibrillin-1 could be found to exist "alone", in a non-elastic fiber context. Since fibulin-5 has yet to be

found independent of elastin, it can be said that fibulin-5 is an elastic fiber-related protein and that its major role appears to be in the process of elastic fiber assembly.

To know the location of binding sites and the interactions between elastic fiber proteins, to elucidate molecular mechanisms and the assembly of elastic fibers, to discover the tissue distribution of fibulin-5 and other elastic fiber proteins or by simply knowing the location of elastic fibers in certain organs, has immense implications in understanding the pathologies that affect elastogenic tissues or genetic diseases that involve elastic fiber proteins. The story of fibulin-5 exemplifies what a complex and interacting world the extracellular matrix is.

CONCLUSIONS

Fibulin-5 is essential for elastic fiber assembly and has a complex relationship with other proteins involved in elastic fibers. In this present study, we have purified full-length fibulin-5 and prepared an anti-fibulin-5 antibody. We have demonstrated that fibulin-5 interacts with tropoelastin by two different methods: solid-phase binding assays and immunoprecipitations. Not only was it shown that fibulin-5 binds tropoelastin, but the use of different constructs enabled us to determine that fibulin-5 binds tropoelastin at two different sites: within the C-terminal (fibulin module) and within the modified cbEGF module in domain I. Surprisingly, fibulin-5 did not require elastin to be able to build a matrix in cell culture. In lieu of this, we then demonstrated that fibulin-5 has another binding partner, fibrillin-1. Solid-phase binding assays with two different fibrillin-1 constructs narrowed down the binding site to the N-terminal half of the fibrillin-1 protein. The tissue distribution of fibulin-5 was also explored using immunohistochemical analysis of seven organs. Fibulin-5 had similar distribution and localization as elastin and fibrillin-1, with the exception of the kidney in which fibrillin-1 was found inside the renal corpuscle and around the tubules. Novel locations of elastic fibers were discovered in the liver capsule, the white pulp of the spleen and the atrial wall. This survey also provided concrete evidence of the presence of elastic fibers in organs that were previously only assumed to contain elastic fibers but not investigated thoroughly. To understand the interactions and location of fibulin-5 and other elastic fiber proteins, has profound implications in understanding the pathologies involving elastic fibers and tissue.

REFERENCES

1. Luis Carlos Junqueira, J.C., Robert O. Kelley, *Basic Histology*. Vol. 9. 1998, Stamford: Appleton & Lange. 89 - 91.
2. Loeys, B., et al., *Homozygosity for a missense mutation in fibulin-5 (FBLN5) results in a severe form of cutis laxa.* Hum Mol Genet, 2002. **11**(18): p. 2113-8.
3. Ramirez, F., et al., *The fibrillin-Marfan syndrome connection.* Bioessays, 1993. **15**(9): p. 589-94.
4. Ramirez, F., *Pathophysiology of the microfibril/elastic fiber system: introduction.* Matrix Biol, 2000. **19**(6): p. 455-6.
5. Kielty, C.M., M.J. Sherratt, and C.A. Shuttleworth, *Elastic fibres.* J Cell Sci, 2002. **115**(Pt 14): p. 2817-28.
6. Mithieux, S.M. and A.S. Weiss, *Elastin.* Adv Protein Chem, 2005. **70**: p. 437-61.
7. Davis, E.C., *Smooth muscle cell to elastic lamina connections in developing mouse aorta. Role in aortic medial organization.* Lab Invest, 1993. **68**(1): p. 89-99.
8. Davis, E.C., *Endothelial cell connecting filaments anchor endothelial cells to the subjacent elastic lamina in the developing aortic intima of the mouse.* Cell Tissue Res, 1993. **272**(2): p. 211-9.
9. Starcher, B.C., *Lung elastin and matrix.* Chest, 2000. **117**(5 Suppl 1): p. 229S-34S.
10. Starcher, B., R.L. Aycock, and C.H. Hill, *Multiple roles for elastic fibers in the skin.* J Histochem Cytochem, 2005. **53**(4): p. 431-43.
11. Keeley, F.W., C.M. Bellingham, and K.A. Woodhouse, *Elastin as a self-organizing biomaterial: use of recombinantly expressed human elastin polypeptides as a model for investigations of structure and self-assembly of elastin.* Philos Trans R Soc Lond B Biol Sci, 2002. **357**(1418): p. 185-9.
12. Vrhovski, B. and A.S. Weiss, *Biochemistry of tropoelastin.* Eur J Biochem, 1998. **258**(1): p. 1-18.
13. Petersen, E., F. Wagberg, and K.A. Angquist, *Serum concentrations of elastin-derived peptides in patients with specific manifestations of atherosclerotic disease.* Eur J Vasc Endovasc Surg, 2002. **24**(5): p. 440-4.
14. Tamburro, A.M., B. Bochicchio, and A. Pepe, *The dissection of human tropoelastin: from the molecular structure to the self-assembly to the elasticity mechanism.* Pathol Biol (Paris), 2005. **53**(7): p. 383-9.
15. Toonkool, P., et al., *Thermodynamic and hydrodynamic properties of human tropoelastin. Analytical ultracentrifuge and pulsed field-gradient spin-echo NMR studies.* J Biol Chem, 2001. **276**(30): p. 28042-50.
16. Toonkool, P., et al., *Hydrophobic domains of human tropoelastin interact in a context-dependent manner.* J Biol Chem, 2001. **276**(48): p. 44575-80.
17. Osakabe, T., et al., *Age- and gender-related changes in ligament components.* Ann Clin Biochem, 2001. **38**(Pt 5): p. 527-32.
18. Szabo, Z., et al., *Sequential loss of two neighboring exons of the tropoelastin gene during primate evolution.* J Mol Evol, 1999. **49**(5): p. 664-71.

19. Liu, X., et al., *Elastic fiber homeostasis requires lysyl oxidase-like 1 protein.* Nat Genet, 2004. **36**(2): p. 178-82.
20. Noblesse, E., et al., *Lysyl oxidase-like and lysyl oxidase are present in the dermis and epidermis of a skin equivalent and in human skin and are associated to elastic fibers.* J Invest Dermatol, 2004. **122**(3): p. 621-30.
21. Indik, Z., et al., *Alternative splicing of human elastin mRNA indicated by sequence analysis of cloned genomic and complementary DNA.* Proc Natl Acad Sci U S A, 1987. **84**(16): p. 5680-4.
22. Parks, W.C. and S.B. Deak, *Tropoelastin heterogeneity: implications for protein function and disease.* Am J Respir Cell Mol Biol, 1990. **2**(5): p. 399-406.
23. Zhang, M.C., et al., *Cutis laxa arising from frameshift mutations in exon 30 of the elastin gene (ELN).* J Biol Chem, 1999. **274**(2): p. 981-6.
24. Debelle, L. and A.M. Tamburro, *Elastin: molecular description and function.* Int J Biochem Cell Biol, 1999. **31**(2): p. 261-72.
25. Piontkivska, H., et al., *Multi-species sequence comparison reveals dynamic evolution of the elastin gene that has involved purifying selection and lineage-specific insertions/deletions.* BMC Genomics, 2004. **5**(1): p. 31.
26. Uitto, J., et al., *Molecular biology and pathology of human elastin.* Biochem Soc Trans, 1991. **19**(4): p. 824-9.
27. Davidson, J.M., *Smad about elastin regulation.* Am J Respir Cell Mol Biol, 2002. **26**(2): p. 164-6.
28. Degterev, A. and J.A. Foster, *The role of NF-1 factors in regulation of elastin gene transcription.* Matrix Biol, 1999. **18**(3): p. 295-307.
29. Conn, K.J., et al., *Insulin-like growth factor-I regulates transcription of the elastin gene through a putative retinoblastoma control element. A role for Sp3 acting as a repressor of elastin gene transcription.* J Biol Chem, 1996. **271**(46): p. 28853-60.
30. Wolfe, B.L., et al., *Insulin-like growth factor-I regulates transcription of the elastin gene.* J Biol Chem, 1993. **268**(17): p. 12418-26.
31. Carreras, I., et al., *Basic fibroblast growth factor decreases elastin gene transcription in aortic smooth muscle cells.* J Cell Biochem, 2002. **85**(3): p. 592-600.
32. Rich, C.B., et al., *Basic fibroblast growth factor decreases elastin gene transcription through an AP1/cAMP-response element hybrid site in the distal promoter.* J Biol Chem, 1999. **274**(47): p. 33433-9.
33. Kahari, V.M., et al., *Tumor necrosis factor-alpha down-regulates human elastin gene expression. Evidence for the role of AP-1 in the suppression of promoter activity.* J Biol Chem, 1992. **267**(36): p. 26134-41.
34. Mauviel, A., et al., *Human recombinant interleukin-1 beta up-regulates elastin gene expression in dermal fibroblasts. Evidence for transcriptional regulation in vitro and in vivo.* J Biol Chem, 1993. **268**(9): p. 6520-4.
35. Reitamo, S., et al., *Interleukin 10 up-regulates elastin gene expression in vivo and in vitro at the transcriptional level.* Biochem J, 1994. **302 (Pt 2)**: p. 331-3.
36. Parks, W.C., *Posttranscriptional regulation of lung elastin production.* Am J Respir Cell Mol Biol, 1997. **17**(1): p. 1-2.

37. Liu, J.M. and J.M. Davidson, *The elastogenic effect of recombinant transforming growth factor-beta on porcine aortic smooth muscle cells.* Biochem Biophys Res Commun, 1988. **154**(3): p. 895-901.
38. Grosso, L.E. and R.P. Mecham, *In vitro processing of tropoelastin: investigation of a possible transport function associated with the carboxy-terminal domain.* Biochem Biophys Res Commun, 1988. **153**(2): p. 545-51.
39. Hinek, A., F.W. Keeley, and J. Callahan, *Recycling of the 67-kDa elastin binding protein in arterial myocytes is imperative for secretion of tropoelastin.* Exp Cell Res, 1995. **220**(2): p. 312-24.
40. Patterson, C.E., et al., *Genomic organization of mouse and human 65 kDa FK506-binding protein genes and evolution of the FKBP multigene family.* Genomics, 2002. **79**(6): p. 881-9.
41. Brown-Augsburger, P., et al., *Identification of an elastin cross-linking domain that joins three peptide chains. Possible role in nucleated assembly.* J Biol Chem, 1995. **270**(30): p. 17778-83.
42. Kagan, H.M. and K.A. Sullivan, *Lysyl oxidase: preparation and role in elastin biosynthesis.* Methods Enzymol, 1982. **82 Pt A**: p. 637-50.
43. Kagan, H.M. and P. Cai, *Isolation of active site peptides of lysyl oxidase.* Methods Enzymol, 1995. **258**: p. 122-32.
44. Umeda, H., M. Takeuchi, and K. Suyama, *Two new elastin cross-links having pyridine skeleton. Implication of ammonia in elastin cross-linking in vivo.* J Biol Chem, 2001. **276**(16): p. 12579-87.
45. Urry, D.W., *Molecular perspectives of vascular wall structure and disease: the elastic component.* Perspect Biol Med, 1978. **21**(2): p. 265-95.
46. Vrhovski, B., S. Jensen, and A.S. Weiss, *Coacervation characteristics of recombinant human tropoelastin.* Eur J Biochem, 1997. **250**(1): p. 92-8.
47. Cleary, E.G., *The Microfibrillar Component of the Elastic Fiber.* "Connective Tissue Disease. Molecular Pathology of the Extracellular Matrix". 1987, Dekker, New York: J. Uitto and A. J. Perejda Editions. p. 55-81.
48. Sakai, L.Y., D.R. Keene, and E. Engvall, *Fibrillin, a new 350-kD glycoprotein, is a component of extracellular microfibrils.* J Cell Biol, 1986. **103**(6 Pt 1): p. 2499-509.
49. Zhang, H., et al., *Structure and expression of fibrillin-2, a novel microfibrillar component preferentially located in elastic matrices.* J Cell Biol, 1994. **124**(5): p. 855-63.
50. Gibson, M.A., et al., *The major antigen of elastin-associated microfibrils is a 31-kDa glycoprotein.* J Biol Chem, 1986. **261**(24): p. 11429-36.
51. Cain, S.A., et al., *Proteomic analysis of fibrillin-rich microfibrils.* Proteomics, 2006. **6**(1): p. 111-22.
52. Reinhardt, D.P., et al., *Fibrillin-1 and fibulin-2 interact and are colocalized in some tissues.* J Biol Chem, 1996. **271**(32): p. 19489-96.
53. Roark, E.F., et al., *The association of human fibulin-1 with elastic fibers: an immunohistological, ultrastructural, and RNA study.* J Histochem Cytochem, 1995. **43**(4): p. 401-11.
54. Nakamura, T., et al., *Fibulin-5/DANCE is essential for elastogenesis in vivo.* Nature, 2002. **415**(6868): p. 171-5.

55. Yanagisawa, H., et al., *Fibulin-5 is an elastin-binding protein essential for elastic fibre development in vivo.* Nature, 2002. **415**(6868): p. 168-71.
56. Reinboth, B., et al., *Molecular interactions of biglycan and decorin with elastic fiber components: biglycan forms a ternary complex with tropoelastin and microfibril-associated glycoprotein 1.* J Biol Chem, 2002. **277**(6): p. 3950-7.
57. Buczek-Thomas, J.A., et al., *Heparan sulfate depletion within pulmonary fibroblasts: implications for elastogenesis and repair.* J Cell Physiol, 2002. **192**(3): p. 294-303.
58. Pereira, L., et al., *Genomic organization of the sequence coding for fibrillin, the defective gene product in Marfan syndrome.* Hum Mol Genet, 1993. **2**(7): p. 961-8.
59. Charbonneau, N.L., et al., *Fibrillins can co-assemble in fibrils, but fibrillin fibril composition displays cell-specific differences.* J Biol Chem, 2003. **278**(4): p. 2740-9.
60. Corson, G.M., et al., *Differential expression of fibrillin-3 adds to microfibril variety in human and avian, but not rodent, connective tissues.* Genomics, 2004. **83**(3): p. 461-72.
61. Carta, L., et al., *Fibrillins 1 and 2 perform partially overlapping functions during aortic development.* J Biol Chem, 2006. **281**(12): p. 8016-23.
62. Baldock, C., et al., *Nanostructure of fibrillin-1 reveals compact conformation of EGF arrays and mechanism for extensibility.* Proc Natl Acad Sci U S A, 2006. **103**(32): p. 11922-7.
63. Reinhardt, D.P., et al., *Fibrillin-1: organization in microfibrils and structural properties.* J Mol Biol, 1996. **258**(1): p. 104-16.
64. Ramirez, F. and L. Pereira, *The fibrillins.* Int J Biochem Cell Biol, 1999. **31**(2): p. 255-9.
65. Wallis, D.D., et al., *Profibrillin-1 maturation by human dermal fibroblasts: proteolytic processing and molecular chaperones.* J Cell Biochem, 2003. **90**(3): p. 641-52.
66. Marson, A., et al., *Homotypic fibrillin-1 interactions in microfibril assembly.* J Biol Chem, 2005. **280**(6): p. 5013-21.
67. Qian, R.Q. and R.W. Glanville, *Alignment of fibrillin molecules in elastic microfibrils is defined by transglutaminase-derived cross-links.* Biochemistry, 1997. **36**(50): p. 15841-7.
68. Reinhardt, D.P., et al., *Initial steps in assembly of microfibrils. Formation of disulfide-cross-linked multimers containing fibrillin-1.* J Biol Chem, 2000. **275**(3): p. 2205-10.
69. Lin, G., et al., *Homo- and heterotypic fibrillin-1 and -2 interactions constitute the basis for the assembly of microfibrils.* J Biol Chem, 2002. **277**(52): p. 50795-804.
70. Jensen, S.A., et al., *Protein interaction studies of MAGP-1 with tropoelastin and fibrillin-1.* J Biol Chem, 2001. **276**(43): p. 39661-6.
71. Rock, M.J., et al., *Molecular basis of elastic fiber formation. Critical interactions and a tropoelastin-fibrillin-1 cross-link.* J Biol Chem, 2004. **279**(22): p. 23748-58.

72. Cain, S.A., et al., *Fibrillin-1 interactions with heparin. Implications for microfibril and elastic fiber assembly.* J Biol Chem, 2005. **280**(34): p. 30526-37.
73. Timpl, R., Sasaki, T., Kostka, G. & Chu, M.L. , *Fibulins: a versatile family of extracellular matrix proteins.* Nat. Rev. Mol. Cell Biol., 2003. **4**: p. 479-489.
74. Argraves, W.S., Greene, L. M., Cooley, M. A. & Gallagher, W. M. , *Fibulins: physiological and disease perspectives.* EMBO Rep., 2003. **4**: p. 1127-1131.
75. Gallagher, W.M., Currid, C. A. & Whelan, L. C. , *Fibulins and cancer: friend or foe?* Trends Mol. Med., 2005. **11**: p. 336-340.
76. Chu, M.L. and T. Tsuda, *Fibulins in development and heritable disease.* Birth Defects Res C Embryo Today, 2004. **72**(1): p. 25-36.
77. Pan, T.C., Kostka, G., Zhang, R. Z., Timpl, R. & Chu, M. L. , *Complete exon-intron organization of the mouse fibulin-1 gene and its comparison with the human fibulin-1 gene.* Birth Defects Res C Embryo Today, 2004. **72**: p. 25-36.
78. Rao, Z.*e.a.*, *The structure of a Ca(2+)-binding epidermal growth factor-like domain: its role in protein-protein interactions.* . Cell, 1995. **82**: p. 131-141.
79. Giltay, R., Timpl, R. & Kostka, G., *Sequence, recombinant expression and tissue localization of two novel extracellular matrix proteins, fibulin-3 and fibulin-4.* . Matrix Biol., 1999. **18**: p. 469-480.
80. Kowal, R.C., Richardson, J. A., Miano, J. M. & Olson, E. N., *EVEC, a novel epidermal growth factor-like repeat-containing protein upregulated in embryonic and diseased adult vasculature.* . Circ. Res., 1999. **84**: p. 1166-1176.
81. Nakamura, T., et al., *DANCE, a novel secreted RGD protein expressed in developing, atherosclerotic, and balloon-injured arteries.* J Biol Chem, 1999. **274**: p. 22476-22483.
82. Jean, J.C., et al., *DANCE in developing and injured lung.* Am J Physiol Lung Cell Mol Physiol, 2002. **282**(1): p. L75-82.
83. Aplin, A.E., Howe, A., Alahari, S. K. & Juliano, R. L. , *Signal transduction and signal modulation by cell adhesion receptors: the role of integrins, cadherins, immunoglobulin-cell adhesion molecules, and selectins.* Pharmacol. Rev., 1998. **50**: p. 197-263.
84. Tsuruga, E., Yajima, T. & Irie, K., *Induction of fibulin-5 gene is regulated by tropoelastin gene, and correlated with tropoelastin accumulation in vitro.* . Int J Biochem Cell Biol, 2004. **36**: p. 395-400.
85. Freeman, L.J., et al., *Fibulin-5 interacts with fibrillin-1 molecules and microfibrils.* Biochem J, 2005. **388**(Pt 1): p. 1-5.
86. Lemaire, R., Korn, J. H., Schiemann. W. P. & Lafyatis, R., *Fibulin-2 and fibulin-5 alterations in the tsk mice associated with disorganized hypodermal elastic fibers and skin tethering.* J. Invest. Dermatol., 2004. **123**(6): p. 1063-1069.
87. Green, M.C., Sweet, H. O. & Bunker, L. E., *Tight-skin, a new mutation of the mouse causing excessive growth of connective tissue and skeleton.* . Am J Pathol, 1976. **82**(3): p. 493-512.
88. Privitera, S., et al., *The 67-kDa enzymatically inactive alternatively spliced variant of beta-galactosidase is identical to the elastin/laminin-binding protein.* J Biol Chem, 1998. **273**(11): p. 6319-26.

89. Mochizuki, S., B. Brassart, and A. Hinek, *Signaling pathways transduced through the elastin receptor facilitate proliferation of arterial smooth muscle cells.* J Biol Chem, 2002. **277**(47): p. 44854-63.
90. Hinek, A., et al., *Lysosomal sialidase (neuraminidase-1) is targeted to the cell surface in a multiprotein complex that facilitates elastic fiber assembly.* J Biol Chem, 2006. **281**(6): p. 3698-710.
91. Rodgers, U.R. and A.S. Weiss, *Integrin alpha v beta 3 binds a unique non-RGD site near the C-terminus of human tropoelastin.* Biochimie, 2004. **86**(3): p. 173-8.
92. Broekelmann, T.J., et al., *Tropoelastin interacts with cell-surface glycosaminoglycans via its COOH-terminal domain.* J Biol Chem, 2005. **280**(49): p. 40939-47.
93. El-Hallous, E., et al., *Fibrillin-1 interactions with fibulins depend on the first hybrid domain and provide an adaptor function to tropoelastin.* J Biol Chem, 2007. **282**(12): p. 8935-8946.
94. Sakamoto, H., et al., *Cell-type specific recognition of RGD- and non-RGD-containing cell binding domains in fibrillin-1.* J Biol Chem, 1996. **271**(9): p. 4916-22.
95. Pfaff, M., et al., *Cell adhesion and integrin binding to recombinant human fibrillin-1.* FEBS Lett, 1996. **384**(3): p. 247-50.
96. Kielty, C.M., et al., *Attachment of human vascular smooth muscles cells to intact microfibrillar assemblies of collagen VI and fibrillin.* J Cell Sci, 1992. **103 (Pt 2)**: p. 445-51.
97. Zheng, Q., et al., *Molecular analysis of fibulin-5 function during de novo synthesis of elastic fibers.* Mol Cell Biol, 2007. **27**(3): p. 1083-95.
98. Pereira, L., et al., *Targetting of the gene encoding fibrillin-1 recapitulates the vascular aspect of Marfan syndrome.* Nat Genet, 1997. **17**(2): p. 218-22.
99. Pereira, L., et al., *Pathogenetic sequence for aneurysm revealed in mice underexpressing fibrillin-1.* Proc Natl Acad Sci U S A, 1999. **96**(7): p. 3819-23.
100. Bunton, T.E., et al., *Phenotypic alteration of vascular smooth muscle cells precedes elastolysis in a mouse model of Marfan syndrome.* Circ Res, 2001. **88**(1): p. 37-43.
101. Markova, D., et al., *Genetic heterogeneity of cutis laxa: a heterozygous tandem duplication within the fibulin-5 (FBLN5) gene.* Am J Hum Genet, 2003. **72**(4): p. 998-1004.
102. Li, D.Y., et al., *Elastin is an essential determinant of arterial morphogenesis.* Nature, 1998. **393**(6682): p. 276-80.
103. Urban, Z., et al., *Isolated supravalvular aortic stenosis: functional haploinsufficiency of the elastin gene as a result of nonsense-mediated decay.* Hum Genet, 2000. **106**(6): p. 577-88.
104. Li, D.Y., et al., *Novel arterial pathology in mice and humans hemizygous for elastin.* J Clin Invest, 1998. **102**(10): p. 1783-7.
105. Dietz, H.C., et al., *Recent progress towards a molecular understanding of Marfan syndrome.* Am J Med Genet C Semin Med Genet, 2005. **139**(1): p. 4-9.
106. Robinson, P.N., et al., *The molecular genetics of Marfan syndrome and related disorders.* J Med Genet, 2006. **43**(10): p. 769-87.

107. Dietz, H.C., et al., *Marfan syndrome caused by a recurrent de novo missense mutation in the fibrillin gene.* Nature, 1991. **352**(6333): p. 337-9.
108. Lee, B., et al., *Linkage of Marfan syndrome and a phenotypically related disorder to two different fibrillin genes.* Nature, 1991. **352**(6333): p. 330-4.
109. Loeys, B., De Backer J., et al., *Comprehensive molecular screening of the FBN1 gene favors locus homogeneity of classical Marfan syndrome.* Hum Mutat, 2004. **24**: p. 140-146.
110. Tsipouras, P., Del Mastro, R., et al., *Genetic linkage of the Marfan syndrome, ectopia lentis, and congenital cantractural arachnodactyly to the fibrillin genes on chromosomes 15 and 5. The International Marfan Syndrome Collaborative Study.* N Engl J Med, 1992. **326**: p. 905-909.
111. Reinhardt, D., Mechling, D., Boswell, B., Keene, D., Sakai, L. and H. Bachinger, *Calcium determines the shape of fibrillin.* J Biol Chem, 1997. **272**: p. 7368-7373.
112. Reinhardt, D., Ono, R. and L. Sakai,, *Calcium stabilizes fibrillin-1 against proteolytic degradation.* J Biol Chem, 1997. **272**: p. 1231-1236.
113. Milewicz, D.M., Z. Urban, and C. Boyd, *Genetic disorders of the elastic fiber system.* Matrix Biol, 2000. **19**(6): p. 471-80.
114. Neptune, E.R., et al., *Dysregulation of TGF-beta activation contributes to pathogenesis in Marfan syndrome.* Nat Genet, 2003. **33**(3): p. 407-11.
115. Ng, C.M., et al., *TGF-beta-dependent pathogenesis of mitral valve prolapse in a mouse model of Marfan syndrome.* J Clin Invest, 2004. **114**(11): p. 1586-92.
116. Pannu, H., et al., *Mutations in transforming growth factor-beta receptor type II cause familial thoracic aortic aneurysms and dissections.* Circulation, 2005. **112**(4): p. 513-20.
117. Mizuguchi, T., et al., *Heterozygous TGFBR2 mutations in Marfan syndrome.* Nat Genet, 2004. **36**(8): p. 855-60.
118. Loeys, B.L., et al., *A syndrome of altered cardiovascular, craniofacial, neurocognitive and skeletal development caused by mutations in TGFBR1 or TGFBR2.* Nat Genet, 2005. **37**(3): p. 275-81.
119. Habashi, J.P., et al., *Losartan, an AT1 antagonist, prevents aortic aneurysm in a mouse model of Marfan syndrome.* Science, 2006. **312**(5770): p. 117-21.
120. Morris, C.A. and C.B. Mervis, *Williams syndrome and related disorders.* Annu Rev Genomics Hum Genet, 2000. **1**: p. 461-84.
121. Urban, Z., et al., *Connection between elastin haploinsufficiency and increased cell proliferation in patients with supravalvular aortic stenosis and Williams-Beuren syndrome.* Am J Hum Genet, 2002. **71**(1): p. 30-44.
122. Ringpfeil, F., *Selected disorders of connective tissue: pseudoxanthoma elasticum, cutis laxa, and lipoid proteinosis.* Clin Dermatol, 2005. **23**(1): p. 41-6.
123. Tassabehji, M., et al., *An elastin gene mutation producing abnormal tropoelastin and abnormal elastic fibres in a patient with autosomal dominant cutis laxa.* Hum Mol Genet, 1998. **7**(6): p. 1021-8.
124. Rodriguez-Revenga, L., et al., *A novel elastin gene mutation resulting in an autosomal dominant form of cutis laxa.* Arch Dermatol, 2004. **140**(9): p. 1135-9.

125. Urban, Z., et al., *Autosomal dominant cutis laxa with severe lung disease: synthesis and matrix deposition of mutant tropoelastin.* J Invest Dermatol, 2005. **124**(6): p. 1193-9.
126. Szabo, Z., et al., *Aortic aneurysmal disease and cutis laxa caused by defects in the elastin gene.* J Med Genet, 2006. **43**(3): p. 255-8.
127. Hucthagowder, V., et al., *Fibulin-4: a novel gene for an autosomal recessive cutis laxa syndrome.* Am J Hum Genet, 2006. **78**(6): p. 1075-80.
128. Hu, Q., et al., *Inflammatory destruction of elastic fibers in acquired cutis laxa is associated with missense alleles in the elastin and fibulin-5 genes.* J Invest Dermatol, 2006. **126**(2): p. 283-90.
129. Stone, E.M., et al., *Missense variations in the fibulin 5 gene and age-related macular degeneration.* N Engl J Med, 2004. **351**(4): p. 346-53.
130. Lotery, A.J., et al., *Reduced secretion of fibulin 5 in age-related macular degeneration and cutis laxa.* Hum Mutat, 2006. **27**(6): p. 568-74.
131. Campochiaro, P.A., et al., *The pathogenesis of choroidal neovascularization in patients with age-related macular degeneration.* Mol Vis, 1999. **5**: p. 34.
132. Green, W.R., *Histopathology of age-related macular degeneration.* Mol Vis, 1999. **5**: p. 27.
133. Zheng, Q., et al., *Normal wound healing in mice deficient for fibulin-5, an elastin binding protein essential for dermal elastic fiber assembly.* J Invest Dermatol, 2006. **126**(12): p. 2707-14.
134. Hirai, M., et al., *Fibulin-5/DANCE has an elastogenic organizer activity that is abrogated by proteolytic cleavage in vivo.* J Cell Biol, 2007. **176**(7): p. 1061-71.
135. Choi, J., Zheng, Q., Starcher, B.C., Yanagisawa, H. & Davis, E.C., *Analysis of Dermal Elastic Fibers in the Absence of Fibulin-5 Reveals a Potential Role for Fibulin-5 in Elastic Fiber Assembly.* Manuscript in preparation.
136. Sasaki, T., et al., *Expression of fibulin-2 by fibroblasts and deposition with fibronectin into a fibrillar matrix.* J Cell Sci, 1996. **109 (Pt 12)**: p. 2895-904.
137. Culling, C.F.A., *Handbook of histopathological and histochemical techniques.* 3 ed. 1974, London: Butterworth.
138. Wang, X., et al., *Decreased expression of fibulin-5 correlates with reduced elastin in thoracic aortic dissection.* Surgery, 2005. **138**(2): p. 352-359.
139. Porto, L.C., et al., *Elastin in human, baboon, and mouse liver: an immunohistochemical and immunoelectron microscopic study.* Anat Rec, 1990. **228**(4): p. 392-404.
140. Vesely, I., *The role of elastin in aortic valve mechanics.* J Biomech, 1998. **31**(2): p. 115-23.
141. Soares, J.C. and A.L. Ferreira, *Contribution to the study of connective fibers in human mitral valve.* Anat Anz, 1985. **158**(3): p. 279-84.
142. Wakui, S., et al., *Subepithelial elastic system fibers of oblique mucosal folds in the rat proximal colon.* Acta Anat (Basel), 1991. **141**(2): p. 119-26.
143. Hermo, L., M. Lalli, and Y. Clermont, *Arrangement of connective tissue components in the walls of seminiferous tubules of man and monkey.* Am J Anat, 1977. **148**(4): p. 433-45.
144. De Menezes, A.P., *Elastic tissue in the limiting membrane of the human seminiferous tubule.* Am J Anat, 1977. **150**(2): p. 349-73.

145. Wiedmer-Bridel, J., A. Vogel, and C. Hedinger, *Elastic fibers in the tunica propria of the seminiferous tubules. Light and electron microscopic investigations.* Virchows Arch B Cell Pathol, 1978. **27**(3): p. 267-77.
146. Saito, H., et al., *Reticular meshwork of the spleen in rats studied by electron microscopy.* Am J Anat, 1988. **181**(3): p. 235-52.
147. Sterzel, R.B., et al., *Elastic fiber proteins in the glomerular mesangium in vivo and in cell culture.* Kidney Int, 2000. **58**(4): p. 1588-602.
148. Schaefer, L., et al., *Regulation of fibrillin-1 by biglycan and decorin is important for tissue preservation in the kidney during pressure-induced injury.* Am J Pathol, 2004. **165**(2): p. 383-396.
149. Porst, M., et al., *Fibrillin-1 regulates mesangial cell attachment, spreading, migration and proliferation.* Kidney Int, 2006. **69**(3): p. 450-456.
150. Streeten, B.W., et al., *The protein composition of the ocular zonules.* Invest Ophthalmol Vis Sci, 1983. **24**(1): p. 119-23.
151. Streeten, B.W., et al., *Immunohistochemical comparison of ocular zonules and the microfibrils of elastic tissue.* Invest Ophthalmol Vis Sci, 1981. **21**(1 Pt 1): p. 130-5.
152. Streeten, B.W. and P.A. Licari, *The zonules and the elastic microfibrillar system in the ciliary body.* Invest Ophthalmol Vis Sci, 1983. **24**(6): p. 667-81.
153. Lu, Y., et al., *Tissue specific differences in fibrillin microfibrils analysed using single particle image analysis.* J Struct Biol, 2006. **155**(2): p. 285-93.

APPENDIX